AD-A107 640 ROYAL AIRCRAFT ESTABLISHMENT FARNBOROUGH (ENGLAND) F/G 13/5
STRENGTH BEHAVIOUR OF FATIGUE CRACKED LUGS (FESTIGKEITSVERHALTE--ETC(U)
JAN 81 W GEIER
UNCLASSIFIED RAE-LIBRARY TRANS-2057 DRIC-BR-80140 NL

1 OF 2
AD A
107640

Trans 2057

UNLIMITED

BR80159
Trans 2057

AD A107040

ROYAL AIRCRAFT ESTABLISHMENT

*

Library Translation 2057

January 1981

NOV 27 1981
E

STRENGTH BEHAVIOUR OF FATIGUE CRACKED LUGS

by

W. Geier

*

DTIC FILE COPY

Procurement Executive, Ministry of Defence
Farnborough, Hants

UNLIMITED

81 9 28 057

Translations in this series are available from:

THE R.A.E. LIBRARY
Q.4 BUILDING
R.A.E. FARNBOROUGH
HANTS

New translations are announced monthly in:

"LIST OF R.A.E. TECHNICAL REPORTS, TRANSLATIONS and BIBLIOGRAPHIES"

UDC 621.886.4 : 539.388.1 : 539.219.2 : 539.4.014.11 : 539.219.2

ROYAL AIRCRAFT ESTABLISHMENT

Library Translation 2057

Received for printing 28 January 1981

STRENGTH BEHAVIOUR OF FATIGUE CRACKED LUGS

(FESTIGKEITSVERHALTEN VON RISSBEHAFTETEN AUGENSTÄBEN)

by

W. Geier

Dissertation Technical University Munich, 1980

Translator

Barbara Garland

Translation editor

J.E. Moon

AUTHOR'S SUMMARY

The aim of this study is to examine the strength behaviour of an important constructional element, the lug, when fatigue cracked, and to propose a stress intensity solution considering the various lug geometries.

First the stress intensity is described on the basis of the linear-elastic principles, which is followed by showing their significance for the strength behaviour in fatigue cracked condition. The investigation of various methods for determining the stress intensity shows the crack propagation method to be particularly appropriate for the lug.

Due to a lack of suitable tests on cracked lugs, a gradual approach to the lug is made, starting with an infinite plate with a hole and continuing with a finite plate with and without pin loaded holes, since stress intensity solutions are already available in this case.

An experimental investigation of the lug not only enables the stress intensity to be determined, but also shows the interrelationship between the essential lug parameters, the crack propagation behaviour and the stress distribution in a non-cracked lug. Finally, it is possible to evolve a stress intensity solution for cracked lugs in the form of a semi-empirical approach, which takes into account the essential lug parameters.

LIST OF CONTENTS

		Page
GENERAL		5
INTRODUCTION		5
1	FUNDAMENTALS OF LINEAR ELASTIC FRACTURE MECHANICS	6
1.1	The Airy stress function	6
1.2	Complex stress function	7
1.3	Solving the crack problems	8
2	STRESS INTENSITY AS BASIS FOR CALCULATION OF RESIDUAL STRENGTH AND CRACK PROGRESSION	10
2.1	Unstable crack propagation	10
2.2	Stable crack propagation	13
3	METHODS OF DETERMINING STRESS INTENSITY	14
3.1	Analytical and numerical methods	14
3.1.1	Analytical methods	14
3.1.2	Method of finite elements as numerical process	15
3.2	Experimental methods of determining stress intensity	17
3.2.1	The compliance method	17
3.2.2	Determination of stress intensity with crack propagation measurements	19
3.2.3	Photoelasticity and strain gauges	20
4	INVESTIGATIONS KNOWN FROM THE LITERATURE FOR DETERMINING STRESS INTENSITY FOR CRACKS EMANATING FROM THE EDGE OF THE HOLE	20
4.1	Infinite plate with unloaded hole	21
4.2	Infinite plate with hole and introduction of force by means of a pin	22
4.2.1	Linear superposition	22
4.2.2	Establishing stress intensity with the aid of the weight function for the loaded hole	22
4.3	Plates with finite dimensions	24
4.3.1	Finite plate with unloaded hole	24
4.3.2	Finite plate with introduction of force by means of a pin	25
4.3.3	Comparison of correction function for the finite plate with hole, with and without introduction of force	26
4.4	Lug	26
4.4.1	Investigation by Impellizerri and Rich	26
4.4.2	Investigation of Liu and Kan	27
5	SUMMARY OF INVESTIGATIONS DRAWN FROM THE LITERATURE	29
6	DEFINITION OF PROBLEM	31
7	INVESTIGATION TO DETERMINE THE STRESS INTENSITY FOR LUGS OF VARYING GEOMETRY	33
7.1	Selection of a suitable method	33
7.2	Specimen and test set-up	35
7.2.1	Dimensions of lugs	35
7.2.2	Material	35
7.2.3	Test set-up	35
7.3	Test procedure and test results	36
7.3.1	Test procedure	36
7.3.2	Test results	37
7.4	Discussion of test results with reference to the stress distribution in the crack-free lug	38

LT 2057

LIST OF CONTENTS (concluded)

		Page
8	EVALUATION OF THE TEST RESULTS TO DETERMINE STRESS INTENSITY	39
	8.1 Premises for the transfer of crack propagation characteristics from specimens to structural components	39
	8.2 Determination of crack propagation characteristics	40
	8.3 Determination of the crack propagation rate for lugs by means of their crack propagation curves	41
	8.4 Determination of stress intensity K_I and its non-dimensional quantity Y for the various lugs	43
	8.5 Comparison of the effect of the essential lug parameters on the correction function, on crack propagation and on stress distribution	45
9	DEVELOPMENT OF AN ANALYTICAL FORMULA TO DESCRIBE THE CORRECTION FUNCTION	46
	9.1 Computation formula for the standard lug	46
	9.2 Extension of the formula to take into account the effect of lug cheek width	48
	9.3 Extension of the formula to take account of the effect of the head height of the lug	49
	9.4 Stress intensity solution for the lug	50
10	VERIFICATION OF THE STRESS INTENSITY SOLUTION FOR THE LUG BY MEANS OF EXPERIMENTALLY DETERMINED CRACK PROPAGATION CURVES	51
11	INVESTIGATION INTO POSSIBLE SOURCES OF ERROR	52
	11.1 Scatter of crack propagation curves and its effect on the correction function	53
	11.2 Divergence of the semi-empirical formula from the experimentally determined correction function	54
12	CONCLUDING OBSERVATIONS	55
Acknowledgment		56
Tables		58
Index of most important abbreviations		64
References		65
Illustrations		Figures 1-11.1

Accession For
NTIS GRA&I
By
Dist
A
Dist
A

GENERAL

Fracture mechanics, *ie* calculation of crack propagation and the critical crack length are gaining increasingly in importance in the most varied technical areas. The reasons are to be found primarily in stricter safety requirements and economic considerations. While, for instance, in aircraft, reactor and pipeline construction the immediate safety of man and environment is of primary importance, it is noticeable that fracture mechanics are applied for economic reasons in areas such as rolling mills, drilling installations, etc.

A shutdown of a large-scale plant due to the unforeseen failure of a component can involve a company in considerable losses per day.

Basically, fracture mechanics can be applied wherever damage development, *ie* crack propagation due to dynamic loading or through stress crack corrosion under static load, cannot be excluded.

Here it is the task of fracture mechanics to predict development of damage and its critical quantity under service conditions in order to be able to take suitable precautions.

A marked drive in the further development of applied fracture mechanics is also likely to come from the area of aircraft construction[1]. Fracture mechanical characteristics have been used for a long time as a criterion in the selection of suitable materials.

Inspection intervals for aircraft components are frequently derived from crack propagation calculations[2]. In the United States, Airforce requirements have already been defined in Mil-Spec 83444 [3] by which aircraft manufacturers must prove that assuming a crack a component will not fail under service conditions within a certain period. Components which cannot be inspected must actually tolerate twofold fatigue life with crack.

Due to these requirements fracture mechanics has become a new dimensioning factor in the USAF in addition to strength and conventional life calculations, the latter based on Woehler curves and linear damage accumulation as Miner. Damage tolerant structure can be achieved by 'fail safe' (redundancy) or 'safe crack growth' requirements. Safe crack growth is achieved structurally both by a low stress level and crack inhibitors and by suitable selection of materials.

The following paper is intended to provide a contribution towards the improvement of life prediction for a typical aircraft and machine element within the framework of damage tolerant design philosophy.

INTRODUCTION

To solve structural and static problems the lug is used by the designer in many ways as an element for transmitting tensile and compressive forces, but without bending.

There are various methods[4-8] of calculating the fatigue strength of this structural element. The known literature does not at present include a stress intensity solution for different lug geometries, assuming a unilateral crack with straight crack front.

LT 2057

PRECEDING PAGE BLANK-NOT FILMED

In practice, the cracks occurring in lugs are predominantly quarter-elliptic edge cracks or semi-elliptic surface cracks. If in the light of dimensioning philosophy (damage tolerance) it is accepted that cracks may be present from the start, then the probability of the presence of *one* crack in the critical lug cross-section is greater than that of a crack on both sides. For this reason it is the aim of this paper to develop a method of calculation for the unilaterally cracked lug.

Starting with the stress intensity solution for a unilateral crack with straight linear crack front, more complicated crack forms could be considered like the edge or surface crack for instance by linear superposition with known answers for cracks with curved crack fronts. Regarding a crack with straight or at least approximately straight crack front has the advantange of reducing the investigation to an essentially two-dimensional problem.

1 FUNDAMENTALS OF LINEAR ELASTIC FRACTURE MECHANICS

Apart from the material characteristics[9,10] which will not be gone into here, the stress intensity plays a decisive part in the calculation of crack propagation and residual strength or critical crack length. It forms the basis of every fracture mechanics calculation. The theoretical fundamentals of the stress intensity K_I within the framework of linear elastic fracture mechanics are outlined below.

The whole derivation of the elastic stress field at the crack tip has already been compiled in Ref 11. The following summary has been extracted from Ref 12.

1.1 The Airy stress function

Within a coordinate system, X, Y, Z of a stressed body the stresses

$$\sigma_x, \sigma_y, \sigma_z, \tau_{xy}, \tau_{xz}, \tau_{yz}$$

can be defined at any point (x,y,z).

For the plane stress state $\sigma_z = \tau_{xz} = \tau_{yz} = 0$.

For the plane strain state $\varepsilon_z = 0$, $\sigma_z = \nu(\sigma_x + \sigma_y)$.

For the plane stress state the following equilibrium conditions result (see Fig 1.2)

$$\frac{\partial \sigma_x}{\partial x} + \frac{\partial \tau_{xy}}{\partial y} = 0 , \qquad \frac{\partial \sigma_y}{\partial y} + \frac{\partial \tau_{xy}}{\partial x} = 0 . \qquad (1\text{-}1)$$

If the displacements in x and y direction are designated u and v , the result for the strains is (see Fig 1.3),

LT 2057

$$\varepsilon_x = \frac{\partial u}{\partial x}, \qquad \varepsilon_y = \frac{\partial v}{\partial y}, \qquad \gamma_{xy} = \frac{\partial u}{\partial y} + \frac{\partial v}{\partial x} \quad . \tag{1-2}$$

The equations between stress and strain in the plane stress state are formulated according to Hooke's Law by

$$\left.\begin{aligned} \varepsilon_x &= \frac{1}{E}(\sigma_x - \nu\sigma_y) \\ \varepsilon_y &= \frac{1}{E}(\sigma_y - \nu\sigma_x) \\ \gamma_{xy} &= \frac{1}{E}\, 2(1+\nu)\tau_{xy} \; . \end{aligned}\right\} \tag{1-3}$$

Equation (1-1) is satisfied when

$$\sigma_x = \frac{\partial^2\psi}{\partial y^2}, \qquad \sigma_y = \frac{\partial^2\psi}{\partial x^2}, \qquad \tau_{xy} = \frac{\partial^2\psi}{\partial x\partial y} \quad . \tag{1-4}$$

Function ψ is termed Airy's stress function.

If equations (1-2) and (1-4) are inserted in (1-3) and differentiated twice the result is the compatibility equation:

$$\frac{\partial^4\psi}{\partial x^4} + 2\,\frac{\partial^4\psi}{\partial x^2\partial y^2} + \frac{\partial\psi}{\partial y^4} = 0 \tag{1-5}$$

or

$$\nabla^2(\nabla^2\psi) = 0 \; . \tag{1-6}$$

In general a plane linear elastic problem can be solved by finding the stress function which satisfies equation (1-6). In addition the stresses calculated from (1-4) must satisfy the boundary conditions of the problem. The stress function for a special case must be estimated on the basis of experience. Approximation solutions are described in detail in Ref 13.

1.2 Complex stress function

A complex stress function can be defined as follows:

$$Z(z) = \mathrm{Re}Z + i\,\mathrm{Im}Z\,; \qquad z = x + iy \; . \tag{1-7}$$

Z should be an analytical function with a unique derivative dZ/dz . This leads to the Cauchy-Riemann conditions:

$$\left.\begin{aligned} \frac{\partial \mathrm{Re}Z}{\partial x} &= \frac{\partial \mathrm{Im}Z}{\partial y} = \mathrm{Re}\,\frac{dZ}{dz} \\ \frac{\partial \mathrm{Im}Z}{\partial x} &= -\frac{\partial \mathrm{Re}Z}{\partial y} = \mathrm{Im}\,\frac{dZ}{dz} \quad . \end{aligned}\right\} \tag{1-8}$$

Various complex forms of the Airy stress function can be used to solve crack problems[14-21].

In the case of crack type I (see Fig 1.1) the function suggested by Westergaard[15] is suitable. While Sih[18] and Eftis and Liebowitz[19] demonstrated that the Westergaard function is not exact, this has no effect as far as the singular expressions of the stress are concerned.

The Westergaard function reads:

$$\psi = \mathrm{Re}\bar{\bar{Z}} + y\mathrm{Im}\bar{Z} \tag{1-9}$$

$\bar{\bar{Z}}$, $\bar{Z}$ and Z' being defined by:

$$\frac{d\bar{\bar{Z}}}{dz} = \bar{Z}\,, \qquad \frac{d\bar{Z}}{dz} = Z\,, \qquad \frac{dZ}{dz} = Z'\,. \tag{1-10}$$

With the Cauchy-Riemann equations (1-8) it follows

$$\nabla^2 \mathrm{Re}Z = \nabla^2 \mathrm{Im}Z = 0 \quad . \tag{1-11}$$

This means that (1-9) automatically fulfils the compatibility equation (1-6).

Using (1-4) produces for stresses

$$\left.\begin{aligned} \sigma_x &= \mathrm{Re}Z - y\mathrm{Im}Z' = \frac{\partial^2\psi}{\partial y^2} \\ \sigma_y &= \mathrm{Re}Z + y\mathrm{Im}Z' = \frac{\partial^2\psi}{\partial y^2} \\ \sigma_z &= -\,y\mathrm{Re}Z' = -\frac{\partial^2\psi}{\partial x\partial y} \quad . \end{aligned}\right\} \tag{1-12}$$

Every analytical function $Z(z)$ will lead to stresses as in equations (1-12). What is required, however, is to find a function $Z(z)$ for the problem in question which also fulfils the boundary conditions.

1.3 Solving the crack problems

For an infinite plate under biaxial stress the following stress function is obtained for crack type I :

LT 2057

$$Z = \frac{\sigma_z}{\sqrt{z^2 - a^2}} , \qquad z = x + iy . \tag{1-13}$$

The function is apart from ($- a \leqslant x \leqslant a$, $y = 0$) analytical. The edge stresses follow from (1-12). At infinity where $|Z| \to \infty$, $\sigma_x = \sigma_y = \sigma$ and $\tau_{xy} = 0$. At the crack face $\sigma_y = \tau_{xy} = 0$. This means that the boundary conditions are satisfied.

In order not to have to replace Z by $(z + a)$ it is logical to shift the co-ordinate system to the crack tip. In the general case, *ie* without taking the boundary conditions into account, Z must take the following form:

$$Z = \frac{f(z)}{\sqrt{z}} \tag{1-14}$$

$f(z)$ must be real and constant at the origin.

In accordance with (1-12) $\sigma_y = \tau_{xy} = 0$ applies at the crack surface.

The required real term and the constant value of $f(z)$ is given at the crack tip by K_I, since

$$Z_{|z| \to 0} = \frac{K_I}{\sqrt{2\pi z}} . \tag{1-15}$$

Using polar coordinates at the origin with $Z = Re^{i\theta}$, the stresses at the crack tip can be calculated from equations (1-12) and (1-15).

$$\left.\begin{aligned}
\sigma_x &= \frac{K_I}{\sqrt{2\pi r}} \cos\frac{\theta}{2}\left(1 - \sin\frac{\theta}{2}\sin\frac{3\theta}{2}\right)(-\sigma) \\
\sigma_y &= \frac{K_I}{\sqrt{2\pi r}} \cos\frac{\theta}{2}\left(1 + \sin\frac{\theta}{2}\sin\frac{3\theta}{2}\right) \\
\tau_{xy} &= \frac{K_I}{\sqrt{2\pi r}} \sin\frac{\theta}{2}\cos\frac{\theta}{2}\cos\frac{3\theta}{2} .
\end{aligned}\right\} \tag{1-16}$$

Parameter K_I in the above equations is termed stress intensity factor. For $r \to 0$ in the elastic case the stresses become infinite. The stress intensity factor is therefore a measure of the stress singularity at the crack tip. Since the material behaviour is assumed to be linear elastic the stress must be proportional to the external loading. In the case of uniaxial load with σ in the infinite K_I must be proportional to σ. K_I must also be proportional to the root of the crack length. For an infinite plate the sole characteristic length is the size of the crack. Consequently K_I must have the following form:

$$K_I = c\sigma\sqrt{a} . \tag{1-17}$$

LT 2057

In the case of biaxial load the stress function is given by (1-13). The shift in the origin of the coordinate system to the crack tip changes (1-13) to

$$Z = \frac{\sigma(z + a)}{\sqrt{z(z + 2a)}} \quad . \tag{1-18}$$

Comparison of (1-15) with (1-18) shows that

$$K_I = \sigma\sqrt{\pi a} \quad . \tag{1-19}$$

As one may assume that the stress system parallel to the crack is not disturbed by the crack, the solution for uniaxial loading must be the same as for biaxial loading. In the case of uniaxial loading factor C in (1-17) assumes the value $\sqrt{\pi}$. In addition to the stresses, the displacements for the plane strain state can also be determined from equations (1-2) and (1-12).

$$\begin{aligned} V &= \frac{1 + \nu}{E} [2(1 - \nu)\mathrm{Im}\bar{Z} - y\mathrm{Re}Z] \\ u &= \frac{1 + \nu}{E} [(1 - 2\nu)\mathrm{Re}\bar{Z} - y\mathrm{Im}Z] \quad . \end{aligned} \tag{1-20}$$

This leads to

$$\left.\begin{aligned} u &= 2(1 + \nu) \frac{K_I}{E} \sqrt{\frac{r}{2\pi}} \cos\frac{\theta}{2} \left[1 - 2\nu + \sin^2\frac{\theta}{2}\right] \\ v &= 2(1 + \nu) \frac{K_I}{E} \sqrt{\frac{r}{2\pi}} \sin\frac{\theta}{2} \left[2 - 2\nu - \cos^2\frac{\theta}{2}\right] \quad . \end{aligned}\right\} \tag{1-21}$$

Equations (1-16) are exact solutions for the stress field in the range $r \approx 0$. These solutions can still be used in a range in which r is small compared with the crack length.

2 STRESS INTENSITY AS BASIS FOR CALCULATION OF RESIDUAL STRENGTH AND CRACK PROGRESSION

2.1 Unstable crack propagation

Calculation of the fracture behaviour of cracked components was carried out by Griffith[22].

The calculation rests on the assumption that fracture occurs in ideally brittle materials when the elastic energy released by crack extension is exactly the same as the energy needed for crack propagation. This energy formula can be described as follows. Imagine an infinite plate with a crack going through the centre. The plate is loaded with a uniaxial stress σ applied at infinity. The potential energy U of the entire system can then be described by the formula

$$U = U_0 - U_a + U_\gamma \tag{2-1}$$

where U_0 = elastic energy of the non-cracked plate
U_a = reduction of the elastic energy by the insertion of a crack
U_γ = increase in surface energy due to enlargement of crack.

With the aid of a stress calculation developed by Inglis[23], Griffith was able to show that

$$U_a = \frac{\pi\sigma^2 a^2}{E} \quad . \tag{2-2}$$

Moreover the surface energy U_γ is equal to the product of the specific surface energy of the material γ_e and the new surface of the crack

$$U_\gamma = 2(2a\gamma_e) \quad . \tag{2-3}$$

The entire elastic energy of the system follows from this.

$$U = U_0 - \frac{\pi\sigma^2 a^2}{E} + 4a\gamma_e \quad . \tag{2-4}$$

Derivation of $\partial U/\partial a$ produces the equilibrium conditions for crack extension

$$\sigma\sqrt{a} = \left(\frac{2\gamma_e E}{\pi}\right)^{\frac{1}{2}} \quad . \tag{2-5}$$

Crack extension in ideally brittle materials is therefore determined by the product of the external stress, the root of the crack length and by material characteristics. With E and γ_e as material characteristics the right-hand side of the equation (2-5) corresponds to a constant which is characteristic of a specified ideally brittle material. It follows from this that crack extension in these materials occurs when the product of $\sigma\sqrt{a}$ reaches a critical value. This value can be determined experimentally for instance with a plate with central crack by measuring σ and a at the moment of crack extension and transferred to other specimen geometries, taking account of the effect of the geometry. It was only the latter which made practical application of fracture mechanics possible in a wide variety of technical areas.

Equation (2-5) can be rearranged as follows:

$$\frac{\pi\sigma^2 a}{E} = 2\gamma_e \tag{2-6}$$

the left-hand side being termed energy release rate G. The right-hand side of the equation represents the crack resistance R_w of the material.

In 1948 Irwin[24] suggested that Griffith's fracture criterion for ideally brittle materials should be transferred by modification to brittle materials and to metals

LT 2057

exhibiting plastic deformations at the crack tip. A similar suggestion was made by Orowan at the same time. According to this the crack resistance of technical materials is composed of the sum of the surface energy and the plastic deformation action. Consequently equation (2-6) was changed accordingly.

$$\sigma\sqrt{\pi a} = \sqrt{2(\gamma_e + \gamma_p)E} \quad . \tag{2-7}$$

A crack becomes unstable when the left-hand side of the equation (2-7) reaches a critical value, i.e. the critical stress intensity K_C . For crack type I the critical stress intensity is designated below with K_{IC} . For the infinite plate with central crack 2 a and external stress σ fracture occurs when equation

$$\sigma\sqrt{\pi a} = K_{IC} \tag{2-8}$$

is satisfied. Ref 25 describes the experimental method of determining the critical stress intensity K_{IC} . It is usual in the literature to designate the critical stress intensity in plane strain state K_{IC} and in plane stress state K_C .

Crack type I which occurs most frequently in practice is always used as basis.

The critical stress intensity K_{IC} in the range of the plane strain state is primarily a material constant. In the range of the plane stress state, however, the critical stress intensity depends on the material thickness.

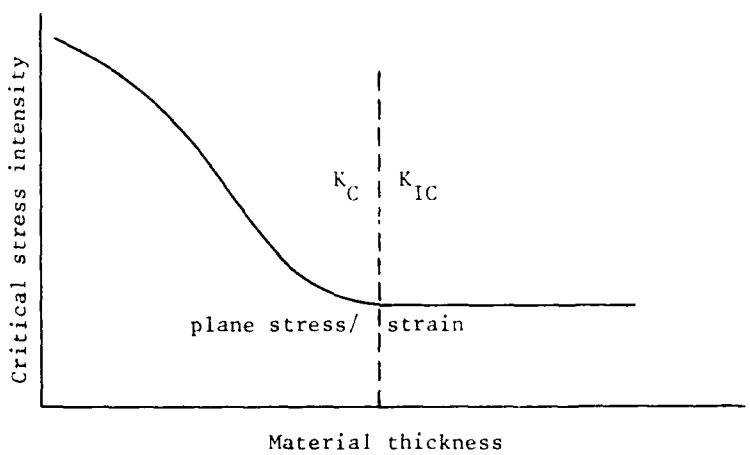

For the critical stress intensity in plane stress and in plane strain state it is assumed that the plastic zone in front of the crack tip is small compared with the length of the crack and the dimensions of the component. This is shown in the test by the linear relationship between force and crack expansion. If linearity no longer exists (elasto-plastic) then the critical stress intensity is dependent on additional factors. Relevant tests were carried out in Ref 26.

LT 2057

Critical stress intensity values are compiled in Ref 27 for a variety of materials.

As soon as one changes from the infinite plate with central crack to specimens resembling components the effect of the crack form, crack arrangement, specimen geometry and type of external load must be accounted for by a correction function Y. Correction functions for the various crack models are compiled in Refs 28 and 29.

$$K_I = \sigma\sqrt{\pi a}Y \quad . \tag{2-9}$$

2.2 Stable crack propagation

Paris[30,31] demonstrated the connection between stable crack propagation due to cyclical loading and stress intensity.

By means of crack propagation tests with constant stress amplitude Paris determined the crack growth per load cycle. In double logarithmic paper plotting the crack propagation rate against the related stress intensity factor range in the middle section B of the curve shown in Fig 2.2 produced a linear relation. Deviations only occur with very small ΔK_I values in section A and in the vicinity of the instability point in section C. This enabled the technically interesting area to be described by a simple exponential function:

$$\frac{da}{dN} = C_p(\Delta K_I)^{np} \quad . \tag{2-10}$$

It has been shown for a number of high strength alloys that the effect of the stress amplitude in the range of fluctuating tensile stresses on crack propagation behaviour is adequately reflected by the Paris equation for a defined stress ratio R.

The material characteristics C_p and n_p in the Paris equation are determined by means of constant amplitude crack propagation tests. These characteristics depend essentially on the material and stress ratio R.

Forman[32] expanded this equation in that he took account of the effect of the mean stress and the crack propagation behaviour on reaching the critical crack length:

$$\frac{da}{dN} = \frac{C_F(\Delta K_I)^{n_F}}{(1 - R)K_{IC} - \Delta K_I} \quad . \tag{2-11}$$

The Forman equation is used very frequently in practice. MBB set up a programme to determine the Forman characteristics[33]. This programme has been included in the structure calculation handbook (HSB) of the German aviation industry.

In practice, however, loading sequences occur frequently with variable amplitudes and mean stress. It has been demonstrated in numerous tests[34-39] that crack propagation on transition from high to lower stress peaks can be delayed appreciably. For this reason, *eg* Willenborg[40] and Wheeler[41] have developed crack propagation retardation models

LT 2057

for the variable load sequence. Besides the Forman equation these retardation models have been evaluated by means of extensive test results which are typical for aircraft construction[42] and suggestions worked out for calculating the crack propagation under operational loads. The retardation models are also based on the stress intensity.

3 METHODS OF DETERMINING STRESS INTENSITY

As already shown in sections 2.1 and 2.2, knowledge of the variation of stress intensity is of considerable importance to the calculation of crack propagation and residual strength. Extensive investigations have therefore been carried out to determine the stress intensity for various components or specimens resembling components. Various methods were used. Analytical methods can be used for very simple geometries. However, in the case of geometries with complex boundary conditions numerical and experimental methods are frequently employed.

Various methods of determining the stress intensity are presented below and evaluated in regard to their applicability to the problem 'lug'. Additional information on several methods is contained in Ref 43.

3.1 Analytical and numerical methods

3.1.1 Analytical methods

The elementary equations to describe the stress and displacement field at the crack tip for the case "infinite plate with central crack" were set up with the aid of these methods.

These results still serve as the starting point for the solution of various crack problems.

The fact that the stress and displacement field for any crack problem always assumes the same shape offers the opportunity of determining the stress intensity indirectly.

From the point of view of the engineer, however, the analytical methods are of secondary importance. In general the boundary conditions are detected precisely by analytical methods. However, this is usually only possible for an infinite plate with central crack.. In determining stress intensity by means of analytical methods the attempt is made to find the Airy stress function corresponding to the crack problem. For crack type I the stress function of Westergaard[15] is frequently used,

$$\phi = \mathrm{Re}\bar{\bar{Z}} + y\,\mathrm{Im}\bar{Z} \quad . \tag{3-1}$$

The solution of this function was given in section 1. Muskhelishvili[14], among others, suggests a complex stress function

$$\phi = \mathrm{Re}\left[\bar{Z}\Phi(z) + \int\Psi(z)dz\right] \quad . \tag{3-2}$$

Using (1-4) it follows

$$\sigma_x + \sigma_y = 4\mathrm{Re}\left[\Phi'(z)\right] \quad . \tag{3-3}$$

LT 2057

Thus it can be shown that

$$\lim_{r \to 0} (\sigma_x + \sigma_y) = \frac{2K_I}{\sqrt{2\pi r}} \cos \frac{\theta}{2} \quad . \tag{3-4}$$

This method was tested in detail by Sih[44] and used by Erdogan[45].

If a simple solution of these equations is not possible numerical methods (difference equations) can be used as approximation solutions.

To solve the technically interesting problem "crack from hole" Bowie[46] used the method of conformal mapping.

3.1.2 Method of finite elements as numerical process

The method of finite elements has been used to an increasing extent recently to calculate the stress field in the vicinity of the crack tip[47]. The versatility of this method enables complicated component geometries to be calculated. The fundamentals and applications of the method of finite elements are described in Ref 48.

In the method of finite elements the elastic continuum is replaced by a limited number of elements which are only connected at their nodal points.

Forces or displacements between the elements can only be transmitted through these nodal points.

The displacements of the nodes are the unknown quantities in an appropriate equation system.

In the plane stress state the sole displacements are u and v. In the simplest case it is assumed that these displacements are linear, *eg* $u = ax + by + c$, $v = ex + fy + g$.

In many cases triangular elements are used with a node at each angle of the element. The displacements of the nodal points are U_1, U_2, U_3 and V_1, V_2, V_3.

The displacements of the nodal points must satisfy the equations for u and v. By inserting the node displacements and node coordinates six equations are obtained with six unknowns a to g for an element.

Solving the equation system produces all the displacements within the element. These assumptions ensure continuity between neighbouring elements, *ie* the linear change in displacements along the contact line of two elements will be the same in both elements because of the common nodal points. It follows from $\varepsilon x = \partial U/\partial x$ and $\varepsilon y = \partial V/\partial y$ that with linear displacements deformations are constant within an element. Of course functions of a higher order are possible to describe the deformations within each element. This considerably improves the accuracy of the FE calculation, especially in the area of steep stress gradients.

The bonding forces between the elements can also be presented as nodal displacements.

Finally, equilibrium equations have to be set up for the nodal points.

LT 2057

In a plane problem the nodal forces have two components, namely in x and y direction. The equilibrium equations are yielded by the sum of the component forces of various elements which meet at the node.

The forces occurring at the nodes of the marginal elements are equated with the external loads or stresses.

The resulting equation system can be solved by electronic computers.

Basically there are two different approximations to determine the stress intensity with the aid of the method of finite elements.

There is the direct method in which the stress intensity is calculated from the stress or displacement field.

In the indirect method the stress intensity is determined via the relationship with other parameters such as stiffness, elastic energy or J integral.

For the direct method the result of general analytical solutions of crack problems is used. The stress intensity can thus be calculated from the stresses and displacements in the vicinity of the crack tip with the aid of equations (1-19) and (1-21):

$$K_I = \sigma_{ij} \frac{\sqrt{2\pi r}}{f_{ij}(\theta)} , \qquad K_I = \frac{U_i}{C\sqrt{r} f_i(\theta)} . \qquad (3\text{-}5)$$

The necessary stresses and/or displacements are obtained from calculation by the finite element method. The stress for an element in the vicinity of the crack tip, the distance r of the centre of gravity of the element from the crack tip and the angle θ (see Fig 1.2) are inserted in equation (3-5), thus yielding the stress intensity at a certain crack length a .

The stress intensity can be calculated in a similar manner from the displacement.

In the ideal case the stresses and displacements of different elements should lead to the same K_I value, provided the elements are in the area of validity of the analytical solution (3-5), *ie* in the immediate vicinity of the crack tip.

To reduce the integration error owing to the finite dimensions of the finite elements very fine subdivision of the grid in the crack area is recommended if elements with linear displacement are used.

To model the crack tip singularity special crack tip elements were developed from the so-called isoparametric elements. For instance the FE programme developed by MARC[49] contains a rectangular element with eight nodes and nine integration points within the element.

Singularity is approximated by shifting together two angle nodes situated on one side.

The advantage of these elements is to be seen in that far fewer elements are needed for idealisation of the crack tip environment with the same accuracy than is the case for elements with linear di placement formula.

LT 2057

For this, approximately 6-8 of these elements are usually required at the crack tip. The computing costs can also be reduced substantially by this means.

The stress intensity can also be calculated indirectly via changes in stiffness with increasing crack length. The procedure corresponds to the experimental compliance method described below. Here the test to be performed in section 3.2.1 is replaced by the FE calculation.

The FE calculation provides the displacement of the force introduction points for various crack lengths.

The change in stiffness as a function of crack length is thus obtained, as in Fig 3.7.

The K value is calculated to equation (3-6).

The J integral can also be used for indirect calculation of the K_I value. As long as elastic deformations are concerned the equation $K_I^2 / E = G_I = J$ applies.

For example Chan, *et al*[50] determined the stress intensity with the J integral for a compact tensile specimen. The external contour of the specimen was used as integration path.

Strain energy density was determined from the nodal point stresses and the nodal point forces used as surface line forces.

The indirect methods have the advantage that extrapolation is not required as in the direct method and according to the known literature no particularly dense element grid is said to be necessary.

3.2 Experimental methods of determining stress intensity

3.2.1 The compliance method

In the compliance method the stiffness of a component at various crack lengths is measured experimentally. The stress intensity is calculated via the crack extension force. According to Irwin the elastic energy U_e changes by the value G_I on extension of the crack. This value is termed crack extension force by Irwin:

$$\frac{\partial U_e}{\partial a} = G_I \quad . \tag{3-6}$$

From the force P and the displacement ΔS of two points, generally the force introduction points, the elastic energy U_e is derived,

$$U_e = \frac{P \Delta s}{2} \quad . \tag{3-7}$$

The displacement Δs can be replaced by the compliance

$$C^{-1} = \frac{1}{C} = \frac{\Delta s}{P} \quad . \tag{3-8}$$

LT 2057

Equations (3-7) and (3-8) produce for U_e

$$U_e = \frac{P^2}{2} C^{-1} \quad . \tag{3-9}$$

If (3-9) is inserted in (3-6) it follows

$$\frac{P^2}{2} \frac{dC^{-1}}{da} = G_I \quad . \tag{3-10}$$

Via the known relationship between stress intensity K and crack extension force G

$$G_I = \frac{K_I^2}{E} \qquad \text{plane stress state}$$

$$G_I = \frac{K_I^2}{E} (1 - \nu^2) \qquad \text{plane strain state}$$

(3-10) can be converted to

$$K_I^2 = E \frac{P^2}{2} \frac{dC^{-1}}{da}$$

$$K_I^2 = \frac{E}{1 - \nu^2} \frac{P^2}{2} \frac{dC^{-1}}{da} \quad . \tag{3-11}$$

The schematic diagrams A, B and C in Figs 3 to 7 show the procedure in experimental determination of the stress intensity K_I .

Fig A shows the specimen extension Δs with increasing force p at different crack lengths a . With increasing length of crack the stiffness of the specimen decreases, *ie* the specimen or component becomes 'softer'.

In B the reciprocal values of the slopes from A are plotted over the length of crack a . A distinct increase in compliance C^{-1} with increasing crack length a can be discerned in this diagram too. If one differentiates in B compliance C^{-1} with respect to crack length a , *ie* forms dC^{-1}/da and plots this in C over the relevant crack length, then the stress intensity K can be calculated with this curve and with equation (3-11).

In the main the stress intensity can be determined only for cracks with linear crack front with the compliance method.

For semi-elliptical surface or quarter-elliptical edge cracks the compliance method would only yield a median value for the entire crack front.

LT 2057

3.2.2 Determination of stress intensity with crack propagation measurements

It has been demonstrated in numerous constant amplitude crack propagation tests that the crack propagation rate can be presented as a function of the stress intensity range.

This means that the same crack propagation rate is always measured, irrespective of crack length, stress and specimen geometry, for a specific stress intensity range. If the stress intensity is to be determined for a component, a crack propagation test under constant amplitude loading must first be performed with the component. From the crack propagation curve the crack propagation rate is determined as a function of the crack length.

A constant amplitude crack propagation test is carried out with a test specimen which agrees with the component in respect of material and thickness under the same conditions (stress ratio, loading frequency, environment). Since the stress intensity for the specimen must be known[52] the crack propagation rate can be presented from the crack propagation curve as a function of the stress intensity range,

$$da/dN = f(\Delta K_I) \quad . \tag{3-12}$$

This crack propagation characteristic, however, can be transferred to the component, as stated at the beginning.

If now a certain value for the crack propagation rate has been determined in the component at a certain crack length, then this must have been brought about by a specific stress intensity range according to (3-12). Therefore the appropriate stress intensity range can be allotted to the crack propagation rate established on the component.

Fig 3.8 shows the procedure in the form of a flow diagram.

It is customary in the literature to quote the correction function as non-dimensional quantity depending on crack length instead of the stress intensity. The stress intensity is used as reference quantity which would result at the same stress and crack length in an infinite plate with central crack under uniaxial load,

$$Y = \Delta K_I / \Delta K_{IO} \tag{3-13}$$

$$\Delta K_{IO} = 2\sigma_a \sqrt{\pi a} \quad . \tag{3-14}$$

As in the Compliance method, this process is suitable primarily for cracks with linear crack front.

This has an important advantage in that this process provides crack propagation curves for the component investigated with which the accuracy of the stress intensity or correction function determined can be verified by re-checking the figures.

LT 2057

3.2.3 Photoelasticity and strain gauges

With the aid of equations (1-19) and (1-21) the stress intensity can be calculated by knowing the stresses or strains in the area of the crack tip. Stresses or strains can be determined experimentally by means of photoelasticity or with the aid of strain gauges.

In contrast to the above experimental methods, photoelasticity offers the possibility of dealing with cracks with curved fronts by 'stress freezing'[53-56].

In this method the crack is replaced by a notch with a finite radius. The difference from the fatigue crack is covered by appropriate correction factors.

The stress intensity is determined with the aid of the shear stresses. The shear stresses themselves are obtained from the isochromatics (= lines of constant principal stress differences) and the related fringe number.

$$K_I = \frac{r}{f(\theta)} \sqrt{2\pi r} \quad . \tag{3-15}$$

Since the K_I value cannot be determined in the immediate vicinity of the notch ($r = 0$), the K values must first be calculated at some distance from the notch. A good approximation value for K at $r = 0$ is obtained by extrapolation (see Fig 3.10).

Fundamentally any method of determining stress intensity can be used which enables stresses or strains to be measured near the crack tip.

For the strain gauge method[57-59] several strain gauges are glued in front of the crack tip and strains ε_x and ε_y measured. The stresses are yielded by the following equations:

$$\sigma_x = \frac{E}{1 - \nu^2} (\varepsilon_x + \nu\varepsilon_y) \ , \qquad \sigma_y = \frac{E}{1 - \nu^2} (\varepsilon_y + \nu\varepsilon_x) \ . \tag{3-16}$$

With these stresses the stress intensity can be determined in the same way as by the photoelastic method.

With this method care must be taken to ensure that the strain gauges lie outside the plastic zone of the crack tip.

4 INVESTIGATIONS KNOWN FROM THE LITERATURE FOR DETERMINING STRESS INTENSITY FOR CRACKS EMANATING FROM THE EDGE OF THE HOLE

In the most varied technical areas fatigue cracks in dynamically stressed structures have frequently proved to emanate from holes. According to an investigation of aircraft frames of the USAF[60], 30% of all fatigue cracks discovered occurred in holes loaded with pins or rivets. Causes of crack generation are usually the relatively high stress concentration, the generation of fretting corrosion in loaded holes and faulty production of the hole. Appropriate stress intensity solutions were therefore determined relatively early for holes affected by cracks, compared with other configurations of cracks of interest in practice.

LT 2057

This applies to the infinite plate as well as the finite plate with hole, solutions being available both for the loaded and unloaded hole.

The lug can be regarded as a special case of a cracked hole. This is due to the finite dimensions in width and head height and the introduction of force which occurs exclusively by means of a pin.

Since lug junctions in structures are frequently not redundant, the failure of this force transmitting element can cause failure of the entire structure. In aircraft, failure of a lug can even lead to a crash.

Although the lug in dynamically loaded structures to a certain extent represents an increased risk and is thus of particular interest for the application of fracture mechanics, there is so far no appropriate stress intensity solution in the known literature. Therefore it appears sensible to approach the more complex problem of the lug by starting from simpler similar crack configurations with known solutions. The effect of the hole, finite dimensions and loaded hole on the stress intensity will be illustrated step by step.

4.1 Infinite plate with unloaded hole

For the case of an unloaded hole with uni- and bilateral crack in an infinite plate Bowie[61] determined the stress intensity analytically by conformal mapping and using the Airy stress function:

$$K_I = \sigma\sqrt{\pi a}Y \quad . \tag{4-1}$$

The correction function Y contains the crack length ratio a/R as parameter. The crack emanating from the edge of the hole is designated a and the radius of the hole R (see Fig 4.2).

$$Y = f(a/R) \quad . \tag{4-2}$$

The correction function for the unilateral crack Y_1 and the bilateral crack Y_2 was indicated by Bowie in the form of tabular values (see Table 4.1).

The Bowie correction can be expressed by the following equations with an accuracy of ±2% (see Ref 63):

$$Y_1 = 0.707 - 0.18\lambda + 6.55\lambda^2 - 10.54\lambda^3 + 6.85\lambda^4 \tag{4-3}$$

$$Y_2 = 1.0 - 0.15\lambda + 3.46\lambda^2 - 4.47\lambda^3 + 3.52\lambda^4 \tag{4-4}$$

$$\lambda = \frac{1}{1 - \frac{a}{R}} \quad . \tag{4-5}$$

If Table 4.1 is studied it will be seen that close to the edge of the hole the correction function compared with that of a central crack of the same length is also greater in an infinite plate.

LT 2057

With a crack length ratio of

$$a/r \sim 2$$

the influence of the hole on the stress intensity can be ignored to a very great extent.

4.2 Infinite plate with hole and introduction of force by means of a pin

In most cases holes are loaded with rivet or screw connections. Grandt[64] developed a stress intensity solution for the 'loaded hole' and compared this with the Bowie solution for open holes.

In determining the stress intensity Grandt used an analytical process suggested by Rice[65] which is briefly described below.

4.2.1 Linear superposition

On the assumption that the stress intensity K_I and the crack opening displacement are known for a particular crack geometry and particular introduction of force, the stress intensity can be calculated for any required introduction of force, as demonstrated by Rice[65].

According to Rice the stress intensity for a given crack geometry under any load can be determined to the following formula:

$$K_I = \int_\Gamma s h d\Gamma + \int_A f h dA \qquad (4\text{-}6)$$

s is the stress vector which at the edge T here acts on the crack tip. f designates a force which occurs within the area bordered by Γ (see Fig 4.3). Vector h is a universal weight function for the given crack geometry and a load with known stress intensity. The weight function is given by

$$h = h(x,y,a) = \frac{H}{2K_I}\frac{\partial u}{\partial a} \quad . \qquad (4\text{-}7)$$

For the constant H

$$H = \begin{cases} E & \text{for the plane stress state} \\ E/(1-\nu^2) & \text{for the plane strain state.} \end{cases}$$

The modulus of elasticity is designated E and the Poisson ratio ν. K_I and u are the known stress intensity and the displacement field for a particular load configuration.

4.2.2 Establishing stress intensity with the aid of the weight function for the loaded hole

For the case of a loaded hole equation (4-6) can be simplified as follows. First the stress vector s is determined. In doing so the reaction stress $p(x)$ in the future crack plane is used instead of the force of the pin acting on the hole radius. The stress distribution $p(x)$ in the crack-free state can be calculated, for example, by the method of finite elements.

LI 2057

The stress vector obtained is then

$$S = \begin{cases} \left.\begin{aligned} S_x &= 0 \\ S_y &= p(x) \end{aligned}\right\} & \text{along the crack planes} \\ S_x = S_y = 0 & \text{along the hole circumference.} \end{cases}$$

.....(4-8)

Since no volume force occurs within the edge Γ , the pin force being replaced by the reaction stress $p(x)$,

$$f = 0 . \tag{4-9}$$

Since the displacement field u shows only one component in y direction due to uniaxial loading

$$U_y = \eta \tag{4-10}$$

is set down.

For the stress intensity of the loaded hole

$$K_I = \frac{H}{K_B} \int_0^a p(x) \frac{\partial \eta}{\partial a} dx \tag{4-11}$$

is obtained.

K_B is the stress intensity solution of Bowie for a unilateral crack in an unloaded hole.

η is the appropriate crack opening displacement. Since Bowie did not give data on the crack opening displacement, Grandt used an approximation[64]:

$$\eta = 4 \frac{K_B}{H} (\zeta/2\pi)^{\frac{1}{2}} \tag{4-12}$$

ζ is defined as

$$\zeta = a - x . \tag{4-13}$$

The approximation solution as equation (4-12) is only valid within the range

$$\zeta < a/10 . \tag{4-14}$$

The stress distribution $p(x)$ was calculated[67] for the loaded hole by the finite element method.

In Fig 4.4 the stress intensity is shown as a fun-tion of the crack length for the loaded and unloaded hole for two different fits. It will be seen that with increasing clearance between pin and hole the stress intensity also increases.

LT 2057

Fig 4.4 also shows that up to about a crack length ratio of $a/R \sim 1$ the stress intensity of the loaded hole is greater than that of the unloaded hole. With increasing crack length, on the other hand, the stress intensity of the loaded hole drops again below that of the unloaded hole.

In contrast to previous observations, the crack propagation direction was assumed under an angle of 81° based on the FE calculation, and not perpendicular to the loading direction (see Fig 4.4).

4.3 Plates with finite dimensions

The stress intensity solutions of Bowie for the unloaded hole and Grandt for the 'loaded hole' can only be used if the hole diameter and the crack are small compared with the dimensions of the plate.

If this is not the case, the plate edge must be allowed for in the stress intensity.

This applies to plates with loaded and unloaded holes.

4.3.1 Finite plate with unloaded hole

Newman[63] developed a stress intensity solution for a plate with finite width and open hole, using the so-called boundary value problem method.

The method is based on finding a stress function which the biharmonic equation (1-6) and the boundary conditions fulfil in a number of points along the edge of the component (see section 4.3.2.1). Thus the following expression of the stress intensity is obtained for the uni- or bilateral crack in an unloaded hole:

$$K_I = \sigma\sqrt{\pi a}\, Y_W Y_{b1} \sqrt{\sec \frac{2R\pi}{W}} \quad . \tag{4-15}$$

The correction function for the stress intensity allows with

$$Y_W = \sqrt{\sec \frac{\pi}{2} \frac{2R + a}{W - a}} \tag{4-16}$$

for the finite width W, with

$$Y_{b1} = f\left(\frac{a}{R}\right) \qquad \text{see equation (4-3)}$$

the effect of the hole according to Bowie and with $\sqrt{\sec (2R)/W}$ the ratio between hole diameter $2R$ and width W.

Index 1 in the correction function designates a unilateral and Index 2 a bilateral crack.

If the correction function of Bowie

$$Y_B = Y_{b1} \qquad \text{(see equation (4-3)}$$

is compared with that of Newman

LT 2057

$$Y_N = Y_W Y_{B1} \sqrt{\sec \frac{2R\pi}{W}}$$

it can be demonstrated with equations (4-15) and (4-3) that: $Y_N \geqslant Y_B$ applies over the entire crack length range.

The correction function and thus the stress intensity according to Newman becomes, compared with the Bowie solution, the greater, the greater the diameter $2R$ in relation to width W and the nearer the crack is to the edge of the plate.

Fig 4.6 shows for $2R = 20$ and $W = 100$ a comparison of the two correction functions.

4.3.2 Finite plate with introduction of force by means of a pin

The best known stress intensity solutions for finite plates with introduction of force by a pin were determined by Newman by the boundary value problem method[63] and by Broek by the superposition method[69]. The two methods will be described briefly below.

4.3.2.1 Boundary value problem method[68,70]

This is a numerical method which is used to determine the unknown coefficients in a stress function series. In Ref 68 an approximation developed by Muskhelishvili based on complex variables was used for the stress function series. With the aid of the stress function series the biharmonic function

$$\nabla^4 \psi = 0 \qquad (4\text{-}17)$$

in which equilibrium and compatibility conditions (see section 1.1) are combined can be presented analytically. Due to symmetry conditions uneven terms of the stress function series can be eliminated. The progression is limited to a certain number of terms. The coefficients are determined through the appropriate boundary conditions. The boundary conditions can be laid down in the form of stresses, forces or displacements.

4.3.2.2 Principle of superposition[69]

The basis of the principle of linear superposition is that the stress intensity solution for a certain crack model with a somewhat more complicated form of loading is built up from already known solutions for the same crack model but with a simpler form of loading.

Fig 4.7 shows this process with a finite plate with hole and introduction of force by means of a pin.

Thus one obtains for K_A

$$K_A = K_B + K_D - K_E \quad . \qquad (4\text{-}18)$$

Since $K_A = K_E$

$$K_A = \frac{K_B + K_D}{2} \quad . \qquad (4\text{-}19)$$

LT 2057

For K_B the Bowie solution (see equations (4-3) and (4-4) can be used and for K_D the known solution

$$K_D = \frac{P}{\sqrt{\pi a}} \quad . \tag{4-20}$$

The boundary effect is allowed for by a width correction $Y(a_{eff}/W)$. Thus the correction function for the loaded hole has the following form

$$\frac{K_A}{\sigma\sqrt{\pi a_{eff}}} = \left[\frac{1}{2}Y_B\left(\frac{a_{eff}}{2R}\right) + \frac{W}{2\pi a_{eff}}\right] Y\left(\frac{a_{eff}}{W}\right) \quad . \tag{4-21}$$

The effective crack length a_{eff} is defined in Fig 4.8.

4.3.3 Comparison of correction function for the finite plate with hole, with and without introduction of force

The correction function Y of Newman and of Broek was determined for the unilateral crack from a hole in a finite plate with force introduction via a pin. Fig 4.9 shows that Broek's correction function yields higher values for Y over almost the entire crack length range than Newman's solution. The same tendency was seen in the unloaded hole (see Fig 4.6).

For purposes of comparison the correction function was given for the bilateral crack according to Cartwright[71] for a loaded hole. Cartwright determined the correction function by the Compliance method described in section 3.2.1. For short crack lengths Cartwright's correction function agrees well with that of Broek. Only at greater crack lengths the loss of supporting effect in the case of a bilateral crack appears to make itself felt by a smaller drop in the correction function.

Fig 4.9 also shows the correction function for a unilateral crack from an unloaded hole in a finite plate.

Up to a crack length ratio of ~0.5 this correction function is distinctly below that of a loaded hole. A reversal takes place only when the cracks are longer. This was also observed in the infinite plate with loaded and unloaded hole (see Fig 4.4).

Irrespective of the plate edge the following can therefore be stated as generally applicable: the correction function Y or stress intensity K_I for the loaded hole is greater than for the unloaded hole in the area of short crack lengths. A reversal takes place for longer crack lengths.

4.4 Lug

Investigations on the lug which have only recently appeared in the literature have been undertaken by L.F. Impellizerri and D.L. Rich[72] and A.F. Liu and H.P. Kan[73].

4.4.1 Investigation by Impellizerri and Rich

The aim of the investigation was to carry out flight-by-flight crack propagation tests on a lug with unilateral crack and then subject the test result to a mathematical check.

LT 2057

It was necessary for this purpose to determine the stress intensity specifically for the lug used in the crack propagation test. The method described in section 4.2.1 was used for the purpose.

The function derived by Bueckner for the lateral crack was used as the weight function (see section 3.2.1).

The stress distribution was determined by the method of finite elements (see Fig 4.10).

Data on the idealisation of the introduction of force in the FE calculation are unfortunately not given. As shown later, however, the pattern of stress and thus also the stress intensity depend on just this. Fig 4.11 shows the pattern of the stress intensity or correction function and the dimensions of the lug.

The correction function includes the correction factor of 1.13 derived by Bueckner for edge cracks. The correction factor is intended to allow for the load-free surface from which the crack emanates. A similar factor has already been quoted for edge cracks by Brown and Srawley[28] at (1-12).

The correction function for lugs Y_A would therefore assume the value $Y_A \to 1.13$ for $a \to 0$ if the stress intensity were based on the stress σ_{max} occurring at the edge of the hole.

4.4.2 Investigation of Liu and Kan

On the principle of linear superposition (see section 4.3.2.2) Liu and Kan first determined the correction function Y_A for uni- and bilateral cracks, varying internal diameter in relation to lug width.

Next the correction function was in addition calculated for a lug with R/W = 0.125 by the finite element method.

Fig 4.13 shows the idealisation of the lug for the finite element calculation.

With the aid of the stress intensity determined by the superposition method crack propagation was calculated for various lugs under constant amplitude load sequence and compared with the test results.

When the results presented in Fig 4.12 are regarded two facts are noted. For one thing the value for the correction function Y_A for $a \to 0$ is considerably higher than that determined by Impellizzeri and Rich.

$$a \to 0 \begin{cases} Y_A = 5 & \text{according to Impellizzeri and Rich} \\ Y_A \sim 8 \to 14 & \text{according to Liu and Kan.} \end{cases}$$

The investigations by Cartwright[71] and Grandt[64] already mentioned make the value determined by Impellizzeri and Rich appear more realistic.

The reason for the values determined by Liu and Kan for $Y_A \sim 8 \to 14$ is probably the too simple approximation process, namely linear superposition. The complexity of the lug seems to be only partially covered by the method of linear superposition already used by Broek[69].

LT 2057

It is probably also due to the approximation method that there is no difference worth mentioning between uni- and bilateral cracks in regard to Y_A. This is contradicted by results by Bowie (see Table 4.1) as also Broek and Cartwright (see Fig 4.9). It is, however, presupposed that the difference between uni- and bilateral cracks in regard to stress intensity is mainly transferable to the lug from infinite plates and strips. In view of the loss of supporting effect consequent on bi-lateral cracking, a distinct difference ought to occur with increasing crack length between uni- and bilateral cracks particularly in the lug.

The results of Liu and Kan show furthermore that for the unilateral as for the bilateral crack the correction function Y_A

$$Y_A \to \infty \quad \text{for} \quad a \to \frac{W - 2R}{2}$$

applies.

Crack propagation tests on lugs[74] have shown at suitably low stress that in a unilateral crack, crack propagation runs steadily through one cheek of the lug whereas the opposite undamaged cheek takes over more and more load until it finally bears the full load. This leads to the conclusion that for a lateral crack the correction function Y_A in the border line case

$$a = \frac{W - 2R}{2}$$

reaches a finite value.

What is surprising about the results of Liu and Kan is that for a lug with $R/W = 0.125$ checking by the method of finite elements agrees fairly well with the result of the superposition method. This would appear to be purely coincidental since the methods used here are fundamentally different approximation solutions.

If one assumes that by using a crack element the stress intensity can be achieved with 1-2% accuracy, then greater deviations can be attributed largely to idealisation of the introduction of force[82].

To determine the stress intensity Liu and Kan assumed introduction of force in the form of

$$p = 2P \cos(\theta/\pi rt) \quad . \tag{4-22}$$

In addition a concentrated point loading introduction of force as well as one of the form of

$$p = 3P \cos^2(\theta/4rt) \tag{4-23}$$

was investigated.

These three distributions are shown in Fig 4.14.

LT 2057

How precisely the stress intensity was determined is shown finally in a comparison carried out by Liu and Kan between crack propagation test and calculation.

The crack propagation characteristics used for the mathematical check were determined with compact tensile specimens (see Fig 8.?).

To allow for the material scatter occurring, crack propagation for the lugs was calculated with the crack propagation characteristics for the upper and lower limit of the scatter band.

As Fig 4.15 shows, the results of crack propagation tests on the lug lie between the upper and lower limit of the crack propagation curves determined mathematically.

The difference between the crack propagation calculation with crack propagation characteristics on the safe and unsafe side can deviate by 3-5 fold from the test result. These are erratic values which completely contradict experience hitherto with constant amplitude crack propagation tests. Deviations of the order of approximately 10-20%, on the other hand, would be realistic. This assumes, however, that the specimens used for determination of the crack propagation characteristics are taken from one batch and the tests performed under the same conditions.

5 SUMMARY OF INVESTIGATIONS DRAWN FROM THE LITERATURE

A table of the crack models examined and methods used to determine the stress intensity is contained in Fig 5.1.

If the most important results of the investigations carried out in Chapter 4 are summarised purely qualitatively, the following effects can be identified in regard to stress intensity and correction function for the different forms of plates with holes.

The ratio between length of crack and radius of hole is of decisive importance for the correction function. The greater the hole radius, the greater is the crack length range in which due to the hole the correction function is increased compared with a crack of the same length in a plate. In the immediate vicinity of the edge of the hole, for instance, the correction function for an unloaded hole with unilateral crack in an infinite plate is for

$$a = 0 \; ; \quad Y(a/R) = 3.39 \qquad \text{(see Table 4.1).}$$

With increasing distance of the crack tip from the edge of the hole the effect of the hole on the correction function also decreases. If the length of the crack amounts to once to twice the hole radius the effect of the hole is removed to a great extent.

If the hole is loaded with a pin this produces an additional increase in the stress intensity or correction function for a crack in the immediate vicinity of the edge of the hole. With increasing crack length, however, the correction function is again progressively reduced (see Fig 4.4).

According to Grandt[64] the fit between pin and hole is also said to have an effect on the stress intensity. According to this greater clearance between pin and hole would also produce higher stress intensity (see Fig 4.4). This may certainly be of importance

for relatively small cracks. For longer cracks, however, it may be assumed that the type of fit is of secondary importance. The overestimation of the effect of fit by Grandt is chiefly attributable to the inadequacy of the method used by him to determine the stress intensity. In the method described in section 4.2.2 the essential quantity used is the stress distribution in a crack-free state which largely depends on the fit.

A further effect on stress intensity arises from the finite size of the plate, *ie* from the edge of the plate. As the crack tip approaches the edge of the plate the stress intensity increases again (see Fig 4.6).

According to the investigations available in the literature[72,73] the hole diameter and lug width are to be regarded as essential influencing parameters in the lug. The head height of the lug has not been taken into account as a parameter in any investigation.

Aside from the preceding purely qualitative description of the stress intensity or correction function with different influencing factors, it seems possible, irrespective of the shape and loading of the plate with hole (see Fig 5.1), to state in a simple manner quantitative values for the correction function at the edge of the hole.

If the investigation of Bowie for the infinite plate with hole (see section 4.1) and of Impellizzeri for the lug (see section 4.4.1) are considered again the following values are yielded for the correction functions:

Plate with hole:	$Y(a = 0)$	= 3.39	according to Bowie[61]
Lug:	$Y(a = 0)$	= 5.65	according to Impellizzeri[72].

Furthermore if the stress at the edge of the hole is considered the result at a nominal stress of $\sigma_N = 1$ is for

Plate with hole:	σ_{max}	= 3.0	according to Petersen[75] and
		3.06	according to Neuber[76]
Lug:	σ_{max}	= 5.0	according to Impellizzeri[72].

For the lug the stress is related to the gross cross-section.

The ratio between correction function and stress yields in both cases, *ie* for the plate with hole and for the lug, a factor of 1.13.

For plates with edge or surface crack this factor is intended to take into account that the edge from which the crack emanates is load-free, *ie* no force occurs parallel to the crack.

On the other hand, in an infinite plate with central crack stresses occur parallel to the crack planes which suppress the opening of the crack to a minor extent. The stress intensity for the infinite plate with central crack is laid down by

$$K_I = \sigma\sqrt{\pi a} \quad . \tag{5-1}$$

If the centrally cracked plate is halved by sectioning perpendicular to the crack plane the result is two plates with lateral cracks while the cut edges are load-free. The stress intensity here is

$$K_I = Y\sigma\sqrt{\pi a} \quad . \tag{5-2}$$

For Y values are quoted between 1.12 and 1.13. Neuber[76] for instance determined a value of 1.1215 for Y for the half plate with crack at the free edge. Since the Airy stress function was determined here by progressive development Y should be regarded as an approximation value which depends to a certain extent on the number of terms used. Bueckner[77] quotes this value as 1.13.

If the nominal stress σ_N is used, which can be related to either the gross or net cross-section, to describe the stress intensity (see equation (5-1)), the correction function for the plate with hole and for the lug as Refs 61 and 72 works out as follows:

$$Y(a = 0) = \alpha_K \cdot 1.13 \quad \text{or} \quad 1.12 \tag{5-3}$$

$$\alpha_K = \frac{\sigma_{max}}{\sigma_N} \tag{5-4}$$

σ_{max} designates the stress at the edge of the hole. The validity of this result was proved theoretically by Neuber.

Neuber showed in Ref 76 for the crack from a notch through a boundary value analysis $a \to 0$ that the factor for stress concentration results from the multiplication of the factors corresponding to the macro amd micro notch. For short cracks

$$\alpha_K = \alpha_0 \alpha_R$$

is valid.

Neuber terms the factor for the stress concentration of the macro notch α_0 and the micro notch (= crack) $\alpha_R \alpha_K$ is equivalent to the correction function Y for a short crack.

Thus a precise value can be stated for the correction function of the lug at the edge of the hole.

This result will be adopted in the later determination of the stress intensity for the various lugs.

6 DEFINITION OF PROBLEM

As already mentioned in the introduction, lugs are essential components of an airframe for which proof of damage tolerance has to be undertaken.

Since the literature does not contain the stress intensity solution for lugs which is required for proof of damage tolerance, the problems posed in the following investigation are:

- selection of a suitable method of determining the stress intensity;
- determination of the stress intensity as a function of the crack length for various forms of lug;
- showing the effect of essential lug parameters on stress intensity;

LT 2057

- setting up a complete formula for calculation of the stress intensity for the lug, allowing for essential parameters;
- checking and evaluating the equation.

Starting point in laying down the types of lug to be investigated are the diemsions of lugs in use in aircraft construction.

If the lug form is specified in a simplified manner by the following parameters

radius of hole R
width of lug W
height of head H and
thickness t

typical lug values result as shown in Table 6.1.

The lug dimensions are defined in Fig 6.1. The cheek width b frequently used later is calculated from

$$b = \frac{W - 2R}{2} \quad . \qquad (6\text{-}1)$$

The geometry of the lugs to be examined is to be laid down in such a manner that on the one hand the typical lug dimensions in Table 6.1 are given predominant consideration and, on the other hand, systematic investigation of the individual parameters in regard to their effect on scress intensity is possible.

It therefore appears logical to stipulate a lug with median dimensions and median geometric relations by means of the values quoted in Table 6.1. For the lug termed 'standard' below the following mean values result

$$\text{Standard lug:} \begin{cases} 2R = 40 \text{ mm} \\ 2R/W = 0.48 \\ 2R/H = 0.9 \\ t = 15 \text{ mm.} \end{cases}$$

In setting down the lug parameters to be examined one cannot rely exclusively on the few investigations quoted in the literature[72,73]. In these tests only the ratio between hole radius and lug width was regarded as essential parameter. In contrast, the numerous fatigue strength tests with lugs[4-8] show that in addition to parameter 2R/W the ratio of 2R/H and the absolute lug size are also significant for crack life.

In a comprehensive lug investigation therefore at least the two parameters 2R/W and 2R/H should be considered. Further influencing parameters such as fit, direction of introduction of force, etc, are not dealt with in this paper. This is reserved for a future investigation which can be based on the results of this paper.

As far as the effect of size is concerned, it may be assumed that with a specific lug geometry at the same nominal stress and the same length of crack the speed of crack propagation and thus also the stress intensity will increase as the size of the lug

LI 2057

increases. The correction function which very probably contains the dimensionless crack length

$$Y = f(a/b) \quad \text{(with } b \text{ as cheek width)}$$

as free parameter, however, ought to be independent of the lug size. This is shown for instance in the crack model "plate strip with cracked hole" (see equation 4-15)). In order to demonstrate this on the lug too the effect of size will also be taken into account in the investigation.

If, as intended in this investigation, the lug is regarded as a plane problem the lug thickness t is not important. It has also been shown in fatigue strength tests[7] that within a technically reasonable range the thickness of the lug has no effect on life.

Table 6.2 lays down values for the parameters $2R/W$, $2R/H$ and the effect of size expressed by $2R$ to be examined.

7 INVESTIGATION TO DETERMINE THE STRESS INTENSITY FOR LUGS OF VARYING GEOMETRY

7.1 Selection of a suitable method

Section 3 presented the various methods which can be used to determine the stress intensity K. However, very few are suitable for application to the lug. Due to the complicated boundary conditions the analytical methods are eliminated from the start. In contrast, the method of finite elements has proved versatile in its use for a variety of crack problems. The results which can be achieved with the use of this numerical method depend decisively on how well the structure or component and the introduction of force can be idealised. Idealising the lug geometry in itself presents no problems. But when the introduction of force and its effect on stress distribution and stress intensity is regarded, modelling can only take place by matching to a known stress distribution. This means that the stress distribution for a lug without crack would first have to be known. For this case the selection of force introduction in the FE calculation would have to be such as to achieve the best possible agreement with the known stress distribution. Next the stress intensity for the cracked lug can be determined. If one wanted to testify on the accuracy of the stress intensity determined by the finite element method, this would have to be done by a comparison between crack propagation test and calculation. For these reasons the finite element method will not be used for the systematic examination of the lug. It should, however, be mentioned here that further work with the finite element method - partial results are already available (see Ref 82) - is being carried out especially for the lug and other typical aircraft components. The most important results of these investigations will be mentioned insofar as they are of interest here.

Finally there is nothing left but experimental methods to determine the stress intensity for the lug.

LT 2057

Of the various experimental methods like

crack propagation
compliance
strain gauges
photoelasticity

the first two methods are particularly of interest. While the strain gauge method could lead to unacceptable integration errors because of the small component dimensions and the relatively wide strain gauges, photoelasticity has the disadvantage of not providing particularly accurate absolute values[80]. A further drawback of the last two methods is that the stress measurements on the cracked component can be falsified because of yielding in the area of the crack tip.

Which of the last two methods, namely the compliance method described in section 3.2.1 or the crack propagation method described in section 3.2.2, should be used for the lug was decided on the basis of preliminary tests in favour of the crack propagation method. The two methods were compared in a preliminary programme from the point of view of scatter of test results and cost of tests. In compliance measurement the difficulty arose that after each crack expansion under constant amplitude load the path measurement equipment had to be readjusted This produced deviations with the compliance method which were of the order of the change in stiffness to be expected. This was particularly evident in the area of short cracks. The technical problems could most probably have been eliminated by appropriate technical effort. But this would appreciably increase the experimental costs which were almost twice as high for the compliance method as for the crack propagation method.

The essential advantage of the crack propagation method can be recognised particularly from an engineering point of view.

Although the stress intensity can be determined by different methods, there remains with all of them, insofar as they are approximation methods, the uncertainty in regard to the accuracy of the stress intensity solution. Proof can only be provided by additional tests.

This proof is superfluous if the stress intensity is derived from crack propagation test results. This method also offers the advantage, particularly in the case of the lug, that the introduction of force does not have to be idealised as in many other methods. This removes a not inconsiderable source of error.

Another reason favouring the crack propagation method is that a considerable measure of experience is already available for the performance and evaluation of crack propagation tests from which this investigation can benefit.

Thus the technical risk can be reduced and the quality of the test results improved.

The reliability of this method has also been demonstrated in an investigation carried out by Huth[78] to determine the stress intensity in bending stressed notches.

LI 7057

7.2 Specimen and test set-up

7.2.1 Dimensions of lugs

In the following investigation the stress intensity is to be determined for seven different types of lug by crack propagation tests. The lugs will be marked 1 to 7. The lug geometry is laid down in Fig 7.1 by the hole radius R, width W and head height H.

In addition the thickness is designated t and the total length of the lug L. The cheek width b which is used below as reference quantity is given by $b = (W - 2R)/2$.

The dimensions of the lugs are shown in Table 7.1.

The crack length, emanating from the edge of the hole, is termed a and the distance from the edge of the hole in the crack-free component x.

Figs 7.2 to 7.4 show the way in which the standard lug No.2 is varied. Fig 7.2 shows the different lug size with the same geometric relations (represented by lugs 1, 2 and 3).

The variation of cheek width with the same hole diameter and the same head height is shown in Fig 7.3, with lugs 4, 2 and 5. The radius for the curvature of the lug head is constant. This applies also to the variation of head height which can be seen in Fig 7.4 with lugs 6, 2 and 7.

7.2.2 Material

Aluminium alloy 7075 T7351 from Messrs. Cegedur was used for the lugs. A 90mm thick plate was available as semi-finished material. The lugs were taken from the plate in grain direction.

The strength and chemical composition of the aluminium alloy is shown in Tables 7.2 and 7.3. While the nominal values were taken from the material specification sheet, the actual values come from workshop tests at MMB, CIVILE No.9337.

For the chemical composition the actual value must lie within the nominal value range. For strength the nominal values are always minimum requirements which must be reached or exceeded by the actual values.

7.2.3 Test set-up

7.2.3.1 Hydropulse equipment

A hydropulse equipment from Messrs. Schenck is used to perform the crack propagation tests.

Fig 7.5 shows a schematic presentation of the entire equipment with input, control and recording units.

The test set-up consists of a base plate, two vertical columns and a traverse. The hydropulse longitudinal cylinder is incorporated in the base plate, as Fig 7.5 shows. The specimen clamp is placed between cylinder and traverse and is mounted flexibly.

LT 2057

The test equipment incorporates an inductive displacement transducer on the cylinder and a dynamometer beneath the traverse to pick up the test values. Additional test value receivers can be fitted to the test object.

The test signals are amplified in (4) and fed to the recorder and the controller (6). There is a monitor socket (3) between test value pick-up and amplifier (4). The controller (6) has the task of comparing test value and nominal value and making adjustments through the servo valves. The control signal is amplified in (7).

The nominal value input leads via the monitor socket (3) to the set point adjuster which is connected to the generator (1). The generator produces periodic sines, triangular and rectangular functions. The static nominal value is preset by a precision potentiometer in the set value transmitter (2) and controlled by the digital display (5). The set value is passed to the controller (6).

With regard to amplitude deviation ΔA the manufacturer quotes the following value:

$$\Delta A < 2\% \quad \text{up to} \quad f_g \sim 30 \text{ Hz} .$$

ΔA is the percentage deviation of the actual value from the set value. The full amplitude deviation is only reached at a limiting frequency of $f_g \sim 30$ Hz. Since the test is performed at a considerably lower frequency the deviation will lie far below 2%.

7.2.3.2 Installation of specimen in machine

Fig 7.6 shows the installation arrangement for the lug. The end of the lug opposite to the hole is fixed between two clamping plates. The introduction of force into the hole of the lug takes place via a steel pin with transition fit H7j6. The steel pin is lodged on both sides in extremely thick steel shackles which are connected flexibly with the traverse. As Fig 7.6 shows, both steel shackles have observation slits for crack propagation measurement. Since this entails a considerable reduction in cross section and steel shackles had to be made thick enough for the hole to take the lug pin not to penetrate the shackles completely.

Although it was intended to examine crack propagation in one direction only, observation slits had to be fitted on the right and left of the pin and in both shackles for reasons of symmetry.

7.3 Test procedure and test results

7.3.1 Test procedure

For the crack propagation test a crack starter notch (see Fig 7.7) is produced by spark erosion at the edge of the hole of the lug.

In preliminary tests with various types of crack starter notch the so-called 'V notch' proved particularly suitable in regard to the generation of a fatigue crack with the straightest linear crack front.

A similar type of crack starter notch but with an acute angle is already used as a chevron notch in the compact tensile test. The shallow angle for the lug (see Fig 7.7)

LI 2057

has the advantage that crack propagation measurement can be started at relatively short crack lengths.

Generation of a fatigue crack with approximately straight crack front offers following advantages for determination of the stress intensity from crack propagation measurements:

- The crack size can be defined by a single parameter, *i.e.* the crack length a (see Fig 7.1), in contrast to the semi-elliptical crack.
- The material characteristic $da/dN = (\Delta K_I)$ required to determine the stress intensity is established with standard specimens (central crack specimen, compact tensile specimen) in which an approximately straight crack front occurs. This enables logical transfer of crack propagation characteristics.

In order to be able to measure crack propagation as precisely as possible the lug was provided with a scale along the crack plane. Using a microscope, crack growth could be read off to an accuracy of 0.1 mm.

Crack propagation took place under constant amplitude sinusoidal loading (see Fig 7.8).

For all lugs the stress was $\sigma_0 = 98.1\ N/mm^2$, the stress σ being related to the nett cross section.

$$\sigma_N = \frac{P}{(W - 2R)t} \tag{7-1}$$

where P indicates the force transmitted by the pin.

The stress ratio selected was $R = 0.1$.

$$R = \frac{\sigma_u}{\sigma_0} . \tag{7-2}$$

The test frequency was 10 Hz.

Measurement of crack propagation started at an initial crack length of $a = 2.5$ mm.

7.3.2 Tes sults

Three crack propagation tests were carried out for each lug. An exception was lug No.1 for which an additional test was carried out because of somewhat greater scatter. The test results for the seven different lugs are shown in Figs 7.9 to 7.15. The number of load cycles to fracture, the appropriate mean value and the standard deviation are also contained in the relevant figures. The small scatter for crack propagation tests is due *inter alia* to the fact that the specimens were taken from one batch of material. A mean curve was plotted through the scatter band of the test values for a lug.

The mean crack propagation curves of lugs 1, 2 and 3(= effect of size) are shown in Fig 7.16. It will be seen that with the scale enlargement of the lug the critical crack length is also increased. The number of load cycles to fracture, on the other hand,

LT 2057

is not affected. This means that the speed of crack propagation also rises with increasing lug size. Fig 7.17 shows the mean crack propagation curves for lugs 4, 2 and 5 (effect of cheek width). It can be seen that with increasing cheek width the critical crack length increases but the number of load cycles to fracture declines. The mean crack propagation curves for lugs 6, 2 and 7 can be seen in Fig 7.18. The increase in head height produces an increase in crack propagation life while the critical crack length remains the same.

7.4 Discussion of test results with reference to the stress distribution in the crack-free lug

To determine the stress intensity for an infinite plate with cracked hole and introduction of force by means of a pin Grandt[64] used the method of linear superposition developed by Rice (see section 4.2.1). If for a crack model with a specific introduction of force the stress intensity and the crack opening displacement as a function of the crack length $V = f(a)$ and for the same model but with changed introduction of force the stress distribution are known in the crack-free model, the stress intensity for the new introduction of force can be calculated analytically by the method of linear superposition. An enquiry into this method in regard to its application was carried out (see Ref 79).

It is essential for this method that the stress distribution in a crack-free state be used in determining the crack intensity. Furthermore Neuber proved that for very small cracks the stress of the macro notch enters directly into the correction function Y (see section 5). It must therefore be assumed that the stress in the immediate vicinity of the crack-free notch has a vital effect on the stress intensity and thus on crack propagation.

In Ref 80 stress measurements were made on lugs on which the present crack propagation tests were later carried out. Photoelasticity and strain gauges were used as methods to determine the stress distribution in the fatigue critical lug cross section. The object of this stress determination was to develop a suitable force introduction model for subsequent examination of the cracked lug with the aid of the method of finite elements (see Ref 82). The stress measurements determined (see Ref 80) for the seven different lugs are shown in Figs 7.19 and 7.21.

If these results are compared with the crack propagation measurements the following relationships may be observed.

Lugs 1, 2 and 3 in Fig 7.19 (= effect of size) as expected show the same stress distribution if the dimensionless stress σ/σ_N with $\sigma_N/P(W - D)t$ is plotted over the also dimensionless quantity x/b (= distance from edge of hole). It can be seen from Fig 7.16 that the three different sized lugs exhibit the same crack propagation life. The increase in critical crack length connected with the size of lug is probably due to the fact that in larger lugs the boundary effect - generally leads to enhanced increase in stress intensity - only makes itself felt at longer crack lengths.

Fig 7.20 shows the stress curve for lugs 4, 2 and 5. It is noted that the stress in the notch area increases considerably with increasing cheek width b . As can be seen from Fig 7.17, crack propagation life declines with increasing cheek width and thus increasing boundary stress. The enlargement of the critical crack length connected with the increase in cheek width is probably also attributable to the boundary effect which only makes itself felt at longer crack lengths.

Fig 7.21 shows that the stress at the edge of the hole is reduced with increasing head height. Comparison with Fig 7.18 shows that here too an increase in stress in the immediate notch area produces a drop in the crack propagation life. Since the cheek width was not changed in this case, lugs 7, 2 and 6 yielded the same critical crack length.

Comparison between crack propagation life and stress in the crack-free area near the notch has shown that the crack propagation life is essentially dependent on the stress. Since stresses in the form of stress concentration factors are already available in the literature[75,81] for most notches, at least qualitative statements can be made with regard to the crack propagation life to be expected if the shape of the notch is changed.

8 EVALUATION OF THE TEST RESULTS TO DETERMINE STRESS INTENSITY

8.1 Premises for the transfer of crack propagation characteristics from specimens to structural components

Determination of the stress intensity K_I and its dimensionless quantity Y takes place in principle by the method described in section 3.2.2.

This method is based on the fact that the crack propagation rate is a function of the stress intensity range

$$da/dN = f(\Delta K_I) .$$

How a particular value of K_I is composed, *ie* which contribution is made by the individual terms such as stress σ , crack length a or correction function Y , is immaterial provided certain conditions are followed:

$$\Delta K_I = \Delta\sigma\sqrt{\pi a}Y .$$

Transfer of crack propagation characteristic determined on specimens with known stress intensity solution

$$da/dN = f(\Delta K_I)$$

to components is permissible if in determining crack propagation for the specimen and for the component conformity exists in the following points:

- Material
  Batch, direction of specimen extraction, thickness of specimen.
- Environment
  Environment medium, temperature, humidity.

LT 2057

- Loading
  Frequency, form of load sequence, stress ratio R .
- Type of crack
  Formation of crack front, type of crack opening.

8.2 Determination of crack propagation characteristics

To determine the crack propagation characteristic which is frequently represented in a diagram by da/dN over ΔK_I , constant amplitude crack propagation tests are performed with specimens with known stress intensity solution. As a rule central crack, compact tensile or bending specimens are used for this purpose. A central crack specimen with dimensions 400 × 160 mm for thickness t = 8 and 15 mm is used here for the crack propagation tests. For a material thickness of t = 20 mm the compact tensile specimen is used. The compact tensile specimen has the advantage here that low loads are required to generate crack propagation in relatively thick specimens.

Figs 8.1 and 8.2 show the two specimens with relevant stress intensity solution.

In order to ensure the transferability of the crack propagation characteristic to be determined to lugs, the following conditions were maintained in regard to the specimens and the performance of the test.

- Material
  AL 7075T7351 same batch as for lugs. Specimen extraction in L-T direction (= longitudinal side of specimen in direction of grain), specimen thickness t = 8 and 15 mm for central crack specimen and t = 20 mm for compact tensile specimen.
- Environment
  Normal laboratory conditions.
- Loading
  Frequency of 10 Hz, sine-shaped load sequence, stress ratio R = 0.1.
- Type of crack
  Crack front approximately straight, type of crack opening I .

The test set-up described in section 7.2.3, was used for performance of the test but with suitable specimen clamping device. Crack propagation measurement was visual with the aid of a microscope. The test results are shown in Figs 8.3 and 8.4.

The test results show that scatter of the crack propagation curves - for the central crack specimens three were carried out for each specimen thickness and for the compact tensile specimen two tests only - is relatively small.

A direct comparison between the crack propagation measurements on compact tensile specimens and central crack specimens is not possible since the two types differ widely in regard to stress intensity. Comparison between the crack propagation measurements on central crack specimens shows, however, that crack propagation life for the 8mm specimen is about 20% longer than that for the 15mm specimen. Various tests have shown that

LF 7057

with increasing material thickness the speed of crack propagation also increases and crack propagation life declines.

The effect of material thickness on the speed of crack propagation, however, is shown in increased measure in the area of the plane stress state[42]. Since the material thicknesses investigated here can already be classified in the transition area to a plane strain state, the speed of crack propagation is likely to increase only slightly with increasing specimen thickness. This is confirmed if the crack propagation rate is plotted against the stress intensity range (see Fig 8.5).

In principle the crack propagation characteristic can be obtained by determining the slope

$$m = \Delta a/\Delta N$$

for a median crack propagation curve at various crack lengths and the appropriate stress intensity range ΔK_I. The quantities required, namely the range of stress $\Delta\sigma$, crack length a and correction function $Y = f(a/W)$ are known.

Evaluation of the crack propagation curves becomes simpler and more accurate if a suitable, constantly differentiable function is laid through the measuring points (= regression analysis). The Forman equation has proved a most suitable regression function. A programme was developed in Ref 33 enabling the Forman equation to be matched to crack propagation curves determined with specimens with known stress intensity solution. The free parameters in the Forman equation, i.e. C_F and n_F (see equation 2.11) are selected so that the least squares of the divergence between test values and analytic function show a minimum. This programme has meanwhile been included in the Handbook for Structural Calculation (HSB) of the German aircraft industry as a generally recognised method.

The crack propagation characteristic for the three different material thicknesses determined with this programme shows that at a certain stress intensity the crack propagation rate increases only slightly with the specimen thickness. Major deviations do not occur until immediately prior to reaching the critical crack length. Fig 8.5 also includes the Forman characteristics for the relevant material thickness. Here it should be noted that the Forman characteristics C_F, n_F and K_c differ considerably from each other in part. If specimens of different thickness exhibit almost the same crack propagation behaviour over a relatively wide range one would expect this to apply to the consistency of the individual characteristics. However, it has to be remembered that C_F, n_F and K_c are dependent on one another. But if the K_c value depends on the material thickness, the C_F and n_F values must change to the effect that in a certain ΔK_I range the Forman equation nevertheless leads to similar crack propagation behaviour.

8.3 Determination of the crack propagation rate for lugs by means of their crack propagation curves

Before the stress intensity K_I or its dimensionless quantity Y can be assigned to lugs through the material characteristic $da/dN = f(\Delta K_I)$ (see Fig 8.5) it

LF 2057

is necessary to determine the crack propagation rate da/dN as a function of the crack length a or a/b for the lug crack propagation curves (see Figs 7.16 to 7.18).

This means that the slope of the crack propagation curves must be determined at different crack lengths.

In order to be able to determine the slope as accurately as possible, the mean crack propagation curves (see Figs 7.16 to 7.18) of the seven lugs are approximated by constant differentiable functions. Crack length a is presented as a function of the load cycle N for the purpose.

The Forman equation, used in section 8.2 for approximation of the crack propagation curves of the central crack and compact tensile specimen, unfortunately cannot be used here since the stress intensity which would be needed is not yet known for lugs and still has to be determined. An attempt is therefore made to approximate the lug crack propagation curves by polynomial formulae. In doing so it has been found that the crack propagation curves can be approximated according to curve piece by piece by two or three polynomials of the second order:

$$a = q_1 + q_2 N + q_3 N^2 \tag{8-1}$$

q_{1-3} being the coefficients to be determined. Since for evaluation the mean lug crack propagation curves are already used, determination of the coefficients q_i was carried out not by 'least squares' (regression analysis) but by introducing three pairs of values (a_i, N_i). This produces three equations with three unknowns. To solve the equations pocket calculator HP-67 was used with a suitable standard programme. This programme handles the equation system in the form of a vector matrix multiplication

$$\bar{a} = |M| \times \bar{q} \quad . \tag{8-2}$$

The programme first forms the inverse of the matrix $|M| \rightarrow |M|^{-1}$ and with it multiplies equation (8-2)

$$|M|^{-1}\bar{a} = \bar{q} \quad . \tag{8-3}$$

Equation (8-3) thus solves equation (8-2) by the unknown coefficients q_i .

Coefficients q_1, q_2 and q_3 for the individual crack propagation ranges are shown in Table 8.1 for the various lug crack propagation curves.

The crack propagation rate is obtained by differentiating equation (8-1)

$$da/dN = q_2 + 2q_3 N \quad . \tag{8-4}$$

Since the polynomials do not exhibit equally good conformity with the crack propagation curve over the entire sub-range of the crack propagation curve, $da/dN = f(a)$ is determined only for those crack lengths or load cycles for which the polynomial

LI 4057

reproduces the crack propagation curve as accurately as possible. The crack propagation rates thus established are shown in Figs 8.6 to 8.8 for the various lugs.

Although the crack propagation rates are not proportional to the stress intensity - the relationship between da/dN and ΔK_I or K_I appears linear only with double logarithmic plotting - some indications can already be gleaned on the future course of the stress intensity. All curves have an initially steep rise shortly after the start of crack propagation in common which in all tests originated at an initial crack length of $a_0 = 2.5$ mm. The crack propagation rate was presumed as $da/dN = 0$ at the initial crack length a_0.

Since the crack length is relative to cheek width b which differs for the various lugs (see Table 6.2), the points at $da/dN = 0$ also diverge partially.

The slope of the curves declines in the median crack length range. An increased slope is then noted in the case of longer cracks.

As Figs 8.6 to 8.8 show, the crack propagation rate depends to a very large extent on all the influencing factors examined, i.e. on the absolute lug size, the cheek width $2R/W$ and the head height $2R/H$.

The effect of size, seen in Fig 8.6, causes the crack propagation rate to increase with lug size at the same crack length ratio a/b. However the variation in cheek width expressed as $2R/W$ has a considerable effect on the crack propagation rate. As shown in Fig 8.7, at the same crack length ratio a/b the crack propagation rate increases considerably with cheek width.

On the other hand, the effect of head height on the crack propagation rate is less pronounced. Here it must be noted that with increasing head height, defined by $2R/H$, the crack propagation rate declines for a certain crack length ratio (see Fig 8.8).

8.4 Determination of stress intensity K_I and its non-dimensional quantity Y for the various lugs

Using the material characteristic $da/dN = f(\Delta K_I)$ determined in section 8.2, appropriate ΔK_I values can be allocated to the crack propagation rate da/dN determined on lugs for different crack lengths a/b. Basically this can be done by extracting from Fig 8.5 the appropriate ΔK_I value with a specific da/dN value of a lug. Since for a lug the stress to generate the crack propagation in the form of R and σ_{max} and the crack length a at which da/dN was determined are known, the dimensionless stress intensity Y, also termed correction function, can be calculated as

$$Y_i = \frac{\Delta K_I}{(1 - R)\,\sigma_{max}\sqrt{a_i}} \quad . \qquad (8\text{-}5)$$

This procedure can be carried out for various crack lengths for which the crack propagation rate of the lug is known. As a result the correction function for the various lugs can be presented as a function of the crack length a or its dimensionless quantity a/b.

LT 2057

The use of the material characteristic shown in Fig 8.5 for assigning the stress intensity to the crack propagation rate of the lug, however, entails the risk of errors in reading, especially since the plotting is double logarithmic.

This source of error can be removed by presenting the material characteristic in the form of a mathematical function, namely the Forman equation. It has already been shown in section 8.2 how the Forman equation can be used to describe crack propagation curves and thus also the crack propagation characteristic.

The connection between da/dN and ΔK_I is laid down in the Forman equation by the characteristics C_F, n_F and K_c, quoted in Fig 8.5, for the various material thicknesses:

$$(da/dN)_{lug} = \frac{C_F \Delta K^{n_F}}{(1 - R)K_c - \Delta K_I} \quad . \tag{8-6}$$

Since the equation cannot be solved according to K_I, K_I must be determined iteratively.

Here again a standard programme of the HP67 is used to determine the zero position

$$0 = \frac{C_F \Delta K^{n_F}}{(1 - R)K_c - \Delta K_I} - \frac{da}{dN} \quad . \tag{8-7}$$

After presetting an estimated value the zero position is calculated by the following recurrence formula

$$X_{i+1} = X_i - f(X_i) \frac{(X_i - X_{i-1})}{f(X_i) - f(X_{i-1})} \quad . \tag{8-8}$$

The zero position or the corresponding ΔK_I value is determined precisely to two decimal places. The possible error is less than 1%.

Expansion of this programme with equation (8-5) produces the appropriate correction function.

The course of correction function Y depending on the crack length a/b for the various lugs is shown in Figs 8.9 to 8.11.

It is revealed that the Y values of lugs 1, 2 and 3, with which the effect of size is to be investigated, lie within one scatter band (see Fig 8.9). This means that despite different crack propagation behaviour lugs of the same geometry but different sizes exhibit the same correction function. This will be of considerable importance in the practical application of the correction functions determined here.

Based on the considerations in section 5, according to which the correction function Y for $a \to 0$ followed from the stress concentration factor of the macro notch and a factor to allow for the load-free surface, the experimentally determined correction function was interpolated between $a = 0$ and the first measuring points.

LI 2057

There were no measuring points available for the technically less interesting range $a/b > 0.8$. This range was therefore presented approximately by extrapolation.

Fig 8.9 also shows values for γ which were determined in Ref 87 with the aid of the finite element method for the uni- and bilaterally cracked lug of the same geometry. Relatively close agreement is found for the unilaterally cracked lug.

As expected, values for the bilaterally cracked lug must be higher since the supporting effect of a cracked lug cheek is less compared with a crack free lug cheek. The greater the crack, the more distinct is the difference.

Fig 8.10 shows the effect of cheek width on the correction function. In the range $a/b < 0.5$ the correction function rises with increasing cheek width. At greater crack lengths $a/b > 0.6$ the cheek width effect is reversed. As can be seen from Fig 8.11, variation of the head height appears to effect parallel displacement of the correction function so that the correction function decreases with increasing head height.

The results available so far can be used to predict the crack propagation of lugs of the same or similar geometry, characterised by the parameters $2R/w$ and $2R/b$. As is customary in part of the literature, the correction function would have to be approximated by a polynomial.

Lug geometries diverging marked.y from those examined here, however, could not be dealt with. It is therefore the aim of this paper to develop a formula which would cover the entire technically viable range of different lug parameters.

In order to present the dimensionless quantity γ more clearly for the lugs examined here the stress intensity is determined with

$$K_I = \sigma_{max}/a\pi$$

Values from Figs 8.5 to 8.11 are also used for this presentation which have only resulted from inter- or extrapolation.

The size of the stress intensity can be seen from Figs 8.12 to 8.14. The results can be compared roughly with the crack propagation rate in Figs 8.6 to 8.8.

8.5 Comparison of the effect of the essential lug parameters on the correction function, on crack propagation and on stress distribution

Table 8.2 compares the results of the stress distribution, crack propagation and correction function to the variation of lug parameters.

Essentially this comparison shows that an increase in stress in the vicinity of the edge of the hole as a consequence of a change in the lug geometry always produces a reduction in crack propagation life and this an increase in the correction function.

The stress in the vicinity of the hole edge or immediately at the edge, where it is expressed by the stress concentration factor, is independent of the arrangement of the lug, providing dimensionless pointing takes place in regard to the stress and the

distance from the edge of the hole. The stress concentration factor and thus the stress in the immediate vicinity of the edge of the hole increase considerably as the cheek width b gets larger. Enlargement of the head height, in contrast, produces a reduction in the stress concentration factor.

The stress concentration factor and the stress in the immediate vicinity of the edge of the hole therefore have a great effect on the crack propagation life and govern the size of the correction function at the edge of the hole, which was pointed out in section 5.

In framing a formula to describe the correction function for the various lugs the stress at the edge of the hole will therefore have to be regarded as an essential quantity.

The course of the stress at a greater distance from the edge of the hole, on the other hand, does not allow conclusions to be drawn on crack propagation behaviour or therefore on the course of the correction function. In this area the edge effect and the rigidity behaviour of the cracked component will be significant for the correction function. The formula to be developed will therefore have to rely on test results in this area.

9 DEVELOPMENT OF AN ANALYTICAL FORMULA TO DESCRIBE THE CORRECTION FUNCTION

It is the aim of the following reflections not to describe each individual experimentally determined correction function by a special function, such as for instance a polynomial, but to cover the entire test results in a complete calculation formula. In principle this would provide a means of describing all forms of lug which lie within or without the range investigated. This, however, presupposes that the effect of the individual lug parameters on the correction function can be regarded separately, which has been confirmed at least in the range examined.

Further it is presupposed that the connection between stress intensity and parameter is established by three test points with adequate accuracy at least within the parameter range examined. Outside the range examined any statement is only permissible to a limited extent.

Direct evidence of these assumptions is not entirely possible since an infinite number of tests would be required. But with the variation of lug geometry it may be assumed with adequate safety that no instability occurs in regard to the effect on the correction function. As far as the stress at the edge of the hole is concerned - the stress is proportional to the correction function there - Frocht and Hill[81] were able to show that the effect of a lug parameter on the stress at the edge of the hole exhibits a steady course.

9.1 Computation formula for the standard lug

Since the variation of the essential lug parameters emanated from lug No. 2 (see Table 7.1) - this lug was therefore termed standard lug - a formula for the correction function will first be developed for this.

As shown in section 5, the following applies in principle to cracks from notches with load-free surface:

$$Y = K_t 1.12 \qquad \text{for} \quad a \to 0 \; .$$

This value Y at the edge of the hole is used for all lugs as so-called 'hanger' of the correction function.

Together with the subsequent decline of the correction function - similar behaviour was also noted in the stress distribution in the crack-free lug - its course will be determined by the following equation:

$$Y = \frac{1.12 K_t A}{A + a/b} \; . \tag{9-1}$$

For lugs 1, 2 and 3 according to Ref 81, $K_t = 2.8$ applies.

Quantity A is fixed in such a way that even in the area of medium and longer crack lengths the function agrees as accurately as possible with the correction function determined experimentally in Fig 8.9.

If equation (9-1) is solved in respect to A

$$A = \frac{Y \frac{a}{b}}{1.12 K_t - Y} \tag{9-2}$$

and A calculated at various crack lengths a/b with the appropriate experimentally determined Y values, it is established that

$$A = f(a/b)$$

(see Table 9.1 and Fig 9.1).

After checking various functions it transpired that the connection between A and a/b can best be shown by an exponential function.

The free parameters in this exponential function are calculated with the help of a standard programme of the HP67 pocket calculator by the method of least squares:

$$A = 0.026 e^{1.895} \left(1 + \frac{a}{b}\right) \; . \tag{9-3}$$

A comparison between the experimentally determined values for the correction function and the values calculated to equation (9-1) is shown in Table 9.1. The mean error over the entire crack length range is approximately 1.8%.

Since there is no size effect in regard to the correction function (see Fig 8.9), equation (9-1) with (9-3) is also valid for lugs 1 and 3.

LT 2057

The correction function can thus also be used for different sized lugs with $2R/W = 0.48$ and $2R/H = 0.9$.

9.2 Extension of the formula to take into account the effect of lug cheek width

The cheek width whose effect on the correction function was examined with lugs No.4 and No.5 (see Fig 8.10) is characterised by the ratio $2R/W$. In order to take full account of this effect the existing formula for the correction function (see equation (9-1)) must be expanded by a term to be determined empirically. First the correction function is calculated with equation (9-1) for lugs No.4 and No.5 at various crack lengths a/b. The following values are used (see Ref 81) for the stress concentration factor K_t.

$$K_t = 2.3 \qquad \text{for lug No.4}$$

$$K_t = 3.85 \qquad \text{for lug No.5.}$$

The values are shown in Table 9.2.

Further the ratio between $Y_{test}/Y_{calculation}$ is determined for the two lugs at the different crack lengths. Y_{test} means the correction function determined in the test, which is shown in Fig 8.10. The correction function calculated to equation (9-1) is termed $Y_{calculation}$. The individual pairs of values Y and a/b and the ratio

$$\frac{Y_{test}}{Y_{calculation}}$$

are also shown in Table 9.2.

Fig 9.2 shows the curve of $Y_{test}/Y_{calculation}$ and its approximation by equation (9-4) as a function of crack length a/b for lug No.4 (k_4), No.5 (k_5) and for No.2 (k_2).

For lug No.2 the additional term to allow for $2R/W$ must be constant over the entire crack length range and assume the value 1.

The task now is to find a function for the three curves k_4, k_2 and k_5 (see Fig 9.2) which fulfils two requirements. First, the connection between k and a/b must be able to be reproduced with adequate accuracy. Second, the function may only contain one free parameter, which again must be a function of $2R/W$. The following formula presents itself as a suitable function.

$$k = e^{r\sqrt{a/b}} \qquad (9\text{-}4)$$

r being a function of $2R/W$.

In order to be able to describe the three curves in Fig 9.2 with equation (9-4) as accurately as possible, r must assume the following values:

$$r = 0.25 \qquad \text{for lug No.4}$$

$$r = 0 \qquad \text{for lug No.2}$$

$$r = -0.48 \qquad \text{for lug No.5.}$$

LI 2057

If k_4 and k_5 are calculated with these r values and compared with $Y_{test}/Y_{calculation}$ (see Table 9.2) the result is for lug No.4 a mean error $\bar{F} = 1.24\%$ and for lug No.5 a mean error of $\bar{F} = 0.89\%$.

The relationship between r and $2R/W$ is established by a polynomial second degree. Since the three r values are reproduced precisely by the polynomial, no additional error occurs here.

$$r = -3.22 + 10.39\left(\frac{2R}{W}\right) - 7.67\left(\frac{2R}{W}\right)^2 \quad . \tag{9-5}$$

9.3 Extension of the formula to take account of the effect of the head height of the lug

The effect of the head height of the lug, characterised by $2R/H$, was examined by means of lugs 6 and 7.

The experimentally determined correction functions are shown in Fig 8.11. The values for Y at different crack lengths are shown in Table 9.3.

If the correction functions are calculated to equation (9-1) with the appropriate formulae (see Ref 81)

$$K_t = 2.6 \quad \text{for lug 6}$$

$$K_t = 3.0 \quad \text{for lug 7}$$

and the ratio

$$Y_{test}/Y_{calculation}$$

formed, values are yielded which, irrespective of crack length, scatter by a specific value (see Table 9.3).

The resultant mean value is used as additional correction U to allow for the effect of the head height.

This produces

$$U = 0.97 \quad \text{for lug 6 with } 2R/H = 0.7$$

$$U = 1.01 \quad \text{for lug 7 with } 2R/H = 1.2$$

$$U = 1.00 \quad \text{for lug 2 with } 2R/H = 0.9.$$

U can thus be shown as a function of $2R/H$.

By using a second degree polynomial the following equation is yielded for U

$$U = 0.72 + 0.52\left(\frac{2R}{H}\right) - 0.23\left(\frac{2R}{H}\right)^2 \quad . \tag{9-6}$$

The mean deviation or the mean error $\bar{F}$ produced by using U instead of $Y_{test}/Y_{calculation}$ over the entire crack length range is

LT 2057

$$\bar{F} = 1.23\% \quad \text{for lug 6}$$

$$\bar{F} = 2.0\% \quad \text{for lug 7.}$$

If equation (9-6) were used over the entire crack length range this would falsify the correction function in the immediate vicinity of the edge of the hole. It is known that at the edge of the hole

$$Y = K_t 1.12 \quad \text{for} \quad a/b = 0 \ .$$

Therefore $U = f(2R/H)$ must be coupled with a carrier function which leads to

$$U \to 1 \qquad \text{for} \quad a/b \to 0 \ .$$

For $a/b > 0 + \varepsilon$ with $\varepsilon \ll 1$ the carrier function must not have any effect worth mentioning on U.

The following equation suggests itself for this purpose:

$$Q = \frac{U\frac{a}{b} + 10^{-3}}{\frac{a}{b} + 10^{-3}} \ . \tag{9-7}$$

At $a/b \to 0$ function Q assumes the value 1 and is for $a/b > 0 + \varepsilon$ almost identical with U. The error is less than 0.06% for $a/b \geqslant 0.05$.

As may be gathered from the data in Table 9.3 and equation (9-6), the effect of the lug head height can already be covered to a very large extent by the semi-empirical formula (see equation (9-1)). Minor divergencies between the correction function Y_{test} determined experimentally and the correction function $Y_{calculation}$ calculated as equation (9-1) (see Table 9.3) are allowed for by the function $Q = f\left(U(2R/H)_i(a/b)\right)$.

9.4 Stress intensity solution for the lug

If the functions determined in sections 9.1 to 9.3 which allow for the effect of the different lug parameters on the correction function, are combined they produce the following solution for the lug:

$$K = \sigma\sqrt{\pi a}\,Y_{sum}$$

$$Y_{sum} = \frac{1.12K_t A}{A + a/b}\,kQ$$

$$k = e^{r\sqrt{a/b}}, \qquad r = -3.22 + 10.39\left(\frac{2R}{W}\right) - 7.67\left(\frac{2R}{W}\right)^2 \tag{9-8}$$

$$Q = \frac{U\frac{a}{b} + 10^{-3}}{\frac{a}{b} + 10^{-3}}, \qquad U = 0.72 + 0.52\left(\frac{2R}{H}\right) - 0.23\left(\frac{2R}{H}\right)^2$$

LI 2057

$$A = 0.026e^{1.895}\left(1 + \frac{a}{b}\right) .$$

This solution applies to the unilaterally cracked lug. The loading direction must point in the direction of the principal axis of the lug. The crack front is assumed to be approximately straight.

Under the premises laid down in section 9 the solution is not only applicable with the accuracy demonstrated in sections 9.1 to 9.3 to the forms of lug investigated here.

The whole purpose of the formula is to cover a whole spectrum of lug forms. It may be assumed that the accuracy of the stress intensity solution for lugs within the parameter field examined should not alter materially. For the calculation of lugs outside the parameter field examined a similar accuracy can be assumed if the 'distance' is not too great.

The types of lug used in practice, however, should be covered to a great extent with adequate accuracy by the formula developed here.

10 VERIFICATION OF THE STRESS INTENSITY SOLUTION FOR THE LUG BY MEANS OF EXPERIMENTALLY DETERMINED CRACK PROPAGATION CURVES

In the selection of a suitable method of determining the stress intensity for a component, section 7.1 pointed to the advantage of the crack propagation method, namely the possibility of checking the results by means of crack propagation measurements.

This decisive advantage will now be used here to demonstrate the accuracy of the stress intensity solution with the aid of the crack propagation measurements.

Since the stress intensity solution was derived directly from the crack propagation tests there should theoretically be exact agreement between the crack propagation investigation using the stress intensity solution (see equation (9-8)) and the crack propagation measurements.

That this cannot be the case can be traced in the main to two causes which will be dealt with in more detail in section 11 in connection with considerations of error. These causes concern the unavoidable material scatter and the divergencies in the approximation of the experimentally determined correction function by analytical functions.

The crack propagation calculation was performed with the Forman equation (equation (2-11)) by numerical integration, using a standard programme of the HP67 pocket calculator.

This programme is used for calculation of the integral of any constantly differentiable functions within given interval limits.

The result is equal to the area which the function encloses within the limits with the abscissa.

LT 2057

$$f(a) = \frac{dN}{da} = \frac{(1 - R)K_C - \Delta K_I}{C_F \Delta K_I^{n_F}} \qquad (10\text{-}1)$$

$$Na = \int_{a_0}^{a_a} \frac{(1 - R)K_C - \Delta K_I}{C_F \Delta K_I^{n_F}} \, da \quad . \qquad (10\text{-}2)$$

Starting from the initial crack length a_0 the number of load cycles N_a to crack length a is obtained by integration of the reciprocal value of the Forman equation. The variable in the Forman equation is the stress intensity factor range ΔK_I which with a given lug geometry and external load only remains a function of the crack length a.

To perform the calculation the standard programme required for integration is first read into the calculator store by means of a magnetic card. The input of the Forman equation follows in which in ΔK_I the entire lug correction function is contained. After input of the number of integration steps, the initial crack length and the crack length up to which the number of load cycles is to be computed, the result yielded is the appropriate load cycle N_a.

The necessary input data are shown in Table 10.1 for the seven lugs.

As in the test, the stress for the crack propagation calculation for the seven lugs was $\sigma_0 = 98.1$ N/mm^2, and the stress ratio R = 0.1.

Figs 10.1 to 10.3 show a comparison between the mean experimentally determined crack propagation curves and the load cycles calculated to Forman for several crack lengths. Relatively close agreement between test and calculation can be noted. The deviation between calculation and test is approximately 10% on average. The greatest deviations arise for lug 3 with 17% and lug 7 with 22%. Experience has shown that deviations of the order found here are within the range of material scatter.

11 INVESTIGATION INTO POSSIBLE SOURCES OF ERROR

As can be seen from Figs 7.9 to 7.15, the crack propagation curves determined for lugs are subject to a certain scatter. Since the correction function for the lugs was derived from these crack propagation curves this too suffers from a corresponding error. Although the mean crack propagation curves were used for the evaluation, the correction function cannot be regarded as the mean value of the basic totality due to the fact that it is not a case here of a basic totality but a random sample of limited extent. A further error of approximately the same size can be traced to the scatter behaviour of the material characteristic required for evaluation.

As far as the correction function in the form of a semi-empirical formula is concerned (see equation (9-8), this too is subject to a certain error.

First, possibilities of error which can be traced to the scatter of experimentally determined crack propagation curves will be examined more closely.

11.1 Scatter of crack propagation curves and its effect on the correction function

Before the scatter occurring in crack propagation tests is determined it must first be defined. One can, for instance, understand by scatter the scatter of crack length at a specific load cycle and in reverse the scatter of the load cycle at a specific crack length. But one can also regard the scatter of the speed of crack propagation as a random event.

No matter which criterion is taken as random event, the scatter connected with crack propagation measurements can be traced to various causes. In the main these are the material, the test specimen, the test set-up and the reliability of the reading of the person performing the test. It is to be assumed that these sources of error are not constant and do not occur at the same intensity during the whole of the experiment.

It therefore seems to make sense to examine only the effect of the various sources of error on the crack propagation life, *i.e.* the sum of their scatter behaviour.

This simplifies consideration of error materially and enables it to be reduced to the following question.

If crack propagation life, *i.e.* the load cycle to fracture, is subject to certain scatter behaviour, what is the error for the correction function which may be expected?

For the rest, the consideration of error will be undertaken by the basic rules of statistics[83] on the assumption of a Gaussian normal distribution.

Since the life of the individual lugs is of different lengths but it may be assumed that the scatter behaviour is independent of lug geometry to the greatest possible extent, the variance coefficient will be used to describe scatter behaviour.

$$V = \frac{s}{\bar{L}_D} \qquad (11\text{-}1)$$

$\bar{L}_D$ signifies the mean value of fatigue life and s its standard deviation.

The following variance coefficients are yielded for the seven lugs.

Lug	1	2	3	4	5	6	7
V	0.103	0.027	0.065	0.046	0.018	0.065	0.028

Further investigation will allow for the mean as well as the maximum variance coefficient.

$$\bar{V} = 0.05$$

$$V_{max} = 0.103 .$$

LT 2057

Furthermore, investigation of error will not be carried out on every lug but only on lug 2 as representative (= standard lug).

To determine the relevant variance coefficient for the correction function the crack propagation life will first be calculated with the aid of the Forman equation (equation (8-6)) with the mean value of $\bar{V}$ as equation (9-8). All crack propagation calculations are performed by numerical integration of the reciprocal Forman equation with the HP67 pocket calculator.

The crack propagation calculation is repeated, assuming different standard deviations for the correction function until the variance coefficient of the calculated life values agrees with those observed in the test.

In regard to the variance coefficient this yields the following connection between life and correction function.

	Variation coefficient	
	Life	Correction function
Maximum value	0.103	0.039
Mean value	0.05	0.014

Shown in a probability diagram the following relationships are produced between the scatter behaviour of the crack propagation curve and the correction function (see Fig 11.11).

If it is assumed that the mean value of the random sample in relation to the basic totality does not occur at 50% (= 100% life), but at 10% or 90% value the error arising in the correction function is 2% or 5% respectively for V_{max}.

In experimental evidence of life it is customary if few test values are available to allot to them a failure probability of 90%. The actual mean value is then smaller according to the standard deviation[84]. Since at least three tests per lug were performed in this investigation allocation of the mean value at the 90% value is fairly conservative. For this reason the error will only be derived from the mean variance coefficient. The error of the experimentally determined correction function is therefore assumed at 2%.

If it is further assumed that the material characteristic, which was also determined by crack propagation tests, may be subject to the same error then the possible error of the correction function is increased.

Thus the total error of the experimentally determined correction function may reach 2.83%. According to Fig 11.1 this would result in an error of approximately 12% for fatigue life.

11.2 Divergence of the semi-empirical formula from the experimentally determined correction function

The divergence between the experimentally determined correction functions (see Figs 8.9 to 8.11) and the semi-empirical formula as equation (9-8) can be shown by simple error observation. It is customary in fracture mechanics[28,29] to state the accuracy of a regression equation over the entire crack length range by the following process:

$$\bar{F} = \frac{1}{n} \sum_{j=1}^{n} \left(\frac{|Y_{test} - Y_{calculation}|}{Y_{test}} \times 100\% \right)_i \quad . \qquad (11-2)$$

$\bar{F}$ is the mean percentage deviation. n is the number of points at which a comparison is carried out. Based on this consideration, the following mean deviations are produced for the correction functions of the seven lugs (see Tables 9.1 to 9.3).

Lug	1, 2, 3	4	5	6	7
$\bar{F}$%	1.8	1.34	0.89	1.23	2.0

The divergence or accuracy of equation (10-8) over the entire crack length range is therefore between 0.89% and 2.0%.

If the crack propagation is calculated after Forman taking account of the correction function, the correction function can be subject to an error of approximately 3.5% - errors from material scatter and regression - at maximum.

The individual errors were added according to the following formula

$$F_{sum} = \left(\sum F_i^2 \right)^{\frac{1}{2}} \qquad (11-3)$$

with F_i individual errors

and F_{sum} the sum of all errors.

An error of approximately 15% can thereby arise for crack propagation life. It is known from experience that errors of this order are in the area of natural material scatter in crack propagation tests.

If crack propagation tests are performed on specimens which either stem from different material batches or from semi-finished materials from different manufacturers the error can amount to up to 100% [85].

Re-calculation of the experimentally determined crack propagation curves for the seven lugs (see Figs 10.1 to 10.3) has shown that the divergence between test and calculation amounted to 10% on average.

12 CONCLUDING OBSERVATIONS

Higher requirements in safety and increased exploitation of the capacity of material to bear stress have led to the extension of fracture mechanics to the most varied technical areas.

An essential constituent of the calculation principles for prediction of crack propagation and the critical crack length is the stress intensity solution.

It was the object of this paper to determine for an important structural component, namely the lug, stress intensity as a function of the typical lug parameters and present it in the form of a complete analytical formula.

First, the stress intensity was described starting from linear elastic principles of strength and its importance for determination of crack propagation and critical crack length demonstrated.

LT 2057

A review of the best known methods of determining the stress intensity followed together with a discussion of their applicability to the problem of the lug.

This revealed that determination of the stress intensity by means of crack propagation curves is a particularly suitable method for the lug.

At the time this work was carried out there was no comprehensive investigation in existence on stress intensity for lugs, especially on the effect of the various lug parameters.

Starting with an infinite plate with hole, through the strip with loaded and unloaded hole, for which known stress intensity solutions were available, the lug was therefore approached step by step.

In a subsequent experimental investigation of the lug it was possible to demonstrate the connections between the essential lug parameters, crack propagation behaviour and stress distribution in the crack-free lug, in addition to determining the stress intensity.

The set aim of the task was finally achieved by succeeding in presenting the stress intensity or its dimensionless quantity Y as a function of the essential lug parameters, such as cheek width, head height and absolute lug size in a complete semi-empirical formula. The accuracy of the formula was demonstrated by re-calculating the crack propagation curves for the various lugs. The difference between test and calculation was 22% maximum and approximately 10% on average.

Strictly speaking, the present stress intensity solution is valid only for the unilaterally cracked lug with an approximately straight crack front.

In practice cracks of this type occur predominantly when caused by fretting corrosion. However, cracks are frequently found in lugs which emanate from the edge of the hole. The crack front then assumes the form of a quarter ellipse or quarter circle.

There is as yet no stress intensity solution specially for this case. If one were to use the stress intensity solution for a crack with straight crack front here the crack propagation life thus calculated would lie considerably on the safe side.

The following procedure should lead to a materially more accurate result.

If the strip with open hole is considered, there is a stress intensity solution for a crack with straight crack front and for a semi-elliptical edge crack[86].

It can be assumed in first approximation that the relationship of the individual stress intensity solutions is transferable to the lug.

Nevertheless, it remains for future investigations on the lug to expand the stress intensity solution for the crack with straight or approximately straight crack front in order to be able to take account of the corner crack and the effect of different directions of load application.

Acknowledgment

This Memorandum originated within the framework of my activities as development engineer with Messrs. Messerschmitt-Bölkow-Blohm GmbH, Aircraft Department, in Ottobrunn near Munich.

I would like to thank Messrs. Dipl.-Ing. V.v. Tein, Head of Development Department, Dipl.-Ing. P. Seibert, Head of Structures and Strength, Dr E. Schreiner, Head of Main Department Strength and Ing. D. Weisgerber, Commercial Head of Material and Life Department, for supporting this work.

Special thanks are due to Prof. Dr. K. Heckel, Head of the Institute of Materials Science at the University of the Bundeswehr Munich and Prof. Dr. Meyer-Jens, Head of the Chair of Light Construction at the Technical University Munich for their constant interest and valuable discussions and suggestions.

I would also like to thank my colleagues, especially Messrs. Ing. R. Bochmann and P. Hahn for valuable discussions.

LT 2057

Table 4.1

VALUES FOR THE CORRECTION FUNCTION FOR CRACKS FROM A HOLE IN AN INFINITE PLATE

$\frac{a}{R}$	Unilateral crack Y_1		Bilateral crack Y_2	
	Uniaxial stress	Biaxial stress	Uniaxial stress	Biaxial stress
0.00	3.39	2.26	3.39	2.26
0.10	2.73	1.98	2.73	1.98
0.20	2.30	1.82	2.41	1.83
0.30	2.01	1.67	2.15	1.70
0.40	1.86	1.58	1.96	1.61
0.50	1.73	1.49	1.83	1.57
0.60	1.64	1.42	1.71	1.52
0.80	1.47	1.32	1.58	1.43
1.0	1.37	1.22	1.45	1.38
1.5	1.18	1.06	1.29	1.26
2.0	1.06	1.01	1.21	1.20
3.0	0.94	0.93	1.14	1.13
5.0	0.81	0.81	1.07	1.06
10.0	0.75	0.75	1.03	1.03
∞	0.707	0.707	1.00	1.00

LI 7057

Table 6.1

TYPICAL VALUES FOR LUGS

2R mm	W mm	H mm	2R/W	2R/H	2R/t
42	96	51	0.46	0.8	2.47
62	120	67	0.46	0.9	2.21
35	58	29	0.6	1.2	2.5
51	70	35	0.73	1.45	1.5
37	75	40	0.49	0.92	1.68
21	42	19	0.5	1.1	2.6

Table 6.2

VALUES FOR THE LUGS TO BE EXAMINED

2R mm	2R/W	2R/H	t mm
40	0.36 0.48 0.6	0.9	15
40	0.48	0.7 0.9 1.2	15
20 40 60	0.48	0.9	8 15 20

Table 7.1

DIMENSIONS OF LUGS Nos. 1-7

Lug No.	Dimension (mm)				
	2R	W	H	L	t
1	20	41.6	22.2	80	8
2	40	83.3	44.4	160	15
3	60	125	66.6	240	20
4	40	66.6	44.4	160	15
5	40	111.1	44.4	160	15
6	40	83.3	57.1	160	15
7	40	83.3	33.3	160	15

LT 2057

Table 7.2

CHEMICAL COMPOSITION OF AL 7075T7351

	Cu	Mg	Mn	Cr	Si	Fe	Ti	Zn
	Composition of alloy by wt.%							
Nominal AMS 4078	1.20-2.0	2.1-2.9	- 0.3	0.18 0.4	- 0.5	- 0.7	- 0.2	5.1 6.1
Actual	1.45	2.66	0.1	0.2	0.13	0.25	0.04	5.81

Table 7.3

STRENGTH VALUES OF A17075T7351

	$\sigma_{0.2}$ N/mm^2	σ_B N/mm^2	δ_5 (%)
Nominal: lengthwise	334	432	6
across	343	432	6
after VFN13314			
Actual: lengthwise	382	462	8.4
across LT	383	464	8.4

Table 8.1

COEFFICIENTS FOR SECOND ORDER POLYNOMIALS FOR APPROXIMATION OF LUG CRACK PROPAGATION CURVES IN SUB-RANGES

Lug No.	As text	Coefficients		
		q_1	q_2	q_3
1	0-1500	2.5	0.2	0.044
	1500-8000	2.529	0.248	0.019
	8000-12000	15.6	-2.85	0.2
2	0-6000	2.5	0.4	0.066
	6000-12000	7.705	1.023	0.159
3	0-7000	2.5	0.701	0.106
	7000-12000	12.25	-1.7	0.25
4	0-9000	2.5	0.144	0.0259
	9000-13500	7.8	-1.03	0.09
5	0-3000	2.5	1.233	0.2
	3000-7000	1.639	1.808	0.104
	7000-8500	19.2	-3.733	0.533
6	0-10000	2.5	0.408	0.035
	10000-13000	6.525	-0.4	0.075
	13000-14500	66.984	-10.043	0.459
7	0-3000	2.5	0.5	0.2
	3000-6000	1.8	1.125	0.063
	6000-8000	25.8	-6.7	0.7

Table 8.2

EFFECT OF LUG PARAMETERS ON STRESS DISTRIBUTION, CRACK PROPAGATION AND ON THE CORRECTION FUNCTION

Parameter	Stress distribution	Crack propagation	Correction function
Effect of size	Same stress curve (see Fig 7.19)	Same crack prop. life; increase in crack propagation rate with lug size (see Fig 7.16)	Same correction function (see Fig 8.9)
Effect of cheek width	Considerable increase in stress at edge of hole with increasing cheek width; reversal with increasing distance from edge of hole $a/b > 0.15$ (see Fig 7.20)	Reduction in crack prop. life with increasing cheek width; increase in crack growth rate with increasing cheek width (see Fig 7.17)	Rise in correction function with increasing cheek width in range $a/b < 0.5$. Reversal in range $a/b > 0.6$ (see Fig 8.10)
Effect of head height	Rise in stress at edge of hole with decreasing head height; reversal at $a/b > 0.05$ (see Fig 7.21)	Reduction in crack prop. life with decreasing head height; higher crack prop. rate at lower head height (see Fig 7.18)	Rise in correction function with decreasing head height (parallel displacement) (see Fig 8.11)

Table 8.1

DATA TO DETERMINE THE EMPIRICAL QUANTITY A

A/b	0.05	0.1	0.2	0.3	0.4	0.5	0.6	0.7	0.8	0.9	1.0
Y test	2.52	2.14	1.79	1.6	1.48	1.43	1.43	1.48	1.55	1.59	1.67
A	0.205	0.215	0.266	0.313	0.337	0.42	0.513	0.626	0.762	0.929	1.139
Y calculation	2.486	2.12	1.74	1.60	1.51	1.45	1.48	1.51	1.58	1.61	1.68
Error %	1.3	0.9	2.8	1.2			3.	2.3	1.3	1.2	.6

LP 2057

Table 9.2

DATA TO DETERMINE THE EFFECT OF WIDTH 2R/W

	a/b	0.05	0.1	0.2	0.3	0.4	0.5	0.6	0.7	0.8	0.9	1.0
Lug No.4	Y test	2.14	1.92	1.64	1.48	1.41	1.41	1.47	1.55	1.6	1.69	1.78
	Y calculation	2.04	1.74	1.44	1.3	1.24	1.21	1.22	1.24	1.28	1.32	1.38
	$\frac{\text{Y test}}{\text{Y calculation}}$	1.05	1.1	1.14	1.14	1.14	1.17	1.2	1.25	1.25	1.28	1.29
	k_4	1.06	1.08	1.12	1.15	1.17	1.19	1.21	1.23	1.25	1.27	1.28
	Error %	0.9	1.82	1.75	0.88	2.63	1.71	0.83	1.6	0	0.78	0.78
Lug No.5	Y test	3.02	2.5	1.95	1.68	1.53	1.44	1.39	1.37	1.39	1.44	1.5
	Y calculation	3.41	2.92	2.41	2.18	2.07	2.03	2.04	2.08	2.14	2.22	2.31
	$\frac{\text{Y test}}{\text{Y calculation}}$	0.89	0.86	0.81	0.77	0.74	0.71	0.68	0.66	0.65	0.65	0.65
	k_5	0.9	0.86	0.81	0.77	0.74	0.71	0.69	0.67	0.65	0.63	0.62
	Error %	1.12	0	0	0	0	0	1.47	1.52	0	3.08	4.6

Table 9.3

DATA TO DETERMINE THE EFFECT OF LUG HEAD HEIGHT

	a/b	0.05	0.1	0.2	0.3	0.4	0.5	0.6	0.7	0.8	0.9	1.0
Lug No.6	Y test	2.16	1.88	1.62	1.44	1.35	1.31	1.32	1.36	1.4	1.46	1.54
	Y calculation according G1 (9.1)	2.31	1.97	1.63	1.47	1.4	1.37	1.38	1.4	1.44	1.5	1.56
	$\frac{\text{Y test}}{\text{Y calculation}}$	0.94	0.95	0.99	0.98	0.96	0.96	0.96	0.97	0.97	0.97	0.99
	U_6	0.97	→									
	Error %	3.19	2.11	2.02	1.02	1.04	1.04	1.04	0	0	0	2.02
Lug No.7	Y test	2.7	2.4	2.0	1.79	1.64	1.58	1.57	1.62	1.66	1.73	1.8
	Y calculation according G1 (9.1)	2.66	2.27	1.88	1.69	1.61	1.58	1.59	1.62	1.67	1.73	1.8
	$\frac{\text{Y test}}{\text{Y calculation}}$	1.01	1.05	1.06	1.05	1.02	1.0	0.98	1.0	0.99	1	1
	U_7	1.01	→									
	Error %	0	3.8	4.7	3.8	0.98	1.0	3.06	1.0	2.02	1.0	1.0

LL 2057

Table 10.1

INPUT DATA FOR CRACK PROPAGATION CALCULATIONS (ALL UNITS OF MEASUREMENT ARE BASED ON NEWTON AND MILLIMETRE

Size	Lug 1	Lug 2	Lug 3	Lug 4	Lug 5	Lug 6	Lug 7
K_t	2.8	2.8	2.8	2.3	3.85	2.6	3.0
C	3.0 E-7	4.02 E-7	8.0 E-7	4.02 E-7	4.02 E-7	4.02 E-7	4.02 E-7
n	2.38	2.34	2.10	2.34	2.34	2.34	2.34
K_c	2400	2255	1400	2255	2255	2255	2255
b	10.83	21.67	32.5	13.33	35.56	21.67	21.67
U	1	1	1	1	1	0.97	1.01
r	0	0	0	0.25	-0.48	0	0

LT 2057

INDEX OF MOST IMPORTANT ABBREVIATIONS

General geometric quantities

a	mm	length of crack
a_0	mm	initial length of crack
a_c	mm	critical length of crack
u, v	mm	displacement in x and y direction
W	mm	width of specimen
t	mm	thickness of specimen
R	mm	radius of hole
b	mm	cheek width of lug
H	mm	head height of lug
L	mm	length of lug
K_t, a_K		stress concentration factor
y		correction function

Quantity related to material

E	N/mm^2	modulus of elasticity
ν		Poisson's ratio
γ_e	N/mm	specific surface energy
γ_p	N/mm	specific plastic deformation action
C	N/mm	stiffness
C^{-1}	mm/N	compliance
C_p, n_p ; C_F, n_F		crack propagation characteristics for Paris or Forman equation
R_W	N/mm	crack resistance
K_{Ic}	$N/mm^{3/2}$	critical stress intensity in plane strain state
K_c	$N/mm^{3/2}$	critical stress intensity in plane stress state

Quantities related to load

P	N	force
σ	N/mm^2	gross stress
σ_N	N/mm^2	nominal stress
σ_0	N/mm^2	maximum stress of a stress cycle
σ_u	N/mm^2	minimum stress of a stress cycle
σ_a	N/mm^2	stress amplitude
K_I	$N/mm^{3/2}$	stress intensity for crack opening mode I
ΔK_I	$N/mm^{3/2}$	stress intensity range
K_{IO}	$N/mm^{3/2}$	stress intensity for an infinite plate with central crack
G	N/mm	crack extension force

LI 2057

REFERENCES

No.	Author	Title, etc
1	K.O. Sippel W. Geier	Fracture mechanics in aircraft construction. DVM papers of the Eighth session of the Arbeitskreis Bruchvorgaenge 1976, Köln-Porz
2	W. Geier	Establishment of inspection intervals with the aid of fracture mechanics. DGLR Symposium "Material maintenance costs for flying systems in the process phase", Köln-Wahn DFLVR 1979
3	-	Airplane damage tolerance requirements. Military specification Mil-A-83444 (USAF) 2 July 1974
4	O. Gökgöl	Estimation of endurance of light metal alloy lugs with interference fit bushes. MBB-UH-25-71, Available as RAE Translation 1861 (1975)
5	A Buch	Estimation of fatigue properties of aircraft lugs with interference fits. Department of Aeronautical Engineering Technion - Israel, Institute of Technology Haifa, Israel, TAE Report No.290, 1976
6	P. Garnatz	Stress measurements and strength investigations for the design of lugs with high fatigue strength. Fortschrittsbericht VDI-Z, Series 1, No.12.
7	J. Schijve	Fatigue strength of lugs of aluminium alloys.
8	O. Buxbaum	Operational strength of lugs made of aluminium alloy 3.1254.7. Laboratorium fuer Betriebsfestigkeit Darmstadt, Report No. FB-59
9	-	Engineering Science Data Unit, Volume 4 Fatigue
10	-	Collection of crack propagation characteristics for high-strength aluminium, titanium and steel alloys. MBB-UFE 214
11	L. Schwarmann	Theoretical principles of the K concept. VFW-Fokker Bremen, Ek 425-B/186, 1975
12	D. Broek	Elementary Engineering Fracture Mechanics. Noordhoff International Publishing
13	S.P. Timoshenko J.N. Goodier	Theory of elasticity. Third edition, McGraw-Hill (1970)
14	N.I. Muskhelishvili	Some basic problems of the mathematical theory of elasticity (1933). English translation Noordhoff (1953)

LT 2057

REFERENCES (continued)

No.	Author	Title, etc
15	H.M. Westergaard	Bearing pressures and cracks. *J. Appl. Mech.*, 61, pp A49-53 (1939)
16	P.C. Paris G.C. Sih	Stress Analysis of cracks. ASTM STP 391, pp 30-81 (1965)
17	G.C. Sih (ed)	Methods of analysis and solutions of crack problems. Noordhoff (1973)
18	G.C. Sih	On the Westergaard method of crack analysis. *Int. J. Fracture Mech.*, 2, 628-631 (1966)
19	J. Eftis H. Liebowitz	On the modified Westergaard equations for certain plane crack problems. *Int. J. Fracture Mech.*, pp 383-392, 8 (1972)
20	J.R. Rice	Mathematical analysis in mechanics of fracture. Fracture II, pp 192-308, Liebowitz ed, Academic Press (1969)
21	J.N. Goodier	Mathematical theory of equilibrium of cracks. Frature II, pp 2-67, Liebowitz ed., Academic Press (1979)
22	A.A. Griffith	The Phenomena of rupture and flaw in solids. Transactions, Royal Society of London, A-221 (1920)
23	C.E. Inglis	Stresses in a plate due to the presence of cracks and sharp corners. Proceedings, Institute of Naval Architects, 60 (1913)
24	G.R. Irwin	Fracture dynamics. In Fracturing of metals, American Society of Metals, Cleveland (1948)
25	-	Standard method of test for plain-strain fracture toughness of metallic materials. ASTM E 399-72
26	W. Geier	Residual strength behaviour of sheets of Al 7475T761, ZTL-Programm 1976, MBB Report No. UFE 1292
27	-	Damage tolerance design handbook. A compilation of fracture and crack growth data for high strength alloys. MCIC-HB-01, Airforce Materials Laboratory, Air Force Flight Dynamics Laboratory Wright-Patterson Air Force base
28	D.P. Rooke D.J. Cartwright	Compendium of stress intensity factors. Printed in England for Her Majesty's Stationery Office by the Hillingdon Press, Uxbridge, Middx. Dd 288672 K24, (1975)

IT 2057

REFERENCES (continued)

No.	Author	Title, etc
29	H. Tada P. Paris G. Irwin	The stress analysis of cracks. Handbook, Del Research Corporation, Hellertown, Pennsylvania (1973)
30	P.C. Paris	The growth of fatigue cracks due to variations in load. Ph.D. Thesis, Lehigh University (1962)
31	P.C. Paris M.P. Gomez W.E. Anderson	A rational analytic theory of fatigue. The trend in engineering, 13, pp 9-14 (1961)
32	R.G. Forman V.E. Kearney R.M. Engle	Numerical analysis of crack propagation in cyclic loaded structures. Journal of Basic Engineering, Trans. ASME, Series D, Vol 89 (1967)
33	W. Geier, W. Krimmel	Analytical determination of the Forman constants. MBB-Aktenvermerk 4, 74 (see also HSB)
34	D.W. Hoeppner W.E. Krupp	Prediction of component life by application of fatigue crack growth knowledge. Engineering Fracture Mechanics, Vol 6, pp 47-70 (1974)
35	T.R. Porter	Method of analysis and prediction for variable amplitude fatigue crack growth. Engineering Fracture Mechanics, p 717, Vol 4 (1972)
36	J.M. Barson	Fatigue crack growth under variable-amplitude loading. ASTM STP 536, p 147 (1973)
37	H.T.M. van Lipzig H. Nowak	Crack propagation behaviour and residual strength of light construction materials under non-constant amplitude loading. DVM paper, Sixth session of the Arbeitskreis Bruchvorgaenge, Freiburg 3, 4 October 1974
38	W.J. Mills	Load interaction effects on fatigue crack growth in 2024-T3 aluminium and A 514 F steel alloys. Lehigh University, Department of Metallurgy and Materials Science (1975)
39	R.B. Sayer	Nonlinear effects of spectrum loading on fatigue crack growth in transport wings. AIAA Paper No.74-984
40	J. Willenborg R.M. Engle H.A. Wood	A crack growth retardation model using an effective stress concept. AFFDL-TM-71-1 FBR AFSC-Wright Patterson Air Force Base, Ohio, January 1971

LT 2057

REFERENCES (continued)

No.	Author	Title, etc
41	O.E. Wheeler	Spectrum loading and crack growth. Journal of Basic Engineering, ASTM, Series D, Vol 19
42	W. Geier K.G. Sippel	Fatigue crack propagation under variable loads. Chapter 8 of the AGARDograph, Practical application of fracture mechanics (1980)
43	D.J. Cartwright	Methods of determining stress intensity factors. RAE Technical Report 73031 (1973)
44	G.C. Sih	Application of Muskhelishvili's method to fracture mechanics. Trans. Chin. Ass. Adv. Studies (1962)
45	F. Erdogan	On the stress distribution in plates with collinear cuts under arbitrary loads. Proc. Fourth US Nat. Congress Appl. Mech (1962)
46	O.L. Bowie	Analysis of an infinite plate containing radial cracks originating at the boundary of an internal circular hole. *J. Math. and Phys.*, 25, pp 60-71 (1956)
47	A.R. Luxmoore R.J. Owen	Numerical methods in fracture mechanics. Proceedings of the First International Conference, Swansea (1978)
48	O.C. Zienkiewicz	The finite element method in engineering science. McGraw-Hill (1971)
49	J.C. Nagtegaal E. Hulst	Analysis of fracture mechanics problems using the MARC system. MARC Analysis Research Corporation, Verrijm Stuartlaan 29 Rijswijk, The Netherlands
50	S.K. Chan I.S. Tuba W.K. Wilson	On the finite element method in linear fracture mechanics. *Eng. Fract. Mech.*, 2, pp 1-17 (1970)
51	K. Heckel	Introduction to the technical application of fracture mechanics. Carl Hauser Verlag München.
52	L.A. James W.E. Anderson	A simple experimental procedure for stress intensity factor calibration. *Eng. Fracture Mechanics*, 1, pp 565-568 (1969)
53	D.G. Smith C.W. Smith	A photoelastic evaluation of the influence of closure and other effects upon the local bending stresses in cracked plates. *Int. J. Fract. Mech.*, 6, 305-318 (1970)
54	W.W. Gerberich	Stress distribution around a slowly growing crack determined by photoelastic coating method. Proc. SESA, 10, pp 350-365 (1962)

LT 2037

REFERENCES (continued)

No.	Author	Title, etc
55	A.S. Kobaya	Photoelastic studies of fracture. Fracture III, pp 311-369, Liebowitz, Ed., Academic Press (1969)
56	J.R. Dixon	Stress distribution around edge slits in tension. Nat. Eng. Lab., Glasgow, Rept 13 (1961)
57	A. Monthulet S.K. Bhandari C. Riviere	Practical methods of determining stress intensity for crack propagation. La Recherche Aerospatiale, pp 297-303 (1971)
58	W. Barrois	Manual on fatigue of structures. AGARD-Man-8-70 (1970)
59	S.K. Bhandari	Experimental study on stress intensity in the vicinity of the tip of a central fatigue crack in a thin sheet by extensometric methods. Thesis, Ecole Nat. Superieure de l'Aeronautique, Paris (1969)
60	R.J. Gran F.D. Orario P.C. Paris G.R. Irwin R.W. Hertzberg	Investigation and analysis development of early life aircraft structural failures. AFFDL-TR-70-149 (1971)
61	O.L. Bowie	Analysis of an infinite plate containing radial cracks originating at the Boundary of an internal circular hole. *Int. Math. Phys.*, April 1956
62	P.C. Paris G.C. Sih	Stress analysis of cracks. ASTM STP 381, p 70
63	J.C. Newman	Predicting failure of specimens with either surface cracks or corner cracks at holes. NASA TN D-8244
64	A.F. Grandt	Stress intensity factors for some through fracked fastener holes. International Journal of Fracture, Vol.11, No.2, April 1975
65	J.R. Rice	Some remarks on elastic crack-tip stress fields. International Journal of solids and structures, 8.6 June 1972
66	P.C. Paris G.C. Sih	Stress analysis of cracks. ASTM STP 381, pp 30-81
67	H.G. Harris J.U. Ojalvo R.E. Hoosen	Stress and deflection analysis of mechanically fastened joints. Technical Report AFFDL-TR-70-49, Wright Pattersen Air Force Base, Ohio (1970)
68	J.C. Newman	Improved method of collocation for the stress analysis of cracked plates with various shaped boundaries. NASA TN D-6376 (1971)

REFERENCES (continued)

No.	Author	Title, etc
69	D. Broek	Cracks at structural holes. Batelle Metals and Ceramic Information Center MCIC Report 75-25
70	B. Gross J.E. Srawley W.G. Brown	Stress intensity factors for a single-edge-notch tension specimen by boundary collocation of a stress function. NASA TN D-2395
71	D.J. Cartwright G.A. Ratcliffe	Strain energy release rate for radial cracks emanating from a pin loaded hole. *Int. Journal of Fracture,* Vol 8, No.2, June 1972
72	L.F. Impellizzeri D.L. Rich	Spectrum fatigue crack growth in lugs. ASTM STP 595, pp 320-336
73	A.F. Liu H.P. Kan	Test and analysis of cracked lug. *Fracture* 1977, Vol 3, ICP 4, Waterloo, Canada, June 19-24, 1977
74	-	Practical application of fracture mechanics. AGARDograph 1980
75	R.E. Peterson	Stress concentration design factors. Library of Congress Catalog Card-Number: 53-111283
76	H. Neuber	The semi-elliptical notch with crack for correlation of micro and macro stress concentration. Ingenieur Archiv 46 , 389-399 (1977)
77	H.F. Bueckner	Weight function for the notched bar. Zeitschrift für angewandte Mathematik und Mechanik, Vol 51 (1971)
78	H. Huth	Crack propagation in notched bars subject to pulsating bending stress. LBF-Einzelbericht 2772-8.2, October 1978
79	-	Determination of stress intensity with the aid of the weight function. TN MBB-UFE 214-7-79
80	-	Stress distribution in the lug. TN MBB-UFE 214-5-78
81	M.M. Frocht H.N. Hill	Stress concentration factors around a central hole in a plate loaded through a pin in the hole. *J. App. Mech.* V, 7, March 1940
82	-	Investigation of the cracked lug with the aid of the finite element method. MBB-Ufe 214-6-78

LT 2057

REFERENCES (concluded)

No.	Author	Title, etc
83	Heinhold Gaede	Engineering Statistics. R. Oldenbourg, München-Wien (1968)
84	E. Haibach H. Ostermann G. Köbler	Covering the risk arising from chance factors of a small number of fatigue strength tests. LBF-TN No.68/73
85	J. Schijve P. De Rijk	The fatigue crack propagation in 2024-T3 Alclad sheet materials from seven different manufacturers. NLR Report TRM.2162
86	A.F. Liu	Engineering Fracture Mechanics. Vol. 4, p 175 (1972)

LT 2057

Figs 1.1-1.3

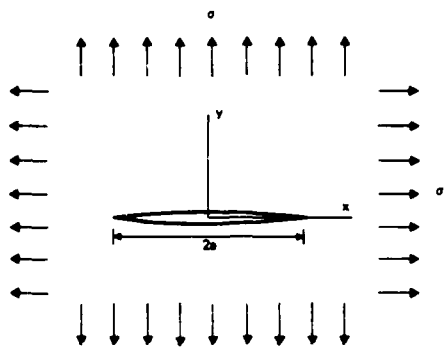

Fig 1.1 Infinite plate with central crack under biaxial stress

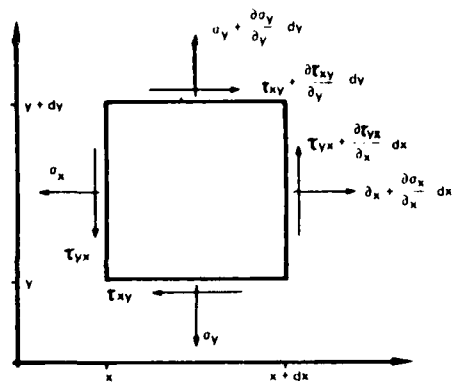

Fig 1.2 Equilibrium conditions in an infinitesimal element

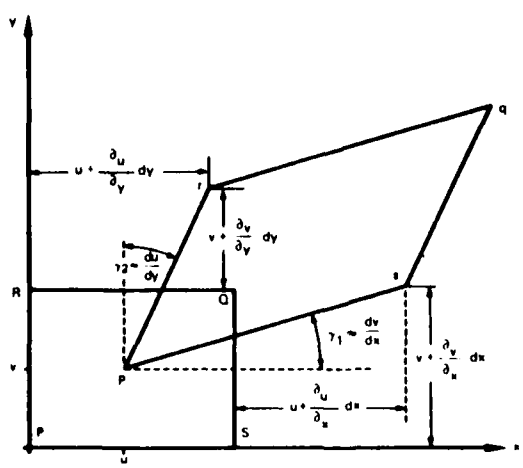

Fig 1.3 Distortions and displacements of an infinitesimal element

LT 2057

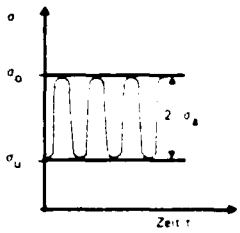

Fig 2.1 Stress sequence with constant amplitude

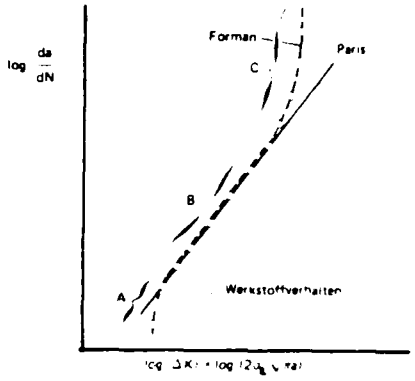

Fig 2.2 Crack propagation rate as a function of the stress intensity range

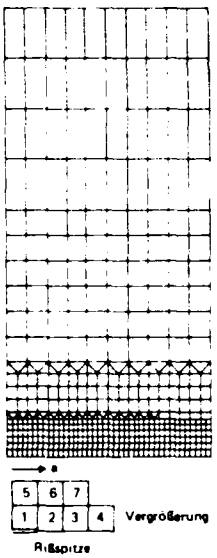

Key:
Vergrösserung = magnification
Rissspitze = crack tip

Fig 3.1 Idealisation of a plate with central crack by finite elements

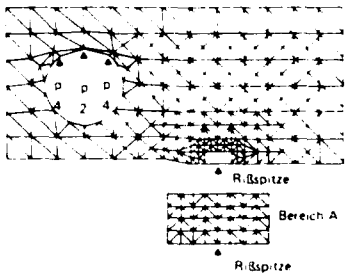

Fig 3.2 Idealisation of compact tensile specimen by finite elements

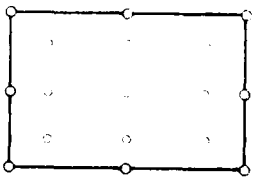

Fig 3.3 Isoparametric element

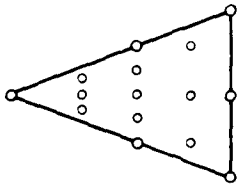

Fig 3.4 Simulation of stress singularity by an isoparametric element

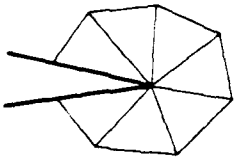

Fig 3.5 Idealisation of the crack tip with the aid of isoparametric elements

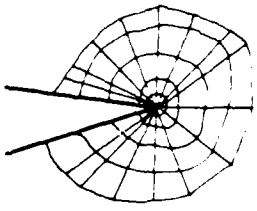

Fig 3.6 Idealisation of the crack tip with the aid of conventional elements

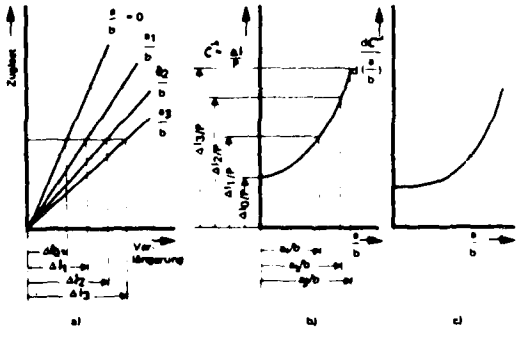

Key:
Zuglast = tensile load
Verlängerung = extension

Fig 3.7 Experimental determination of $dC^{-1}/d\left(\frac{a}{b}\right)$ from Ref 51

LI 2057

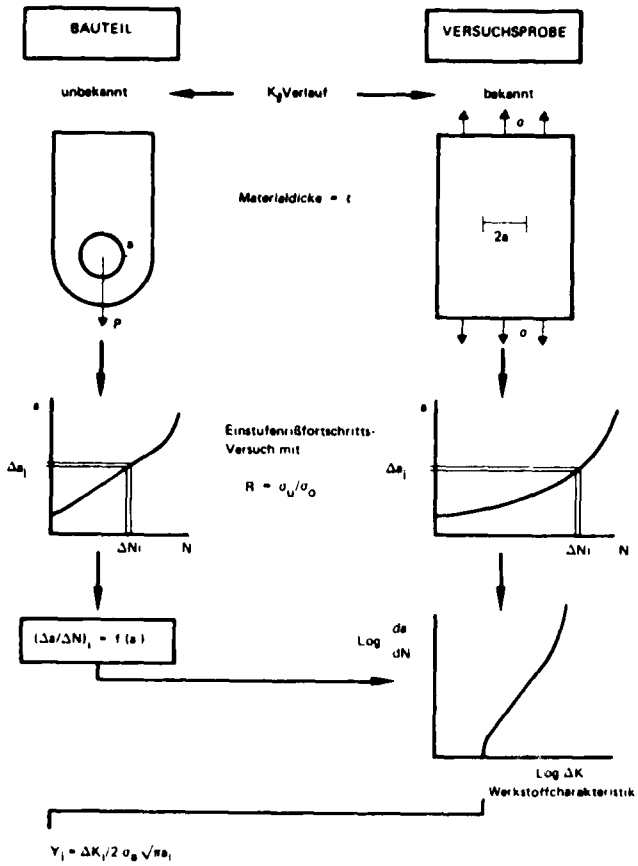

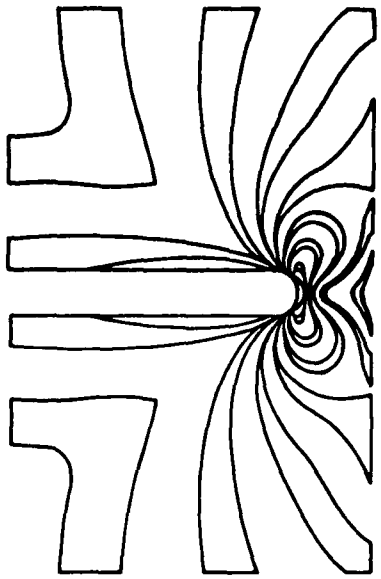

Fig 3.9 Plot of isochromatics in the area of a sharp notch

Key:

Bauteil	= component
Versuchsprobe	= test piece
(un)bekannt	= (un)known
Verlauf	= course
Materialdicke	= material thickness
Einstufenrissfortschritts-Versuch	= constant amplitude crack propagation test
Werkstoffcharakteristik	= material characteristic

Fig 3.8 Procedure in determining stress intensity with the aid of the crack propagation method

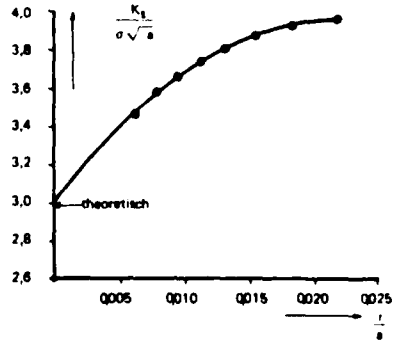

Fig 3.10 Determination of stress intensity for an edge crack specimen

LT 2057

Figs 4.1-4.4

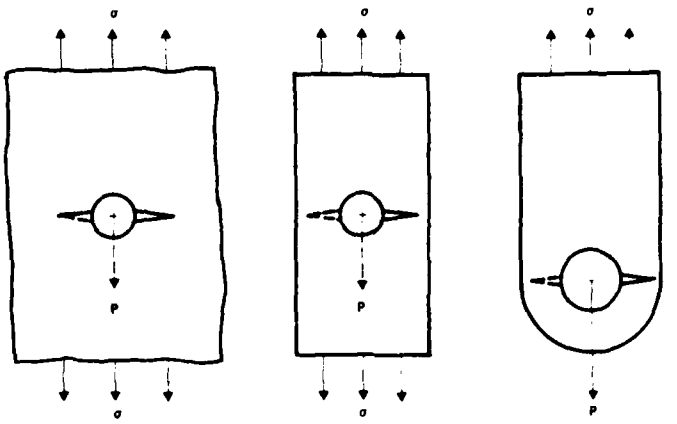

Fig 4.1 Loaded and unloaded hole with crack in infinite and finite plate

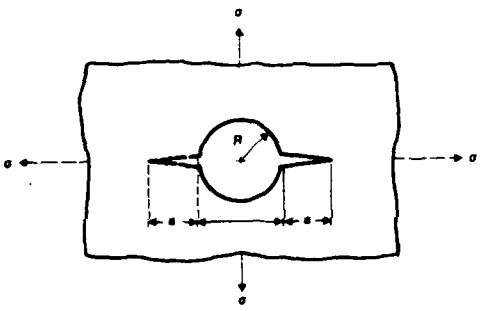

Fig 4.2 Uni- and bilateral crack from unloaded hole in an infinite plate

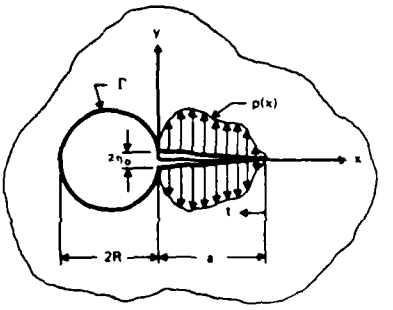

Fig 4.3 Open hole with crack under load p(x)

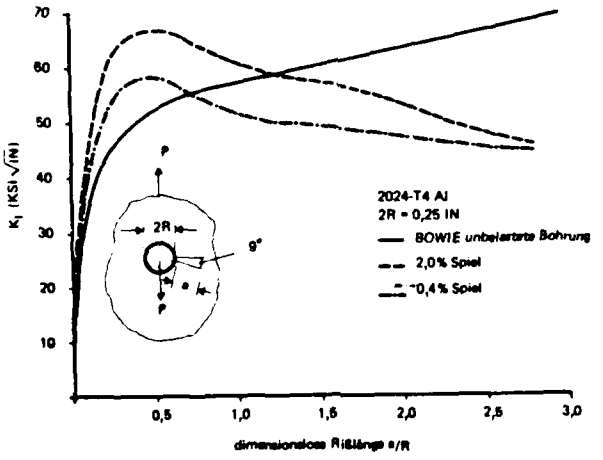

Key:
Unbelastete Bohrung = unloaded hole
Spiel = clearance
Dimensionslose Risslänge = dimensionless crack length

Fig 4.4 Curve of stress intensity for an open hole and for a loaded hole with different pin fit

LT 2057

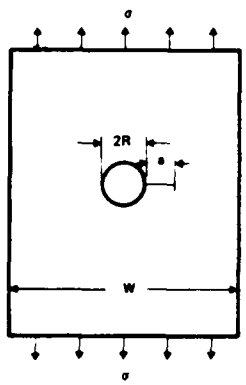

Fig 4.5 Finite plate with unloaded hole

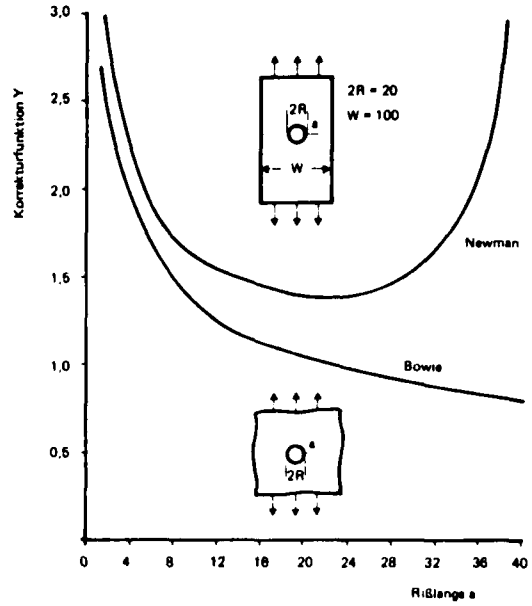

Fig 4.6 Effect of plate edge on correction function

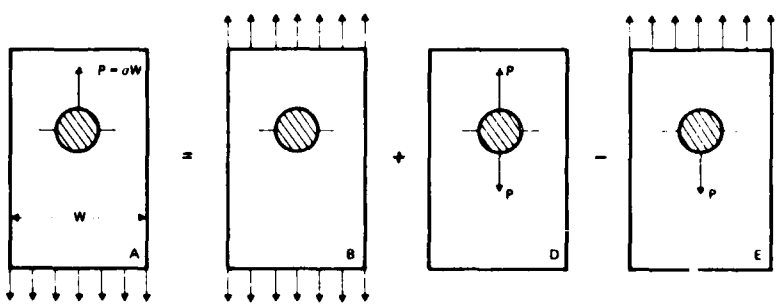

Fig 4.7 Illustration of principle of superposition by means of a finite plate with loaded hole

Fig 4.8 Effective crack length for the unilateral and bilateral crack in a hole

LT 2057

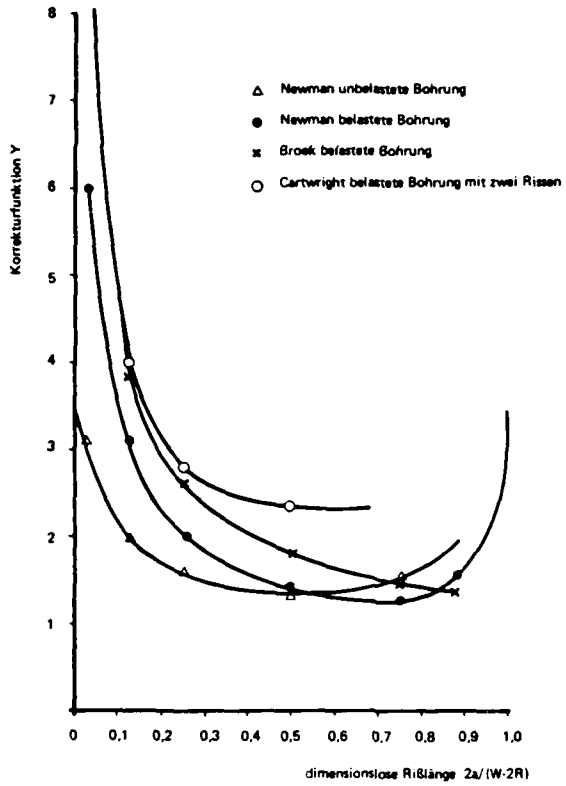

Key:
(un)belastete Bohrung = (un)loaded hole
mit zwei Rissen = with two cracks
Dimensionslose Risslänge = dimensionless crack length

Fig 4.9 Comparison of correction functions for the loaded and unloaded hole

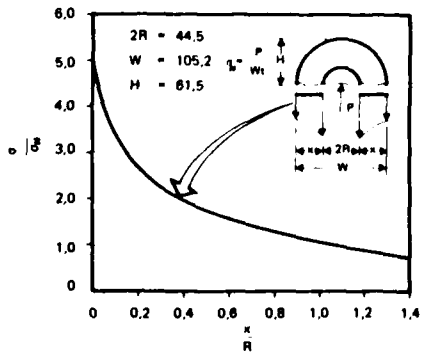

Fig 4.10 Stress distribution in the non-cracked lug

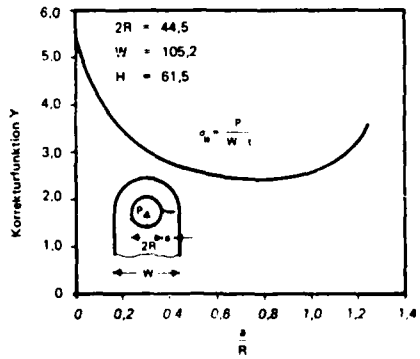

Fig 4.11 Correction function for a lug

LT 2057

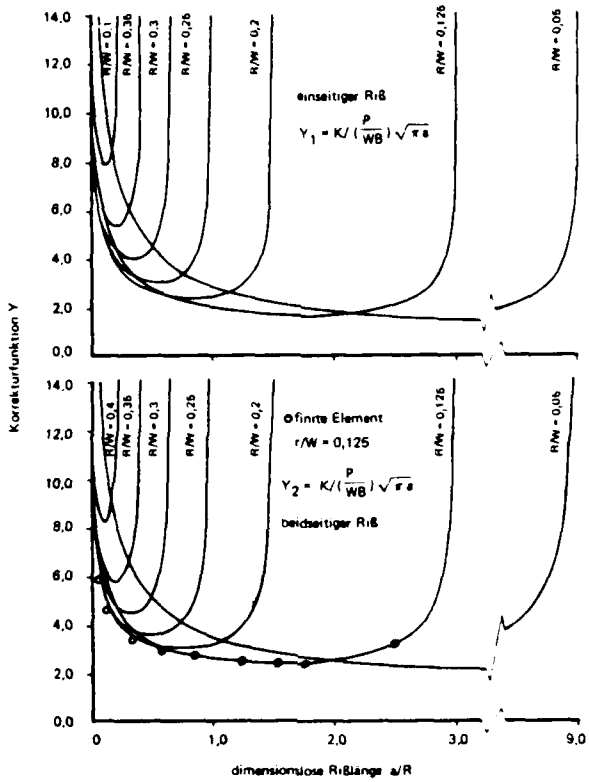

Fig 4.12 Effect of cheek width R/W on the plot of the correction function for the uni- and bilaterally cracked lug by the method of linear superposition

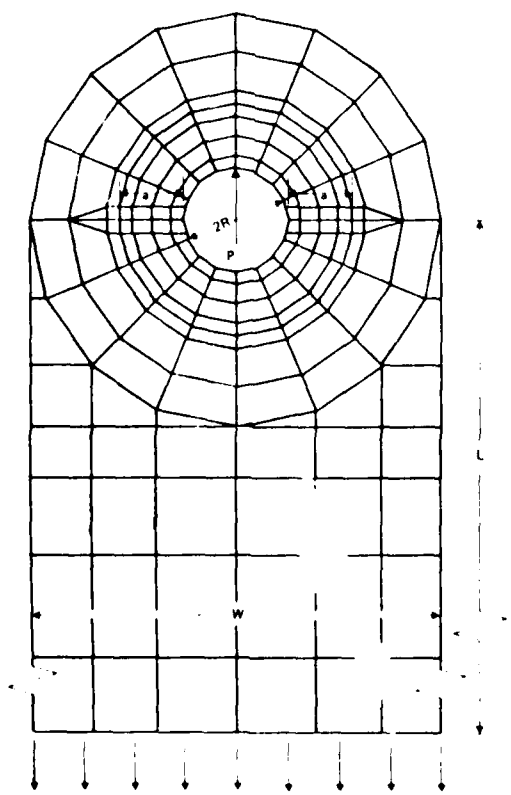

Fig 4.13 Finite element model for the bilaterally cracked lug

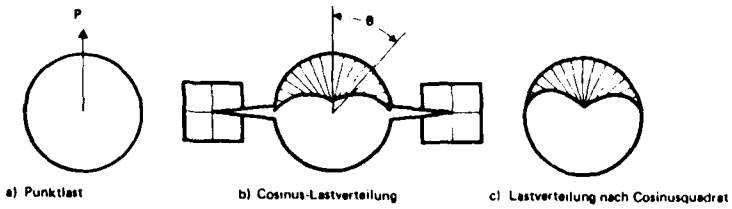

Key:
(a) concentrated load at centre of hole
(b) cosine load distribution
(c) cosine square load distribution

Fig 4.14 Different means of idealisation of introduction of force into the lug

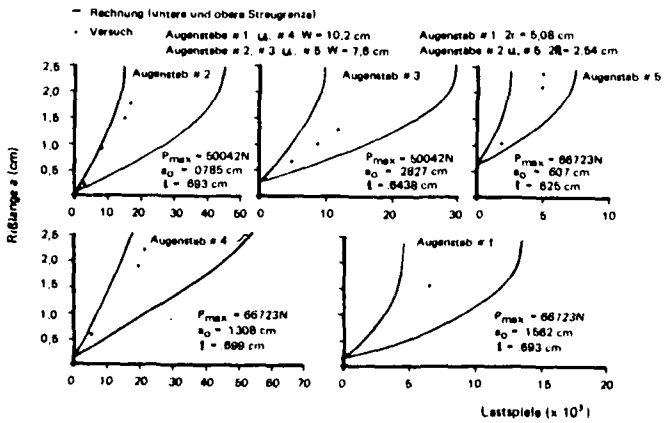

Key:
Rechnung (untere etc) = calculation (lower and upper scatter limit)
Lastspiele = stress cycles

Fig 4.15 Comparison between test and calculation

I.T 2057

Crack model		Method	Described in section:	Reference No.
Sketch	Description			
	Infinite plate with crack from open hole	Analytical stress function conformal mapping	4.1	Bowie (61)
	Infinite plate with crack from hole and force introduction by means of a pin	Analytical linear superposition with aid of 'weight function'	4.2.2	Grandt (64)
	Plate strip with open hole	Numerical solution of stress function series (boundary collocation)	4.3.1	Newman (63)
	Plate strip with hole and force introduction by a pin	Numerical solution of stress function series	4.3.2.1	Newman (63)
		Superposition, superimposing known solutions	4.3.2.2	Broek (69)
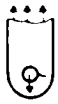	Lug	Analytical, linear superposition with aid of 'weight function'	4.4.1	Impellizzeri and Rich (72)
		Superposition, superimposing known solutions	4.4.2	Liu and Kan (73)

Fig 5.1 Survey of different crack models and methods to determine stress stress intensity

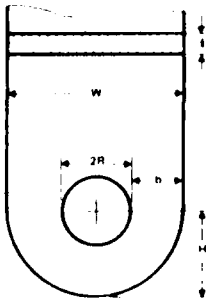

Fig 6.1 Definition of notations for the lug

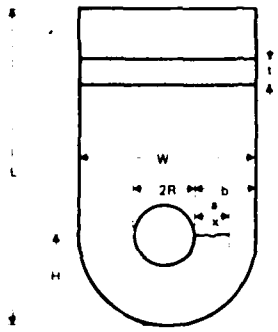

Fig 7.1 Laying down lug geometry by typical parameters

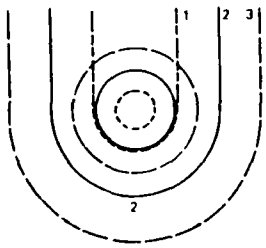

Fig 7.2 Variation of lug by scale enlargement

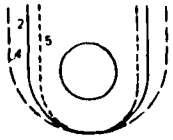

Fig 7.3 Variation of lug width W

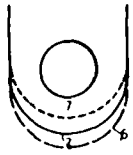

Fig 7.4 Variation of head height H of lug

LT 2057

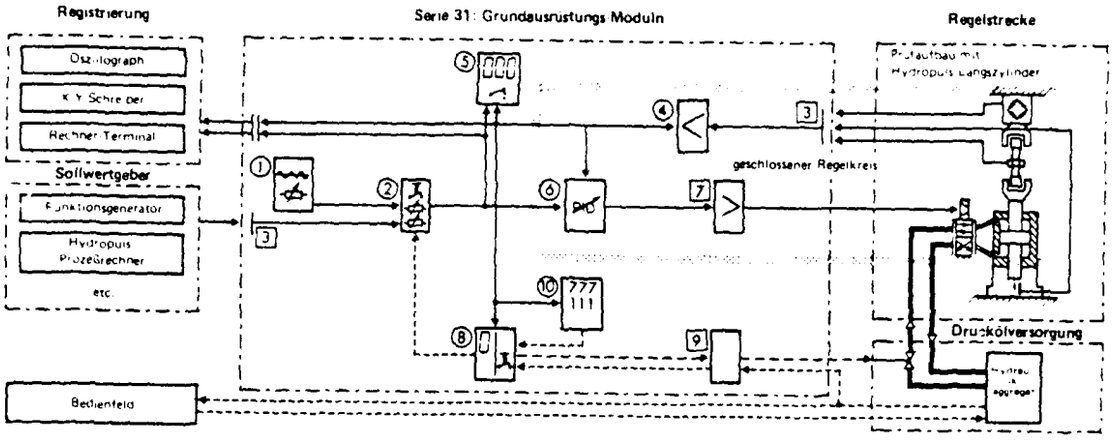

Key:

Registrierung	= recording
X-Y-Schreiber	= X-Y recorder
Rechner-Terminal	= computer terminal
Sollwertgeber	= setting transmitter
Functionsgenerator	= function generator
Prozessrechner	= process computer
Bedienfeld	= operating field
Geschlossener Regelkreis	= closed control circuit
Regelstrecke	= control section
Prüfaufbau mit Hydropuls-Längszylinder	= test set-up with Hydropulse longitudinal cylinder
Druckölversorgung	= pressure oil supply
Hydraulikaggregat	= hydraulic control unit

Fig 7.5 Plan of hydropulse equipment - Series 31: Basic equipment module

LT 2057

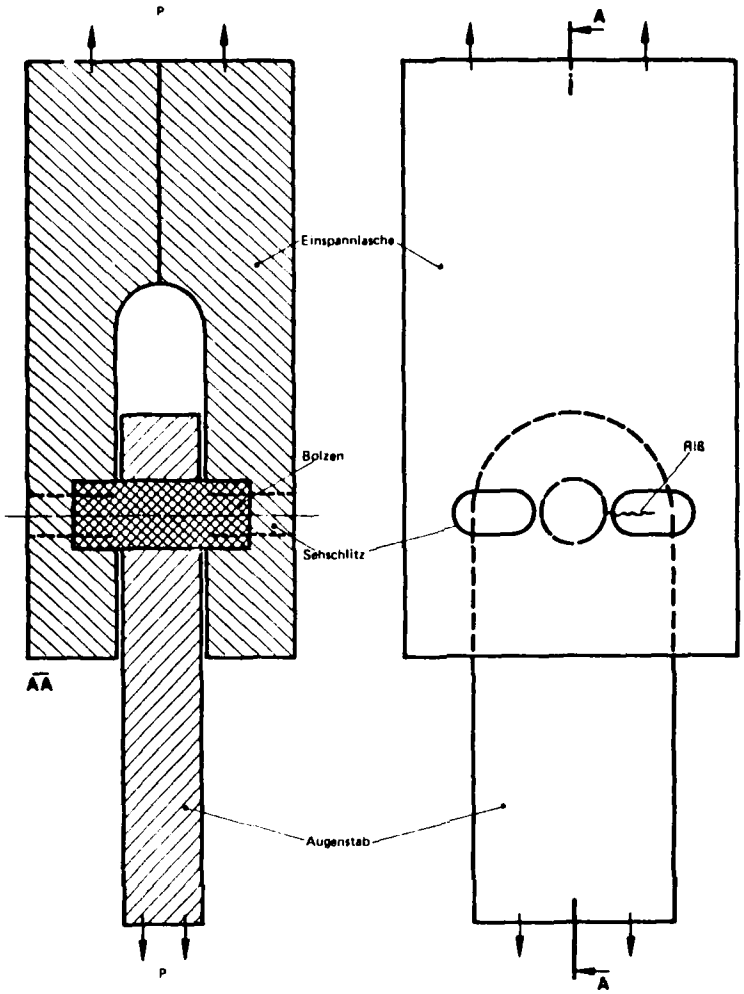

Key:
Einspannlasche = shackle
Bolzen = pin
Sehschlitz = inspection slit
Riss = crack

Fig 7.6 Mounting device for the lug

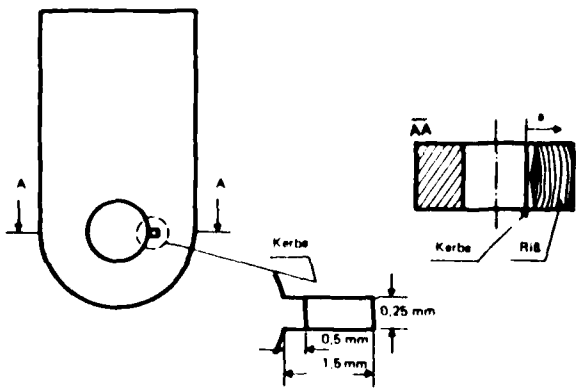

Key:
Kerbe = notch

Fig 7.7 Crack starter notch at the edge of the hole in the lug

LT 2057

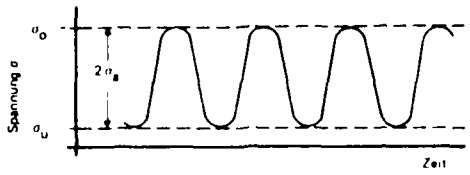

Key:
Spannung = stress
Zeit = time

Fig 7.8 Constant amplitude load sequence

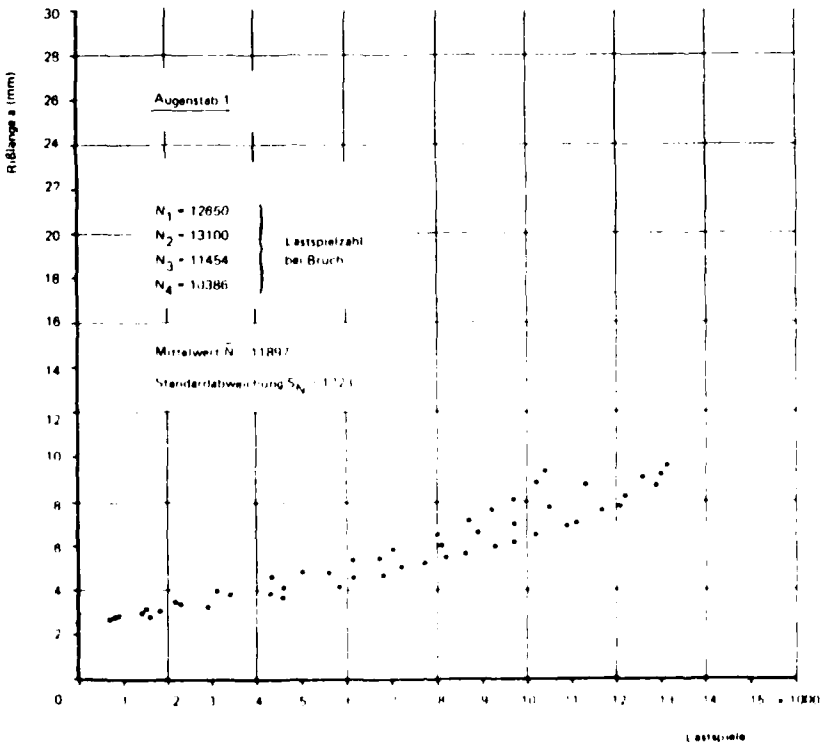

Key:
Lastspielzahl bei Bruch = load cycle on fracture
Mittelwert = mean value
Standardabweichung = standard deviation

Fig 7.9 Crack propagation investigation of lug 1

LT 2057

Figs 7.10&7.11

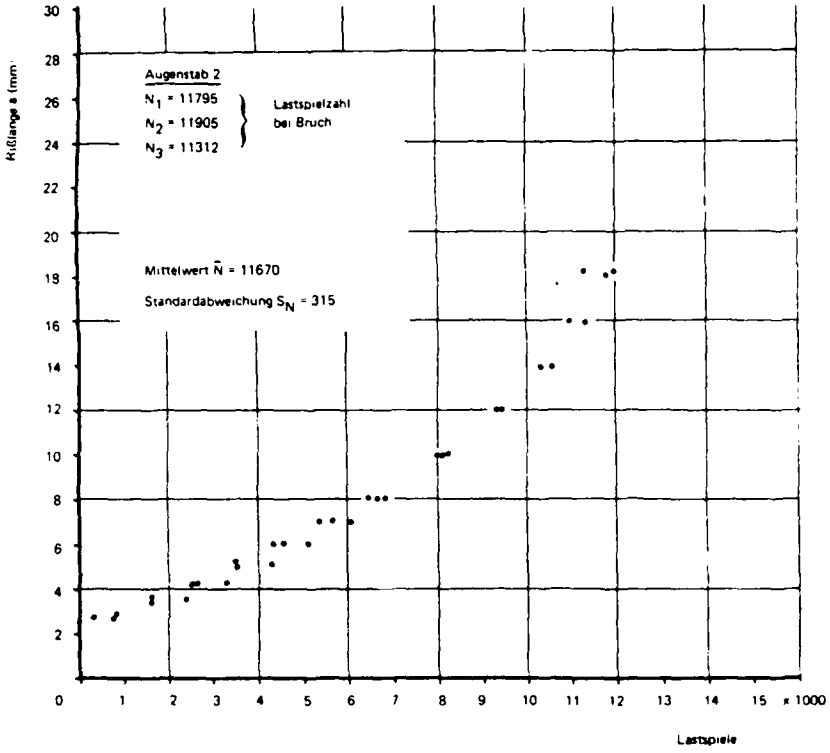

Fig 7.10 Crack propagation investigation of lug 2

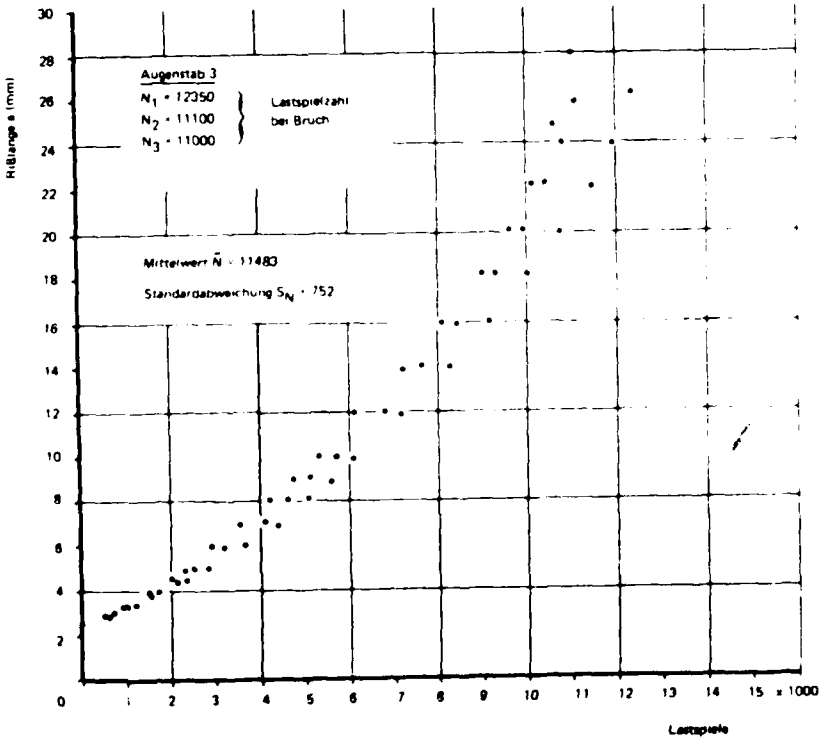

Fig 7.11 Crack propagation investigation of lug 3

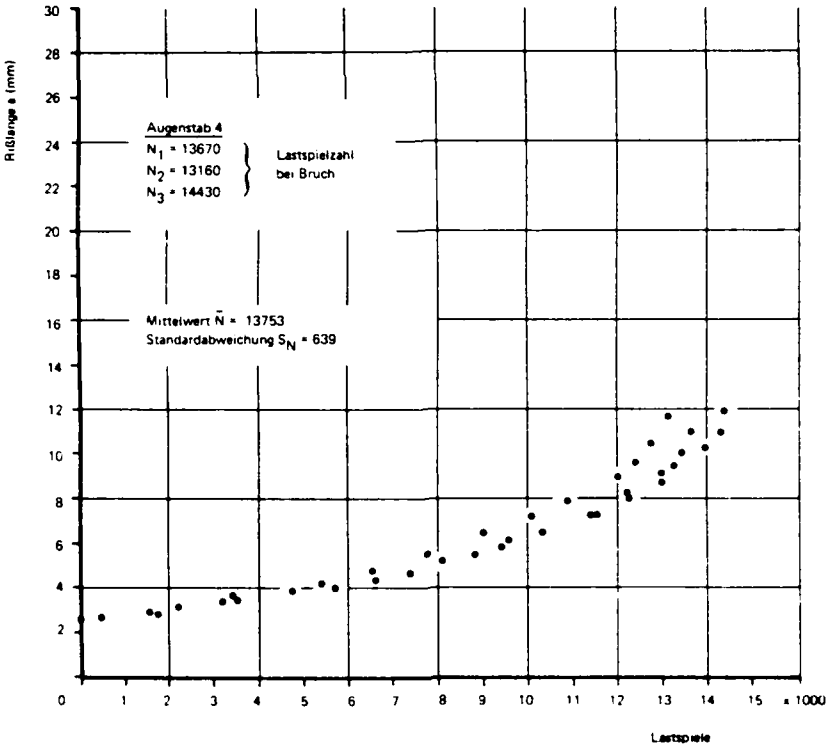

Fig 7.12 Crack propagation investigation of lug 4

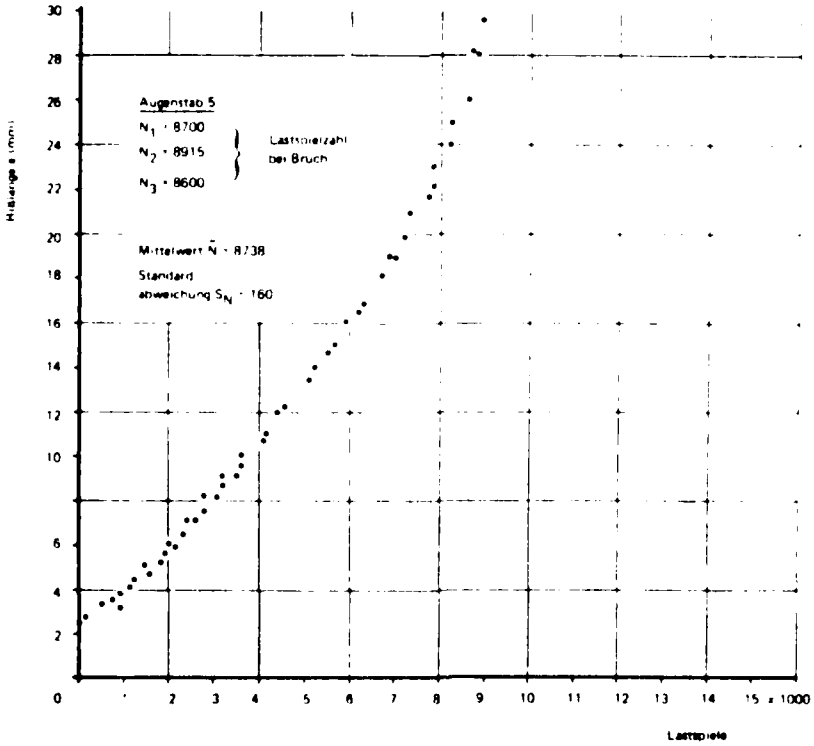

Fig 7.13 Crack propagation investigation of lug 5

Figs 7.14&7.15

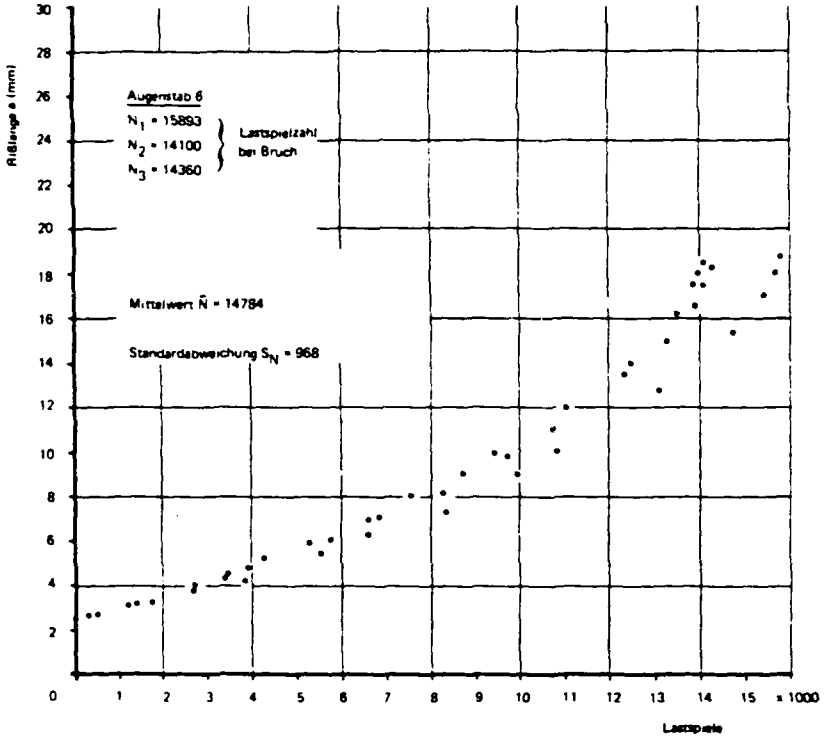

Fig 7.14 Crack propagation investigation of lug 6

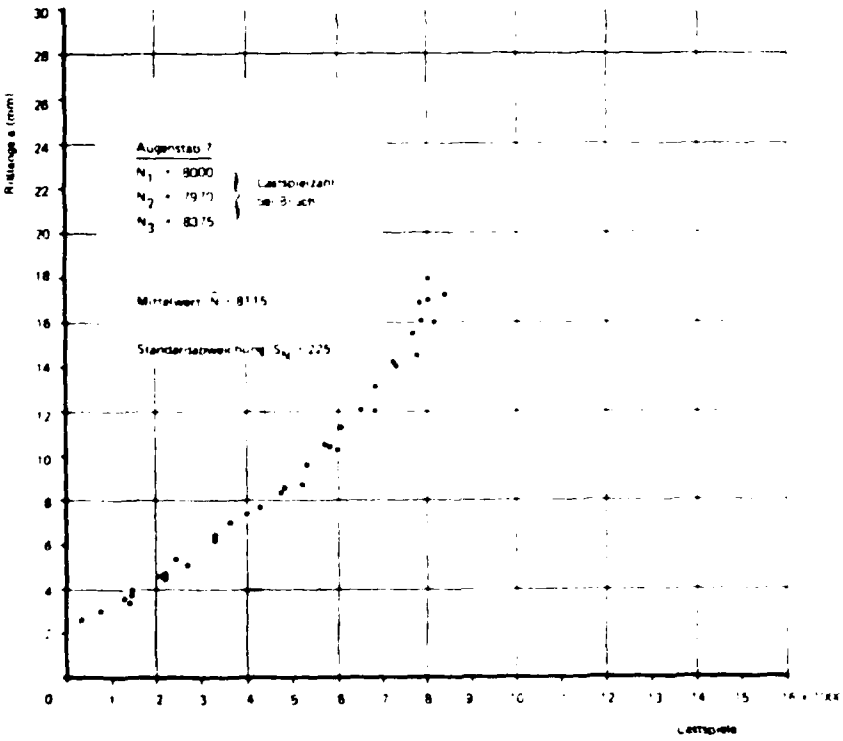

Fig 7.15 Crack propagation investigation of lug 7

LT 2057

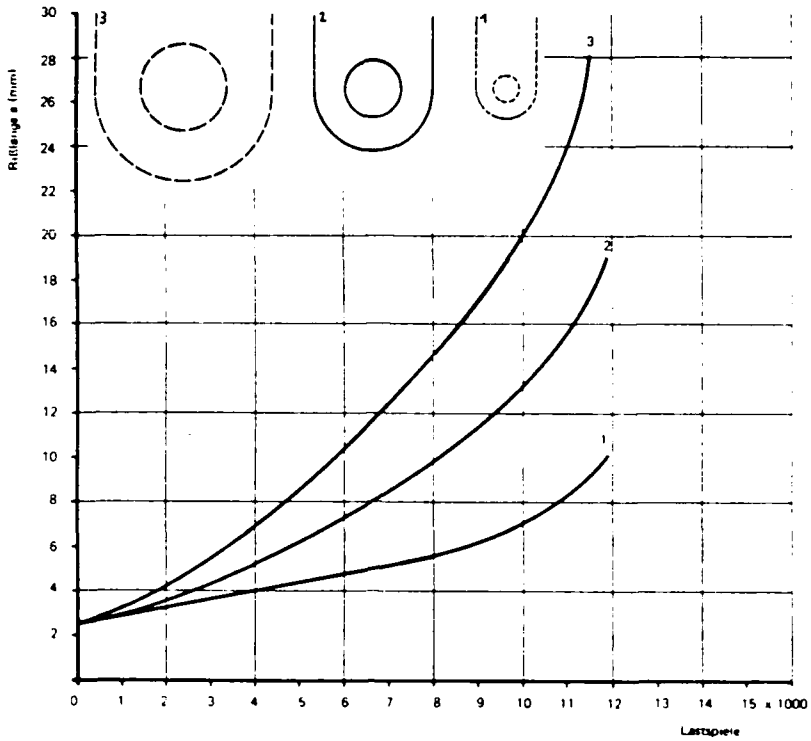

Fig 7.16 Mean crack propagation curves for lugs 1, 2 and 3

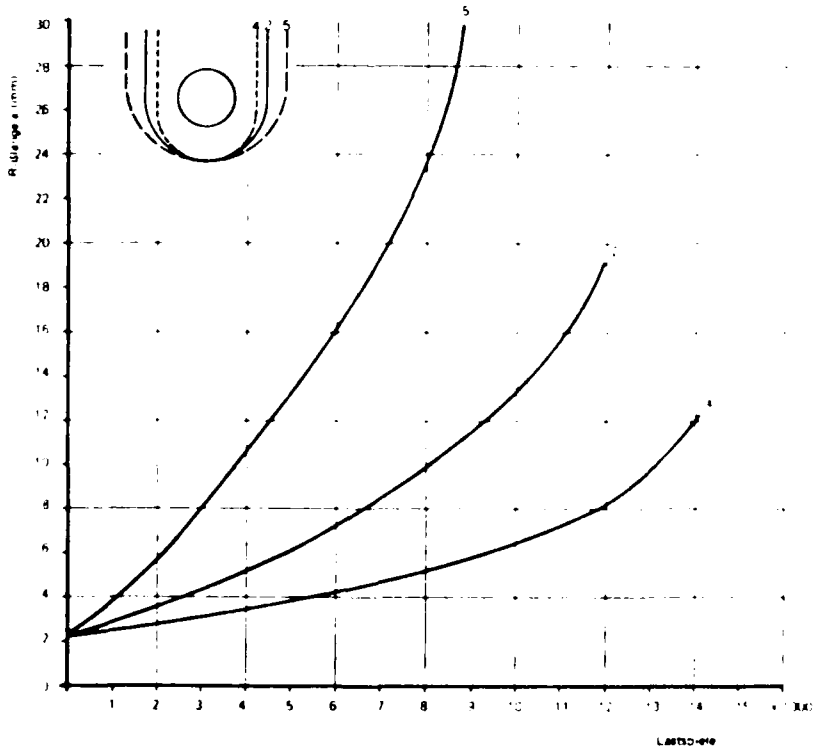

Fig 7.17 Mean crack propagation curves for lugs 2, 4 and 5

LT 2057

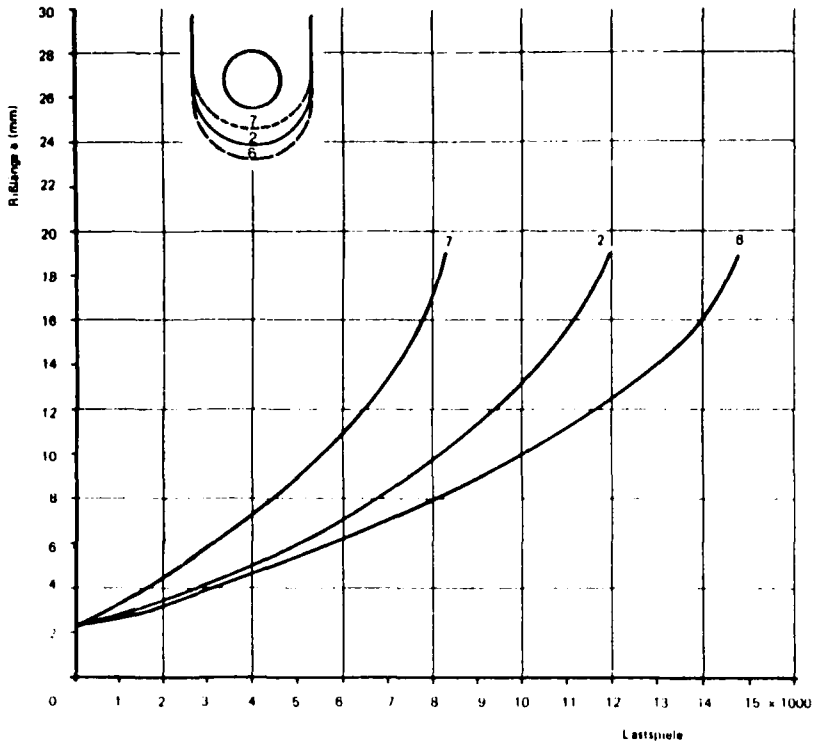

Fig 7.18 Mean crack propagation curves for lugs 2, 6 and 7

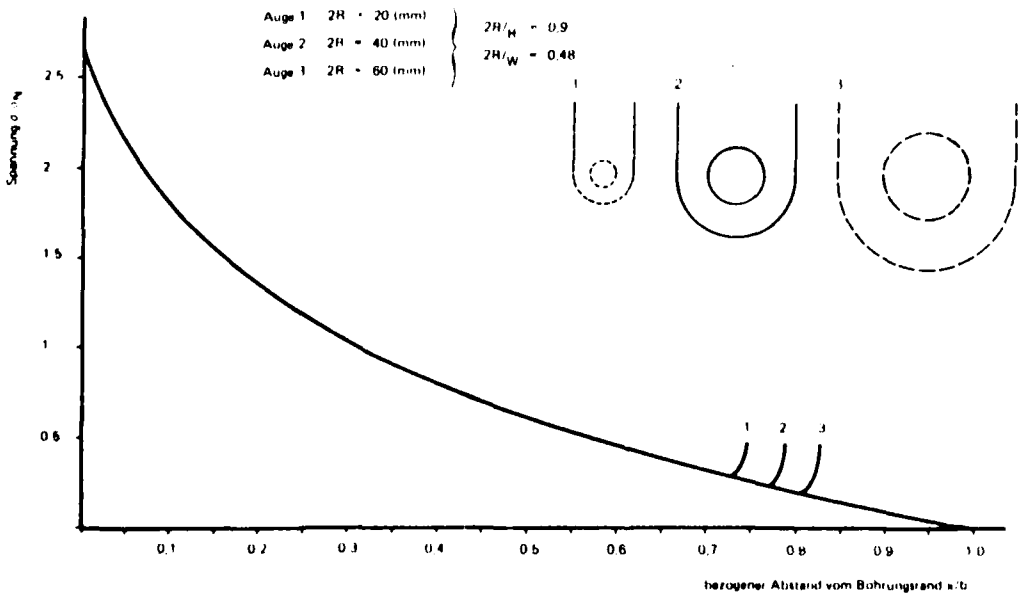

Key:
Bezogener Abstand vom Bohrungsrand = relative distance from edge of hole

Fig 7.19 Stress distribution for lugs 1, 2 and 3

LT 2057

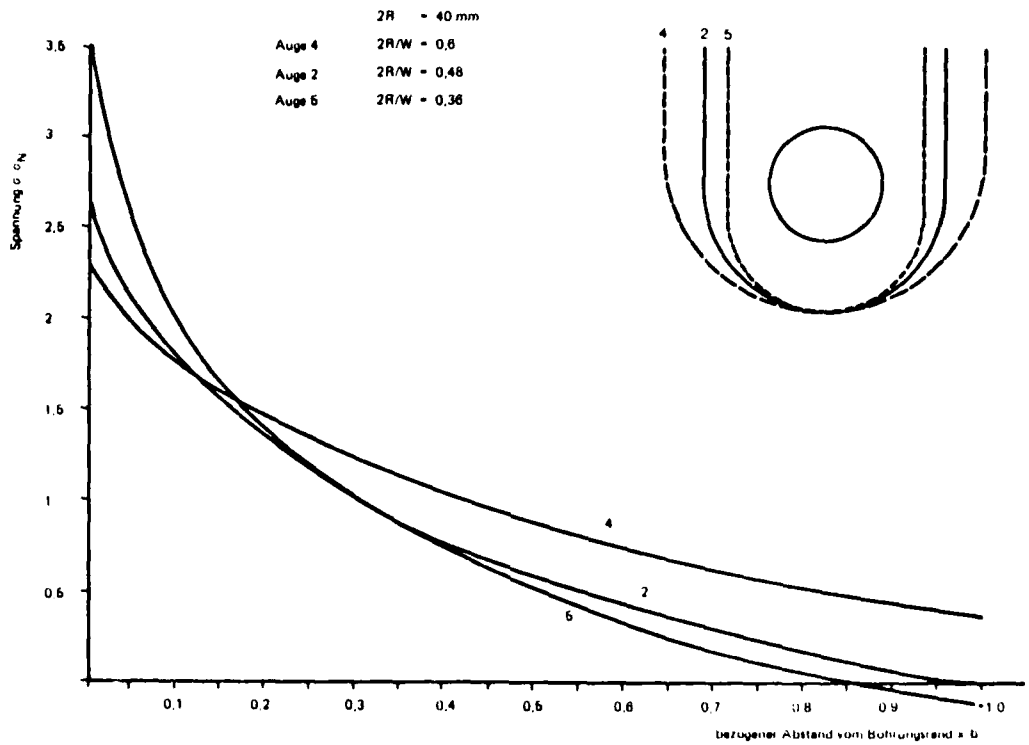

Fig 7.20 Stress distribution for lugs 4, 2 and 5

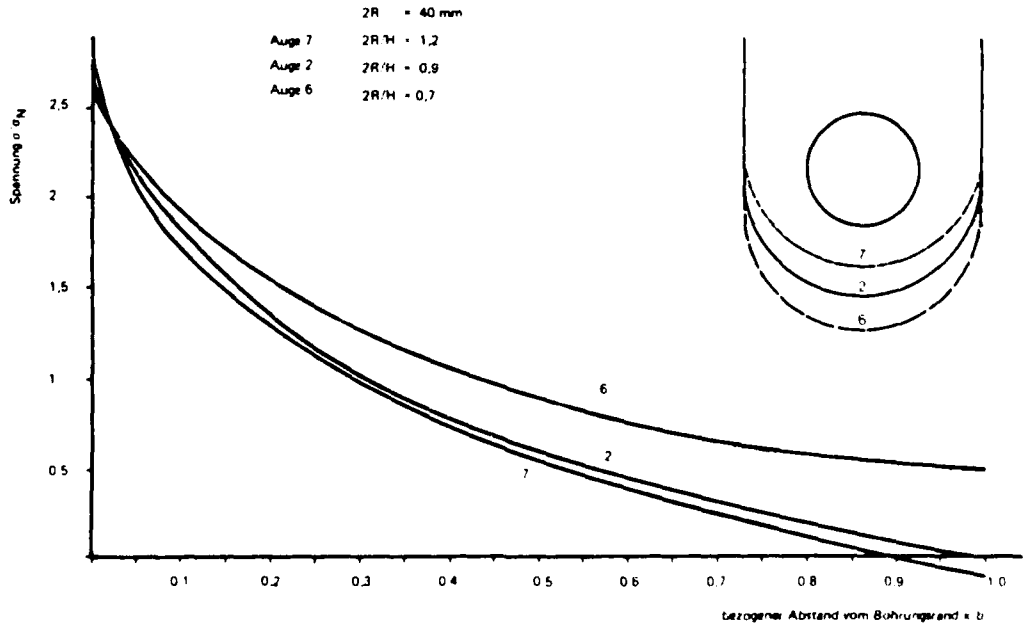

Fig 7.21 Stress distribution for lugs 6, 2 and 7

LT 2057

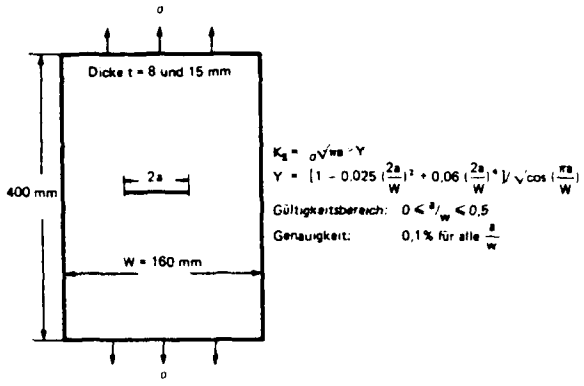

Key:
Dicke = thickness
Gültigkeitsbereich = area of validity
Genauigkeit = accuracy

Fig 8.1 Central crack specimen for determination of crack propagation characteristic

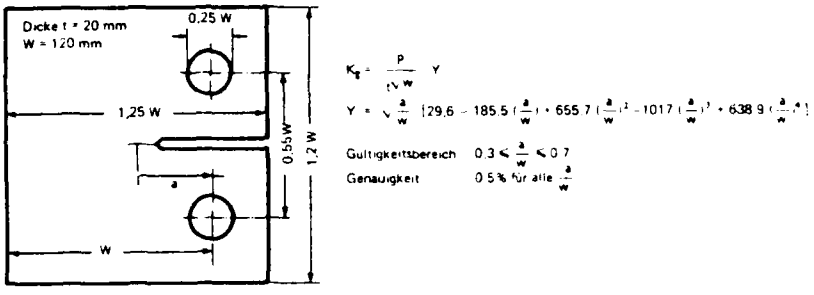

Fig 8.2 Compact tensile specimen for determination of crack propagation characteristic

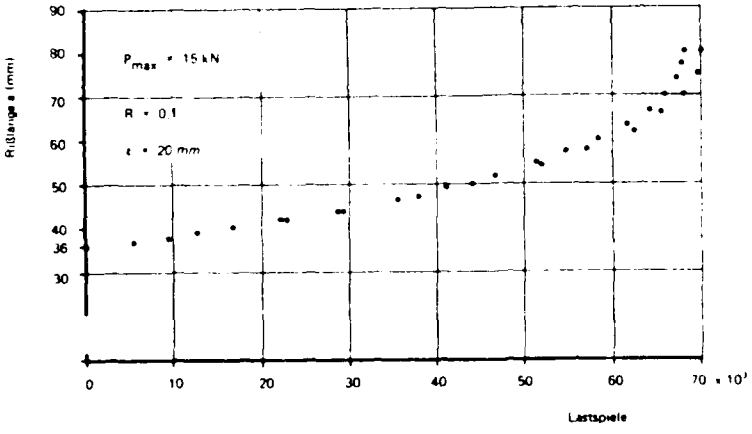

Fig 8.3 Crack propagation measurements on compact tensile specimens

LT 2057

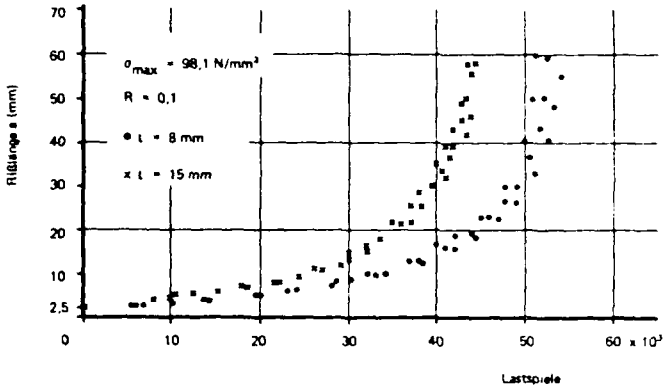

Fig 8.4 Crack propagation measurements on central crack specimens

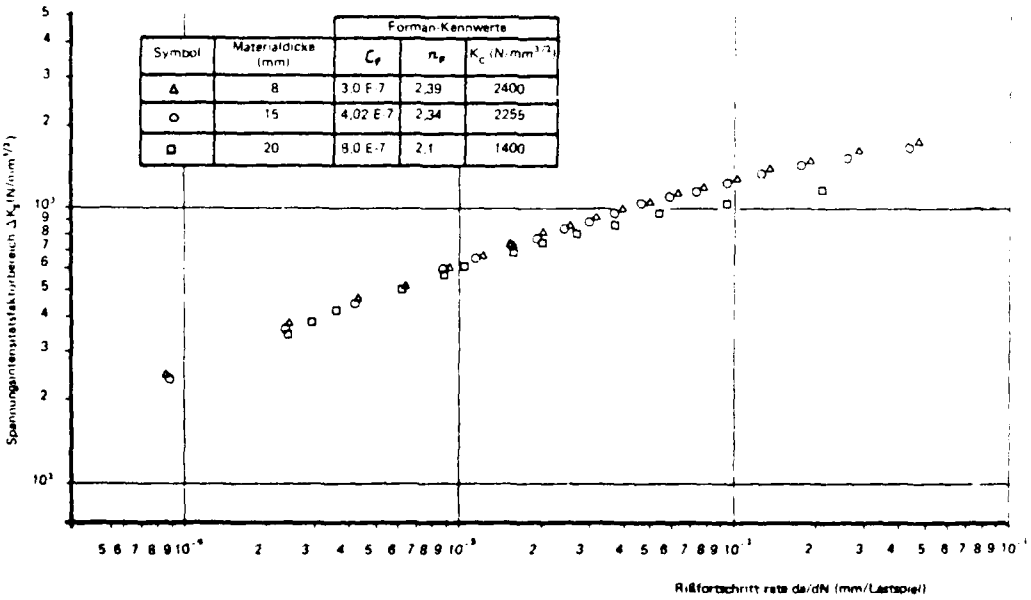

Key:
Spannungsintensitätsfaktorbereich = stress intensity factor range
Rissfortschrittsrate = crack propagation rate

Fig 8.5 Crack propagation characteristic for aluminium alloy 7075T7351 with differing specimen thickness

LT 2057

Figs 8.6-8.8

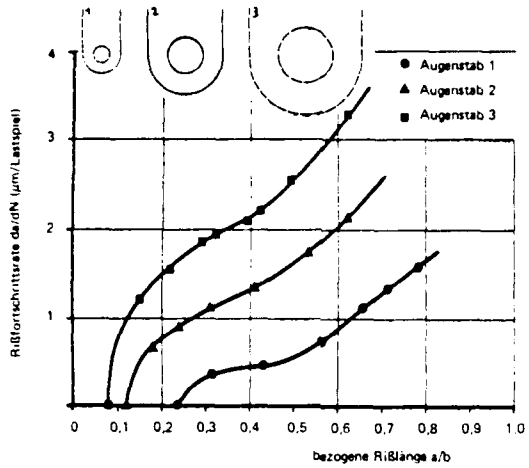

Key:
Bezogene R·,slänge = relative crack length

Fig 8.6 Crack propagation rate for lugs 1, 2 and 3

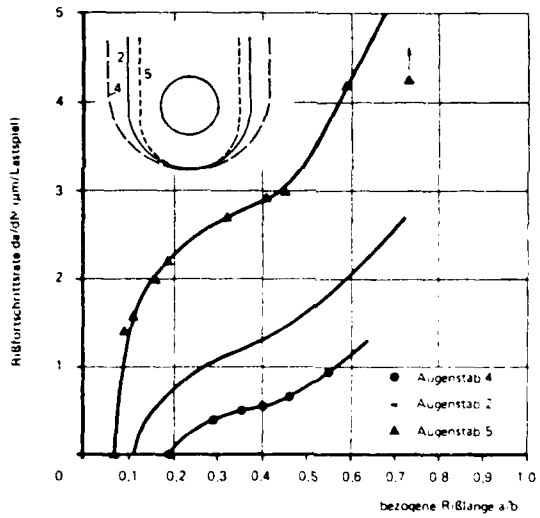

Fig 8.7 Crack propagation rate for lugs 2, 4 and 5

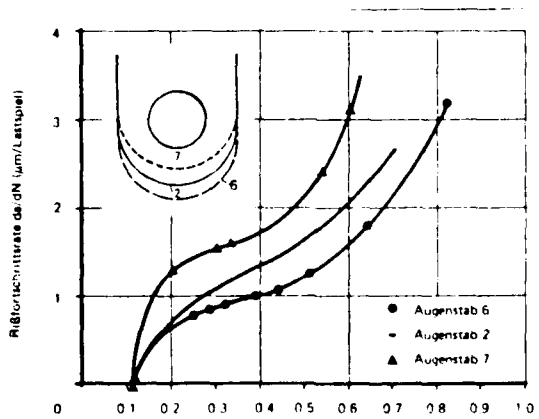

Fig 8.8 Crack propagation rate for lugs 2, 6 and 7

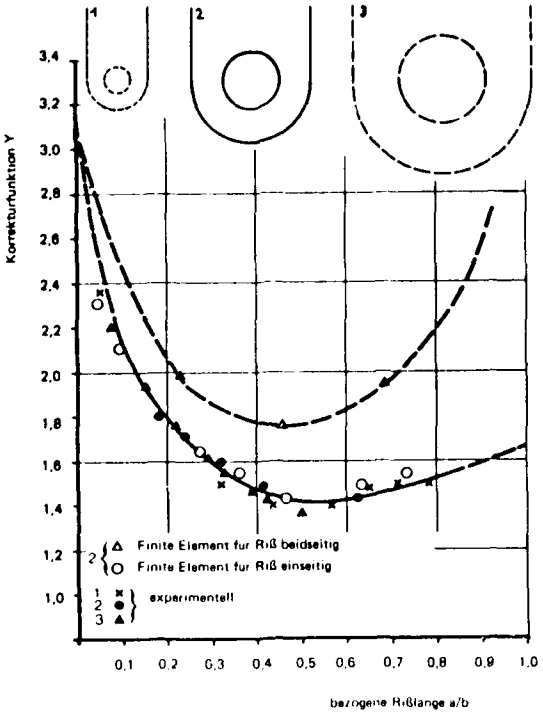

Key:
Finite Element für Riss = finite element method for
(beidseitig) einseitig (bilateral) unilateral crack

Fig 8.9 Correction function Y for lugs 1, 2 and 3

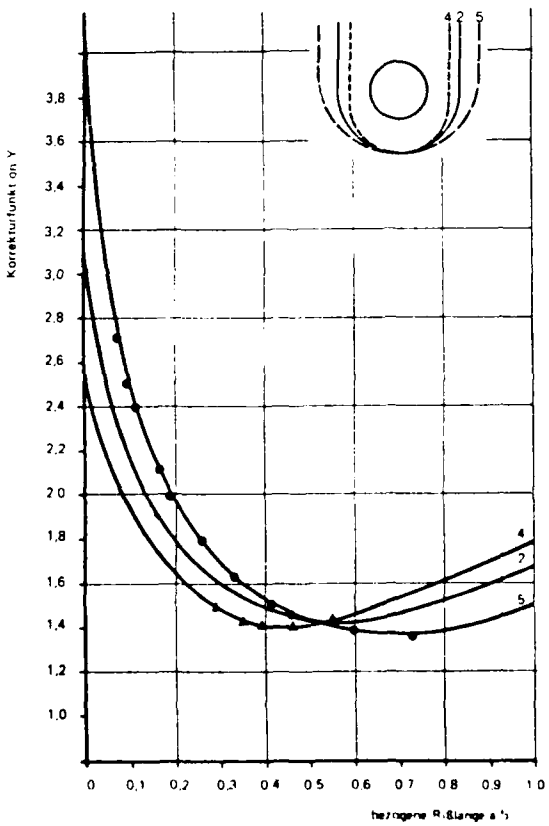

Fig 8.10 Correction function for lugs 2, 4 and 5

AD-A107 640 ROYAL AIRCRAFT ESTABLISHMENT FARNBOROUGH (ENGLAND) F/G 13/5
STRENGTH BEHAVIOUR OF FATIGUE CRACKED LUGS (FESTIGKEITSVERHALTE--ETC(U)
JAN 81 W GEIER
UNCLASSIFIED RAE-LIBRARY TRANS-2057 DRIC-BR-80140 NL

2 OF 2
AD A
107640

END
DATE
FILMED
1-82
DTIC

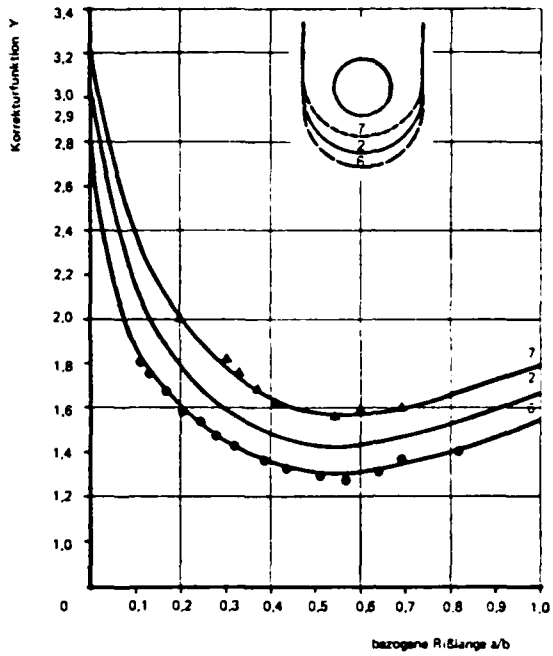

Fig 8.11 Correction function for lugs 2, 6 and 7

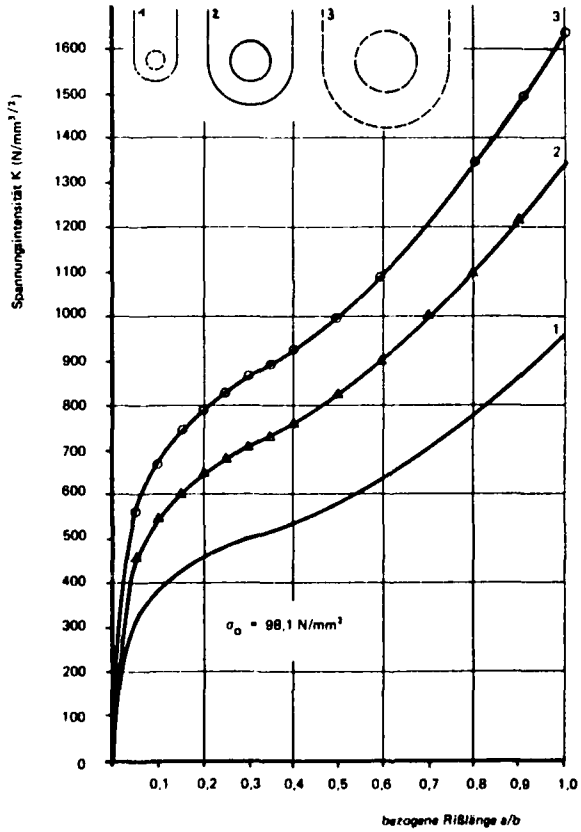

Fig 8.12 Stress intensity for lugs 1, 2 and 3

LT 2057

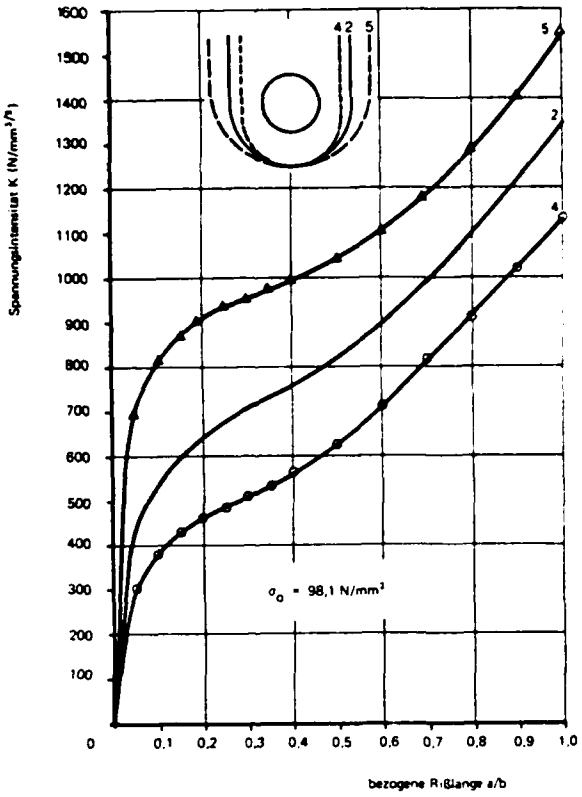

Fig 8.13 Stress intensity for lugs 2, 4 and 5

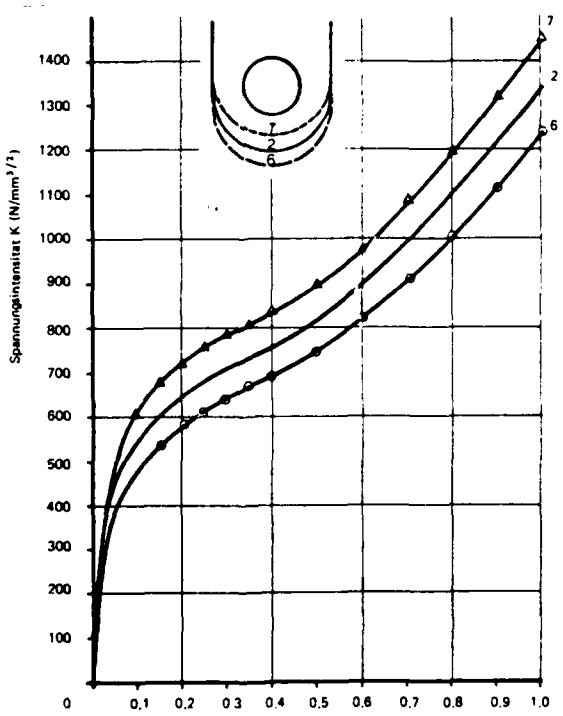

Fig 8.14 Stress intensity for lugs 2, 6 and 7

LT 2057

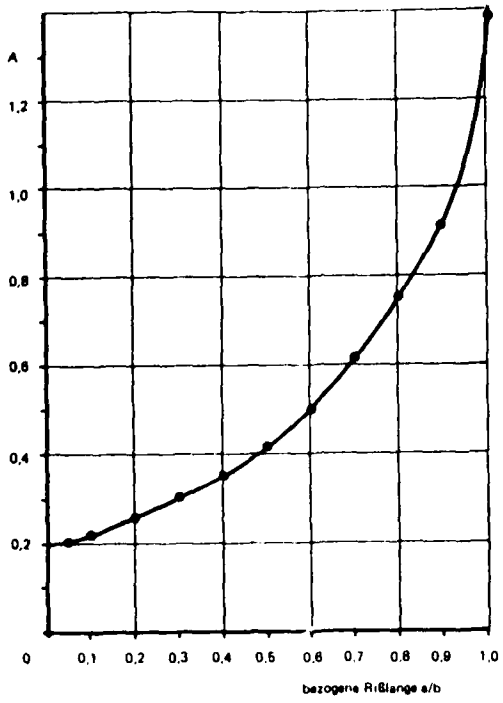

Fig 9.1 Relation between the empirically determined quantity A and crack length

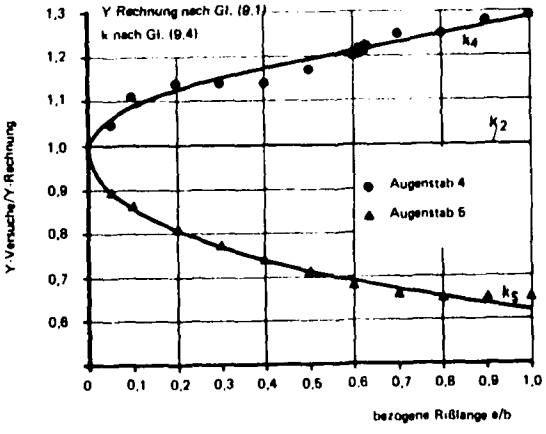

Fig 9.2 Relationship between correction function determined experimentally and to equation (9-1) as a function of crack length for lugs 4 and 5, as well as approximation with equation (9-4)

LT 2057

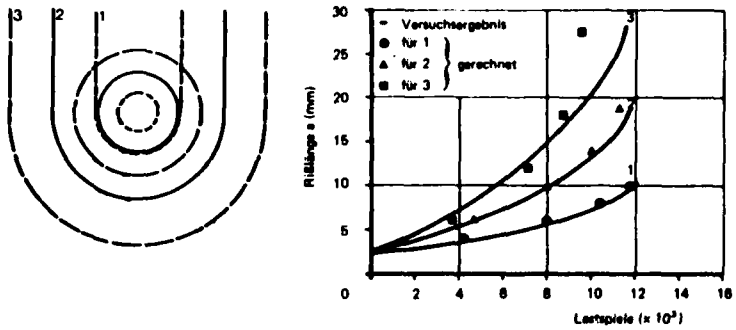

Fig 10.1

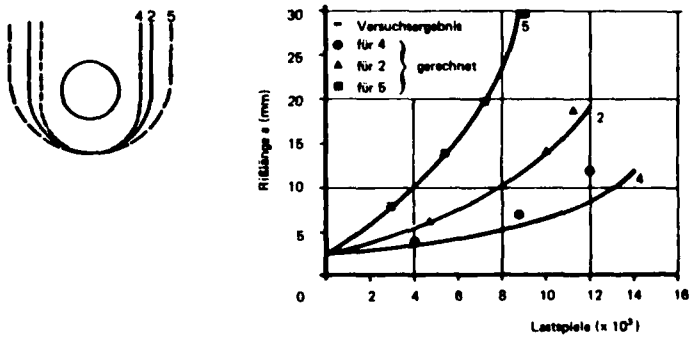

Fig 10.2

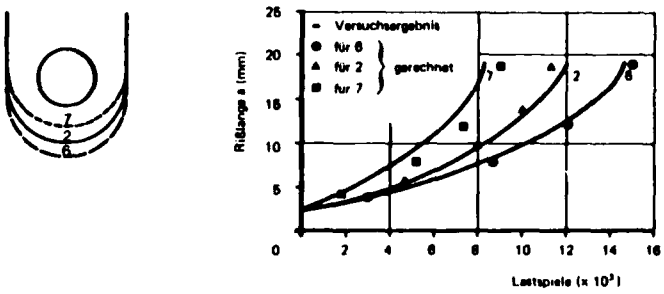

Fig 10.3

Key:
Versuchsergebris = test result
Gerechnet = calculated

Figs 10.1-3 Comparison between crack propagation curves determined experimentally and calculated as Forman, using equation (9-8)

Figs 11.1

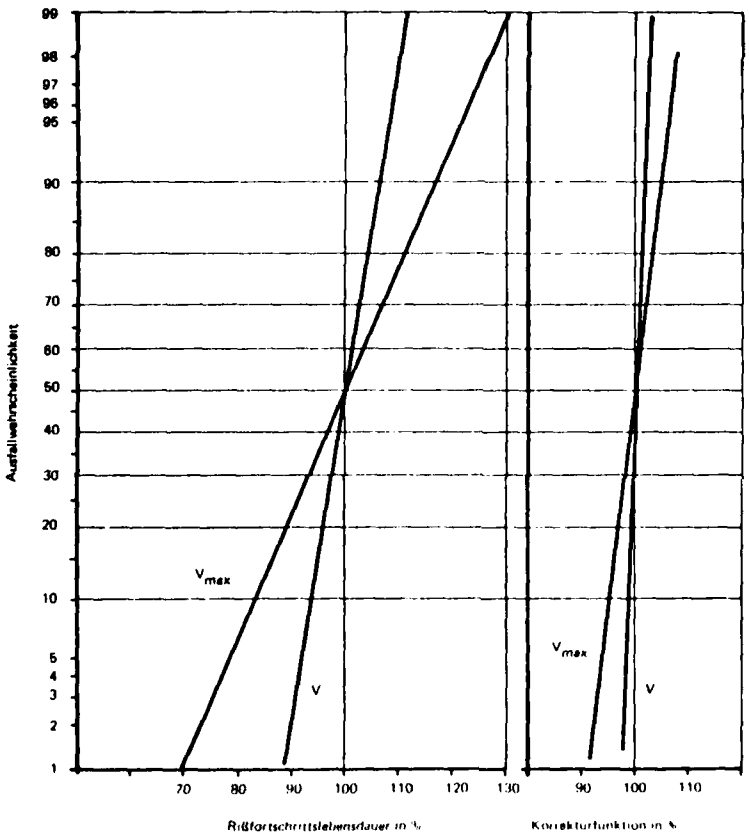

Key:
Ausfallwahrscheinlichkeit = failure probability
Rissfortschrittslebensdauer = crack propagation life

Fig 11.1 Scatter behaviour of the crack propagation curves and their influence on the correction function

LI 2057

ADVANCE DISTRIBUTION:

RMCS
ITC
DRIC 70

BAe, Hatfield
Library, NGTE

RAE

Deputy Director
Main Library
Structures Dept 15